Deformation of Breakwater Roundheads under Construction

Additional Thesis

Delft, April 5th, 2014

Victoria Curto
4257162

Preface

Proper understanding of construction activities as well as design processes is an essential component of a successful civil engineer. For a structure to perform efficiently, it is imperative to have a strong link between design and construction since the two are not independent of one another. It is as important for a contractor to fully understand the basis upon a design was based, as it is for a designer to know the forcing and ambient conditions, to which a structure might be exposed such as, a breakwater under construction.

Breakwaters are in integral part of port infrastructure and coastal defense. In this research, not only did I have the opportunity to learn about the behavior of breakwaters under construction but also, I completed in The Netherlands, which is known worldwide for her coastal defense systems. This Additional Thesis was carried out in TU Delft, institution leader in the coastal engineering field, and my tenure consisted of literature review, detailed data processing, and data analysis.

The following report presents the Additional Thesis titled “Deformation of Breakwater Roundheads under Construction,” and it is part of the MSc. Hydraulic Engineering curriculum at the TU Delft Civil Engineering and Geosciences Faculty.

To end, I would like to acknowledge and thank Prof. Henk Jan Verhagen for guiding me and giving me the opportunity to expand on the exceptional work carried out by his former student, Patrick Mulders. For me, it has been a humbling experience to learn from Prof. Verhagen which brings an aptitude for sharing knowledge as well as for transmitting it. Also, I would like to thank Ir. Patrick Mulders for openly sharing his suggestions which were fresh in his mind withstanding the test of time; for his valuable input, attention, and insight, I am genuinely grateful.

Victoria Curto.

Abstract

Breakwaters under construction are prone to undesired deformation because the breakwater core is not designed to withstand severe or moderate wave loads. The reshaping mechanisms for a complete (finished) breakwater have been comprehensively studied; however, few research studies have been undertaken to analyze the deformation mechanisms of the breakwater core (or a breakwater under construction). It is imperative for the contractor to understand how the reshaping takes place because reshaping requires construction schedules to be adjusted as well as additional material and therefore, additional costs. The present study focusses on the deformation rubble mound breakwater roundheads undergo during the construction phase.

Mulders (2010) performed physical model tests for breakwaters under construction exposed to wave attack. To investigate the deformation processes, twelve scaled physical model tests were performed by varying the wave height (8cm for low and 10cm for high wave heights), wave angle (0°, 30°, and 45°), and material grading (f_g= 1.3 for narrow and f_g=6 for wide grading). The data from Mulders' tests was used in this study to analyze the breakwater deformation, with emphasis on the roundheads, via volumetric changes (initial and final test conditions) for a given control volume. The control volumes included the overwash, the overall breakwater, and the roundheads using radial and angular sectioning methods. The radial sections depicted the cross-shore transport while the angular sections illustrated the longshore sediment transport at the roundheads.

As expected, the overwash volumes were proportional to wave load and angle of wave attack. Regarding the breakwater overall behavior, wide graded material caused a volume increase due to the transverse movement of the coarse fractions while the narrow graded material (fine fraction) decreased in volume thus, increasing the packing density. This sorting mechanism was also noticeably present in the roundheads for the radial sections.

For the roundheads, distinctive percentage losses (sectors with low resistance to wave loading) were clearly present in the radial sectors; thus, transverse (radially outward) sediment transport was the dominant deformation mechanism over longshore transport. Longshore transport did contribute to roundhead deformation; however, no maximum losses were found because the volume losses were nearly equal throughout the angular sectors. As a result, the angle of wave incidence did not affect the volume losses in the angular direction. With regards to material sorting at the roundheads, wide graded material caused a volume increase at the outer radii due to the transverse movement of the coarsest fraction potentially reducing the packing density. On the other hand, grading did not influence the roundhead negative percent changes in the radial direction; thus, grading appeared to be indifferent to volume losses but relevant for volume gains.

Keywords: breakwater, roundhead, core, construction, deformation, grading, wave obliquity, reshaping.

Table of Contents

List of Figures

List of tables

1 Introduction

1.1 Breakwaters overview

Coastal areas are considered highly valuable because of activities and growth opportunities associated with the sea. For instances, major cities have developed along the coasts because of different industries such as fishing, tourism, and trading. Trading via shipping plays a major role in the economy of a country thus; port infrastructure is vital. The benefits of being close to the sea also come with a price. It is as crucial for a port to be protected from wave attack as it is for a recreational beach to be protected from erosion, and breakwaters are a typical structure used for such purposes.

Different breakwater types exist such as, rubble mound (stones, loose blocks), monolithic (concrete caissons), and composite (rubble mound and monolithic combination). Rubble mound is one of the most commonly used breakwaters; the topic of this research lies on the behavior of core material under construction. A typical cross-section of conventional rubble mound is shown on Figure 1.

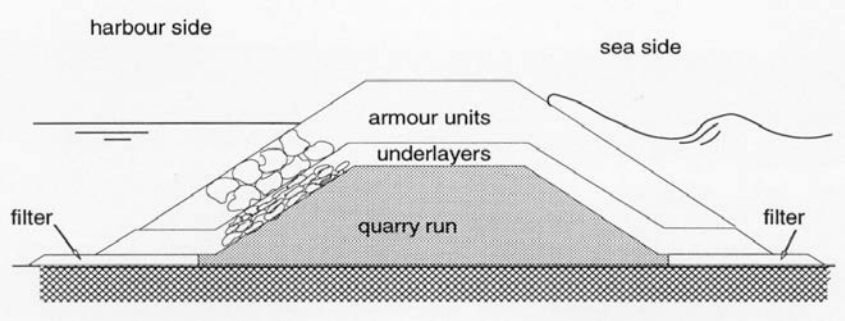

Figure 1 Typical cross-section of conventional rubble mound breakwater (Kennisbank Waterbouw, 2013)

“While these breakwaters are designed to withstand the governing boundary conditions after completion, in the design phase often little attention is given to hydraulic loads during the construction phase” (Mulders P. , 2010) Because of the grading, lack of armoring, and exposure, cores are vulnerable to wave attack. To minimize exposure time, breakwaters might be constructed in work fronts (Figure 2); thus, the exposed end of the breakwater at a given time could be considered a roundhead.

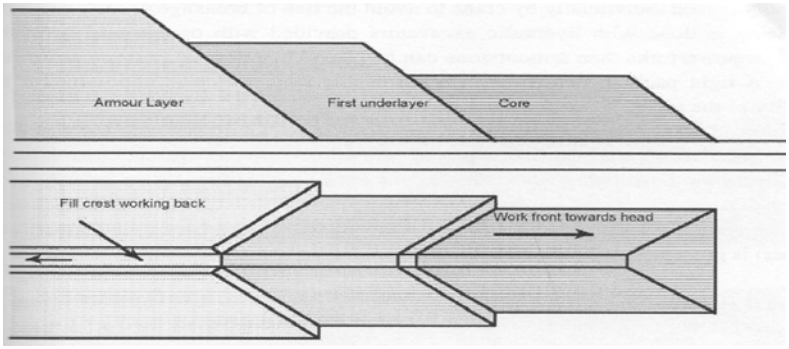

Figure 2 Breakwater under construction work fronts (Verhagen, D'Angremond, & Van Roode, 2012)

Currently, little is known about the roundhead core reshaping but an effort has been made to associate deformation patters with the existing understanding of rubble mound behavior. The goal of this research is to bridge the knowledge gap between deformation and breakwater roundheads under construction.

1.2 Description research

Problem analysis

Breakwaters under construction are prone to undesired deformation because the breakwater core is not designed to withstand severe or moderate wave loads. The reshaping mechanisms for a complete (finished) breakwater have been comprehensively studied; however, few research studies have been undertaken to analyze the deformation mechanisms of the breakwater core (or a breakwater under construction). It is imperative for the contractor to understand how the reshaping takes place because reshaping requires construction schedules to be adjusted as well as additional material and therefore, additional costs. The present study focusses on the deformation rubble mound breakwater roundheads undergo during the construction phase.

Problem definition

Currently, limited information is known about the deformation/reshaping mechanisms the core of a breakwater roundhead made of quarry run suffers when exposed to wave attack.

Research background

This research study is a continuation of a previous MSc thesis completed at TU Delft. In 2010 for his MSc thesis work, Patrick Mulders performed physical model tests to assess the behavior of exposed breakwater trunks (core material consisting of quarry run) with different gradings (D_{85}/D_{15}), wave loading, and angle of wave attack. Using the experimental data obtained by Mulders during physical model tests, a detailed deformation analysis of breakwaters mainly focusing on the roundheads is presented in this report.

Objective

The overall purpose of the research is to provide insight and to bridge the gap in the current knowledge related to the behavior of breakwaters during construction with an emphasis on roundhead deformation. The aim of this research study is to answer the following main research question:

How does the exposed core of a breakwater roundhead (or a breakwater under construction) deform due to wave attack?

With the following research sub-questions:

- Do different material gradings (narrow vs. wide) cause different deformation patterns in the overall breakwater and if so, is this behavior occurring at the roundheads?
- Does the material suffer any changes on its packing density?

- For the roundheads, is there a dominant deformation mechanism such as, cross-shore or longshore transport?
- Do different wave loads (low vs. high wave height) have different impacts on roundhead deformation?
- Do different angles of wave attack (head-on vs. oblique waves) have different impacts on roundhead deformation?
- Do different angles of wave attack have influence the roundhead longshore transport?
- Do different material gradings make an impact on roundhead deformation?
- Is the overwash representative of angle of wave attack?

Approach

The first step was to gain a better theoretical understanding by means of literature review. Therefore, berm breakwater design was introduced including reshaping and roundhead stability. Mulders procedures and findings were studied in detailed; his recommendations were analyzed and all in all, the information was used to draft the problem definition, research questions, and approach to fill the information gap and establish the research beginning.

Because this research is based on previously completed physical model tests, the next step was to acquire the experimental raw data. The data was carefully analyzed prior to any form of data processing. Meanwhile, it was noted that filtering and interpolation were indispensable and the necessary measures were taken. Based on the data available, it was decided a numerical volumetric approach to data analysis was to be taken; thus, the need to specify the control volumes of interest became apparent. Different control volumes were defined and processed, each one with particular objective in mind. After all the data was processed, the results were analyzed by means of comparison and contrasting a variable of interest having the remaining variables fixed. Finally, all the information was gathered and the final research report was completed.

1.3 Report outline

This report proceeds in the following fashion: Chapter 2 provides a literature review, Chapter 3 is a recapitulation of the physical model tests performed by Mulders (2010), Chapter 4 gives an explanation of the data processing completed by the author, and Chapter 6 concludes the finding and provides future work recommendations. In addition, Appendix 7.1 illustrates the roundheads visual schematizations, and Appendix 7.2 provides the complete graphical results for all twelve tests.

2 Literature Review

As previously mentioned, conventional rubble mound breakwaters are commonly used in practice. They consist of a core layer composed of quarry run, followed by underlayers, and outer armoring units (Figure 1). In addition to the conventional rubble mounds, also known as statically stable breakwaters, there is also the reshaping berm breakwater type (consisting of rubble mound as well). A schematic representation of conventional and reshaping rubble mound berm breakwaters are shown on Figure 3.

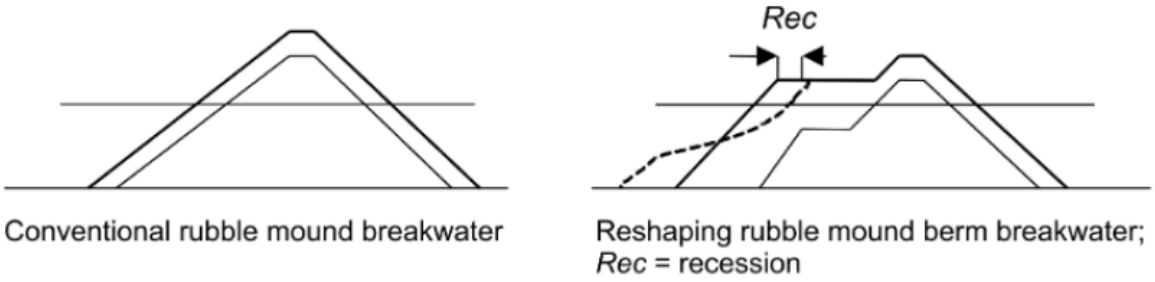

Figure 3 Conventional rubble mound breakwaters and reshaping rubble mound berm (IRIA, CUR, & CETMEF, 2007)

Berm breakwaters are not always statically stable; in fact, "in accordance with the recommendations of PIANC (2003a) – [they can] be divided into three types:

- Type 1: Non-reshaping statically stable, in this case few stones are allowed to move, similar to the conditions for a conventional rubble mound breakwater.
- Type 2: Reshaped statically stable; in this case the profile is allowed to reshape into a stable profile with the individual stones also being stable.
- Type 3: Dynamically stable reshaping; in this case the profile is reshaped into a stable profile, but the individual stones may still move up and down the slope" (IRIA, CUR, & CETMEF, 2007)

As Mulders (2010) points out, "in case of the last two classes extra material is placed on the sea side of the breakwater allowing deformation without jeopardizing the structure itself. Caused by breaking and the following inertia a water mass is driven up the slope. Upon reaching the highest point the water flows back by gravity until elimination by the following wave. Due to this motion grains will be displaced resulting in a possible change of the profile. Material is removed from zones where it is unstable and is relocated into more stable positions. Severe wave attack then leads to reshaping of the outer slope into a more stable S-curve." The S-curve is shown in the dashed line on Figure 3.

The behavior of the breakwater core under construction is comparable to the reshaping mechanism of a rubble mound breakwater. Previous studies have analyzed the stability of rock slopes and berm breakwaters via stability number:

$$H_0 = \frac{H_s}{\Delta D_{n50}}$$

With H_0 *stability number,* H_s *significant wave height,* Δ relative density, D_{n50} median nominal diameter

For instances, Van Hijum & Pilarczyk (1982) developed a model for the dynamically stable profile of gravel beaches with stability numbers between 12 and 35; later, Van der Meer (1988) extended their research to stability numbers ranging from 3 to 250. These researchs studied in detail deformations in the cross-shore direction; since then, a set of parameters are used to described the deformed equilibrium profile: local origin (intersection of the profile and still water level), crest point (upper point of the beach crest), and step point (gentle to steep sloping transition).

The studies mentioned above are based on berm breakwaters or on shingle beaches and even though, they may be comparable to the behavior of breakwater cores, few studies have aimed at the specifics of breakwater core deformation under construction. As pointed out in the previous chapter, in 2010 Mulders completed physical model tests with the objective of getting a "better understanding of the two-dimensional deformation and longshore transport at exposed cores; regarding the influence of grading, wave obliquity and wave load" (Mulders P. , 2010). However, his analysis excluded the roundhead deformation.

Some research has been conducted on roundhead behavior itself: for rock armor by Vidal *et al* (1991) and Matsumi *et al* (2000), for concrete armor units by Jensen (1984) and Maciñeira & Burcharth (2008), and for roundheads during construction by Van Gent & Van der Werf (2011). Refering to Figure 4, Van Gent and Werf (2011) performed physical model tests on temporary roundheads (roundhead in the construction phase with a submerged berm) and on completed roundhead (roundhead with a straight slope to the bottom without submerged berm): "by performing a systematic test program in a wave basin, the stability of rock armor on roundheads during the construction phase [was] studied compared to completed roundheads."

Figure 4 Left completed roundhead, Right temporary roundhead (Van Gent & Van der Werf, 2011)

In closing, although the deformation of berm breakwaters, the behavior of breakwater trunks under construction, and the stability of rock armor on roundheads during construction have been investigated in different occasions, there is an information deficit regarding the deformation of roundhead cores under construction. Thus, the analysis and results presented in this report targets this information shortage and provides ample focus on behavior of breakwater cores under construction when exposed to wave attack.

3 Physical Model Testing

As pointed out, the data analysis and results presented hereto are based on the physical model tests performed by Patrick Mulders during 2009 and 2010 for his MSc Thesis in the Delft University of Technology wave basin. An excerpt from (Mulders & Verhagen, 2012) summarizing the conducted tests will be presented in this section; for further consideration, refer to Mulders' Chapter 3 "Experimental set-up" (Mulders P. , 2010).

"In total 12 tests were executed in which two different gradings were tested: a narrow grading, f_g = 1.3, and a wide grading, f_g = 6 [$f_g = D_{n85}/D_{n15}$ representing stone grading]. Other parameters varied were the wave spectrum, with values for H_{m0} of 0.08m and 0.10m, and the angle of wave attack with values of 0°, 30° and 45°. To keep the different tests apart every test was given a name composed of the values of the varied parameters. In this name the 'N' stands for the narrow grading of 1.3, while 'W' represents the wide grading of 6. The significant wave height is indicated in centimeters. [Table 1] shows the test schedule as executed.

Table 1 Test Schedule

fg = 1.3						fg = 6					
0°		30°		45°		0°		30°		45°	
0.08m	0.10m	0.08m	0.10m	0.08m	0.10m	0.08m	0.10m	0.08m	0.10m	0.08m	0.10m
N-0-8	N-0-10	N-30-8	N-30-10	N-45-8	N-45-10	W-0-8	W-0-10	W-30-8	W-30-10	W-45-8	W-45-10

The breakwater model had a geometrical scale of 1:20 and was divided in a test section consisting of loose stones and a fixed part. The base of the model had a length of 6.7m and a width of 2.2m. Together with a slope of 2:3 and a height of 0.55m this led to a crest width of 0.55m. The radiuses of respectively the crest and the base of the roundhead were 0.275m and 1.1m. In the following drawings (Figure 5, Figure 6, Figure 7), the test section is represented by the hatched part […].

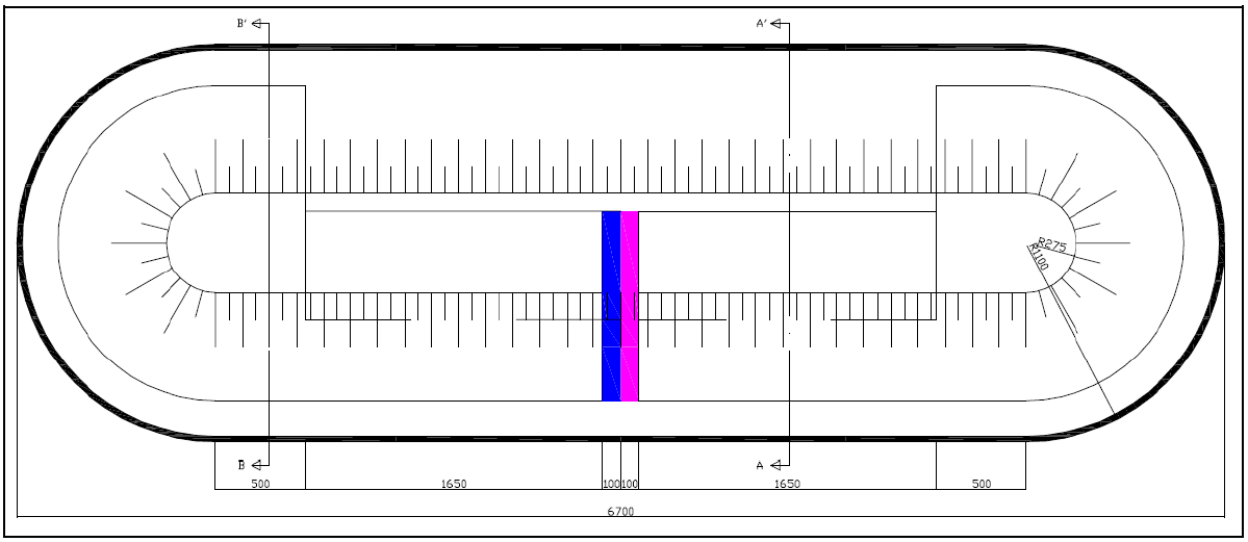

Figure 5 Plan view breakwater model

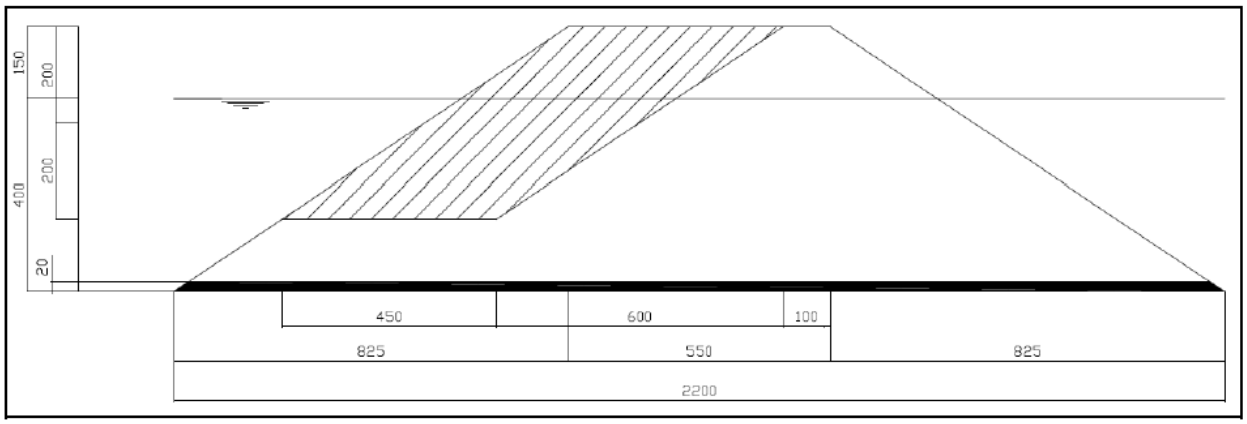

Figure 6. Cross-section A-A

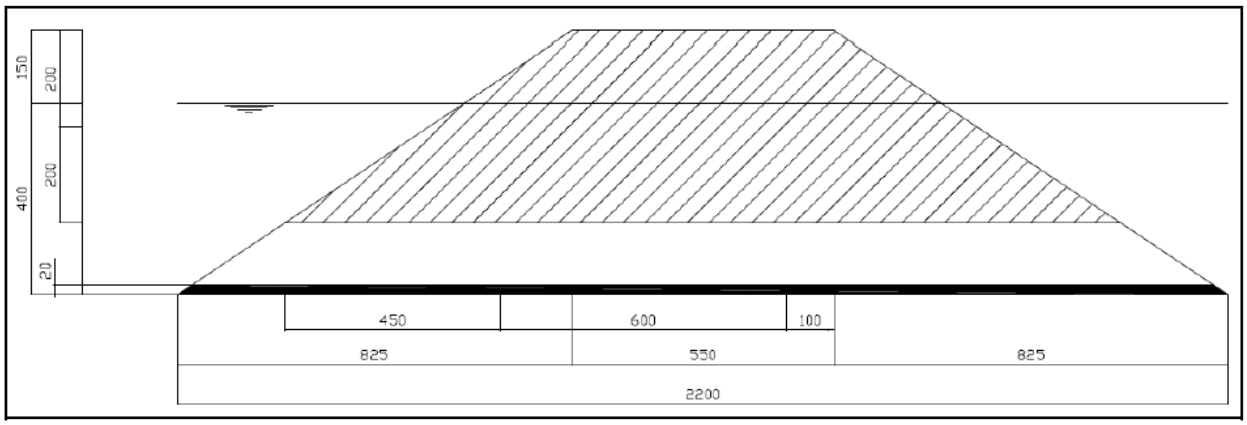

Figure 7. Cross-section B-B

In order to compose the narrow and wide gradings, while keeping the nominal diameter the same at D_{n50} = 12.1mm, five different stone fractions were used. The stone samples were mixed in such a way that the mixtures were representative of respectively armor stone material (f_g = 1.3) and quarry run (f_g = 6). Table 2 shows the characteristics of both mixtures and Figure 8 shows final result on the breakwater model itself.

Table 2. Nominal diameters and weights of narrow and wide grading

Grading	f_g = 1.3	f_g = 6	f_g = 6 (scale factor 20)	W(kg) ($\rho_s D_{n3}$)
D_{n15} (mm)	10.4	5.2	103.7	3.0
D_{n50} (mm)	12.1	12.1	241.6	37.6
D_{n85} (mm)	13.8	31.1	621.7	640.7
D_{n85}/D_{n15}	1.33	6.00	6.00	

Figure 8. Final results of the mixtures on the breakwater model

For the wave load itself two different JONSWAP spectra were generated, in which the significant wave height was varied, H_{m0} = 0.08m and 0.10m, while the fictitious peak wave steepness s_{0p} was kept constant at 0.030. The total durations of the tests were varied for the two different spectra so that the number of waves was the same, approximately 3500 waves. In order to check the actual occurring wave spectra during the tests together with the directional spectrum of the waves, five resistive wave gauges were place in a spatial distribution. The different angles of wave attack were obtained by rotating the model itself. The final test set-up is visualized in Figure 9.

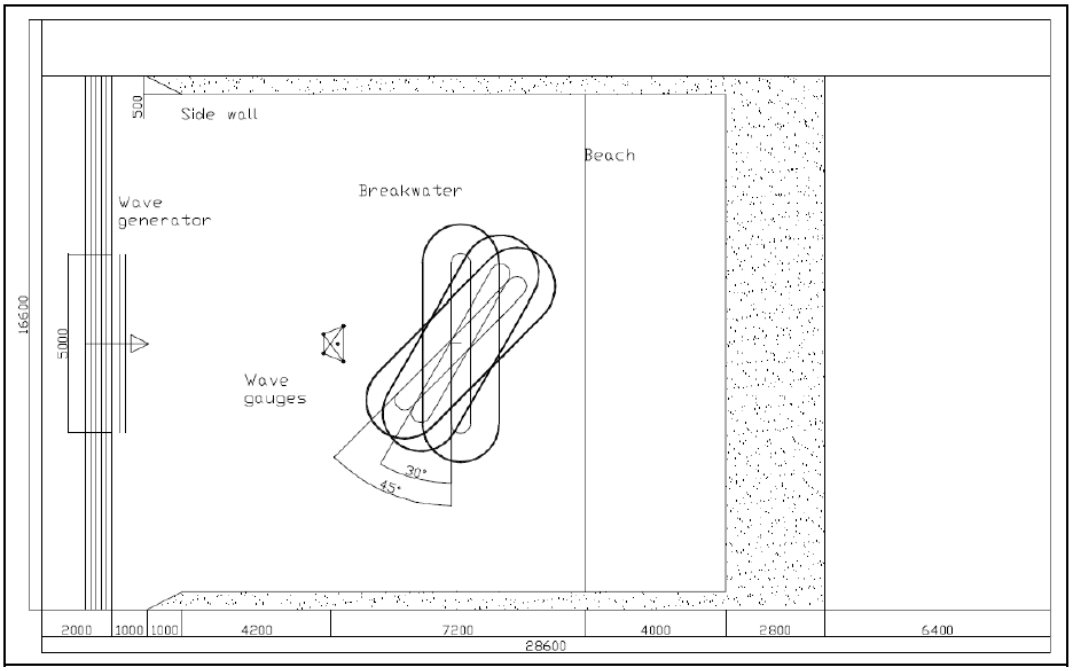

Figure 9 Rotation of breakwater model inside the wave basin

Profile measurements were done both prior to and after the tests by means of laser profiling. The measurements were taken according to the following cross-sectional plan, displayed in Figure 10:

- At the roundhead every 15°
- At the trunk every 0.5m […]

Due to extensive damage additional measurements were sometimes necessary at the roundhead to provide for extra information" (Mulders & Verhagen, 2012).

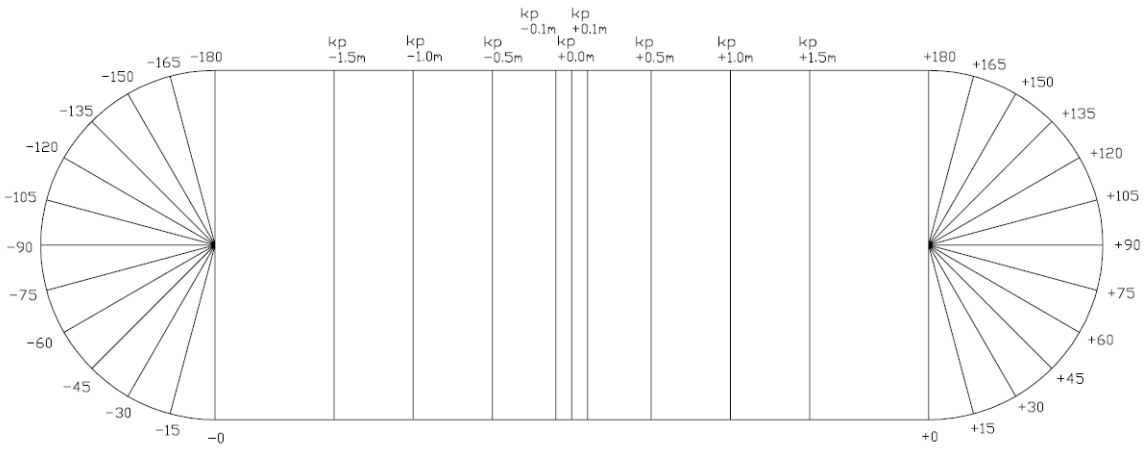

Figure 10 Cross-sectional measuring plan

4 Data Processing

Following Mulders' results from 2010, the raw data was processed to assess the breakwater deformation via a volumetric change approach with an ample emphasis on the roundheads. This chapter describes how the laser profiling data was processed and used in the analyses. Section 4.1 covers the general steps taken to arrive to the volume calculations from the raw data sets, sections 4.2 through 4.4 illustrate the different control volumes used to analyze the volumetric changes of the whole structure, overwash, and the roundheads at the radial and angular level, respectively, and section 4.5 calls out the model limitations.

4.1 General data processing

Based on the work completed by Mulders (2010), for all twelve tests listed on Table 1, laser profiling was recorded for initial and final conditions; meaning, topographic measurements were taken prior and after each test for a total of 24 data sets. For comparison purposes, the raw data sets were converted to a Cartesian coordinate system (x- longitudinal distance from roundhead to roundhead, y- cross sectional distance, z- elevation, all in millimeters). Further data processing was carried out by the author.

Using the plots of all 24 data set (via Matlab), a visual inspection was conducted. It was observed the laser profile had recorded negative elevation as well as off-set elevations with respect to the structure layout; such elevations were considered an instrument error and were filtered accordingly. Negative elevations were initially removed from the data sets; however, it was noted, based on the plot inspections, such elevations actually need to be accounted as zero millimeter readings; thus, the negative z-readings were replaced with a value of zero instead of eliminating them from the data set. On the other hand, the off-set elevations were carefully selected and filtered out of the data set as they were considered noise; see Figure 11 and Figure 12.

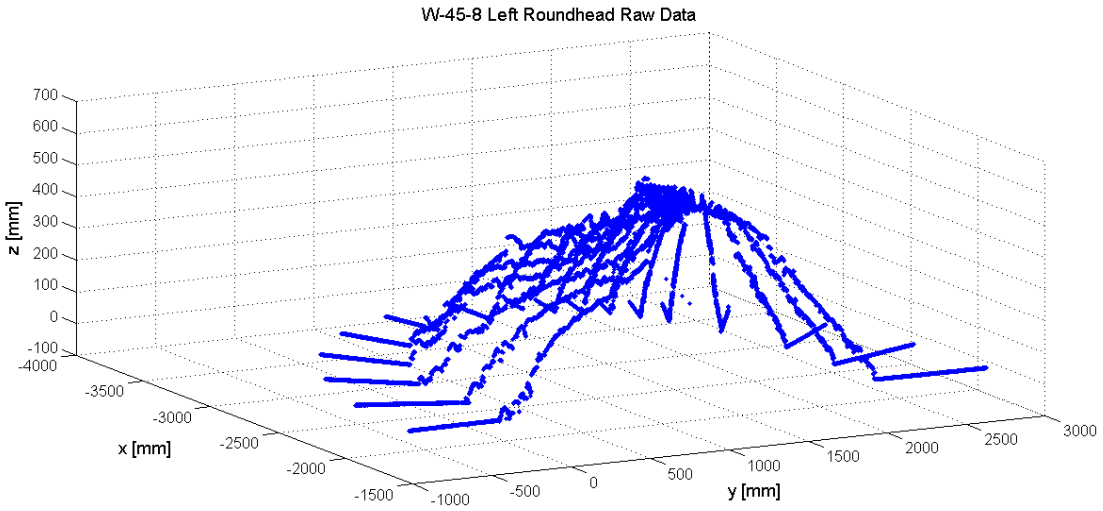

Figure 11 Example of raw data plot

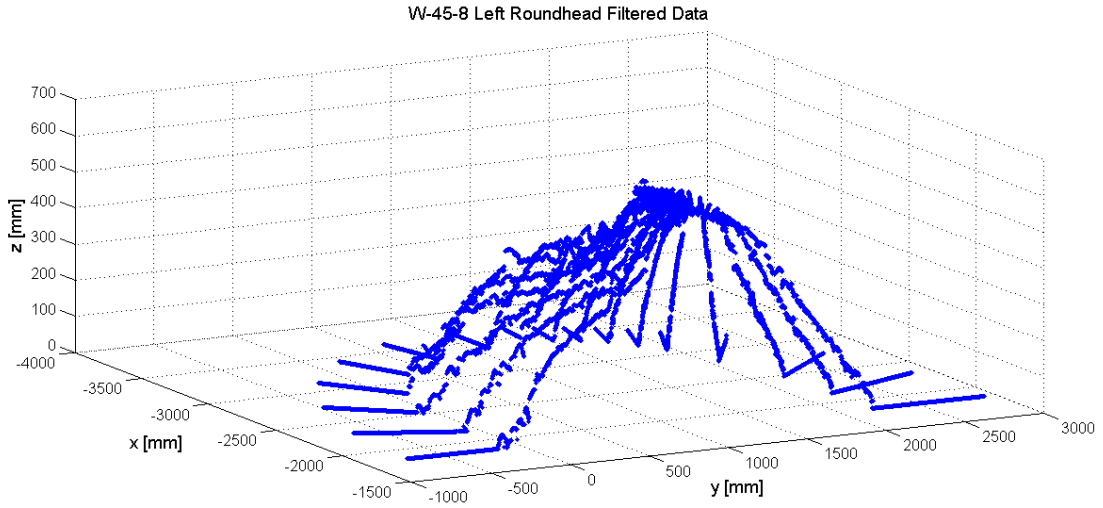

Figure 12 Example of filtered data plot

Additionally as Mulders (2010) points out, the measuring frame was shifted at the roundheads to account for excessive deformation and/or to account for the data corresponding to the first 10 linear centimeters with respect to the measuring frame. This shifting resulted in a relative mismatch of the laser profile transect readings at the roundheads – the x and y components of the initial conditions (in most cases) did not match the final x and y coordinates. Figure 13 exemplifies the structural changes a breakwater may undergo after testing and the necessary measures taken to collect a proper topographical data set: even though the initial structure actual configuration is represented by the red lines (see Figure 5 and Figure 13), the initial and final laser profiling were completed following the blue (frame shifting) and green lines (excessive deformation), respectively. Thus, 3D surface interpolation was conducted to evaluate the elevations corresponding to the predetermined measuring plan Figure 10 (red lines on figure below). In order to optimize software running time, linear interpolation was employed for this purpose, and extrapolation was never considered.

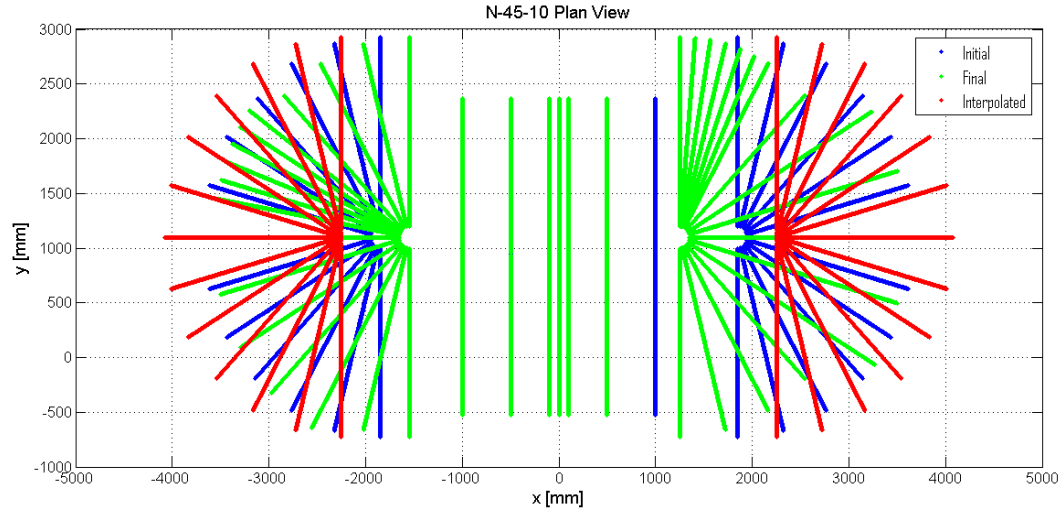

Figure 13. Example of deformed breakwater plan view

Finally, for a given control volume (discussed below), the corresponding filtered ordered triple data sets were interpolated to a regular matrix using the “meshgrid” and “griddata” Matlab commands; the volume between the xy-plane and the encompassed surface was numerically estimated using

the Trapezoidal rule twice, in the x and y directions. The volumetric percentage changes were calculated by the volume difference between the final and initial condition and divided by the initial volume amount:

$$percent\ volume\ change = \frac{volume_{final} - volume_{initial}}{volume_{initial}} \times 100$$

4.2 Overall breakwater control volume

A closed control volume, which included the entire spatial domain of the structure, was used to assess any potential variations in volume of the structure as a unit. In this case, the system is considered closed because no sediment can leave or enter the domain – all the material has been accounted in the topographical data set. Thus, variations in initial and final volumes in a closed system should result from changes in packing density, porosity, and/or sediment sorting mechanisms. Examples of overall breakwater control volumes are illustrated on Figure 14 and Figure 15.

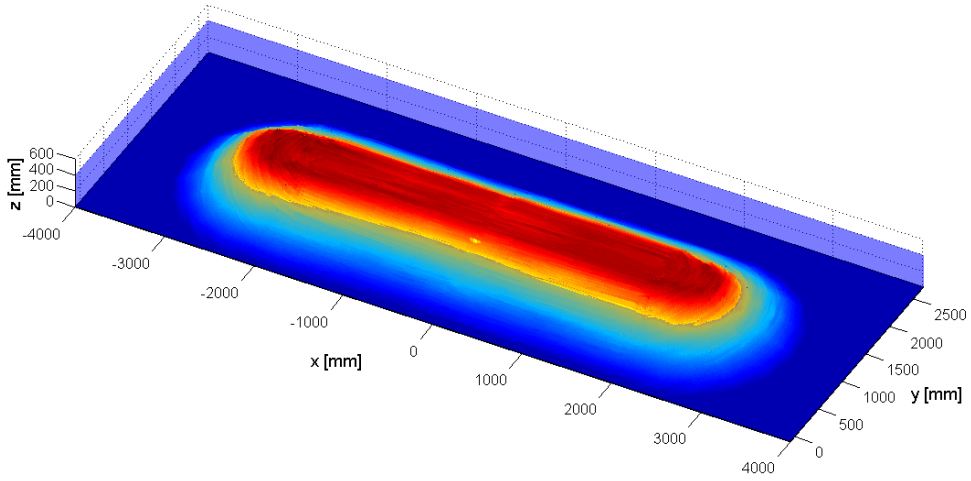

Figure 14 Example of overall breakwater control volume initial condition (W-45-10 Initial)

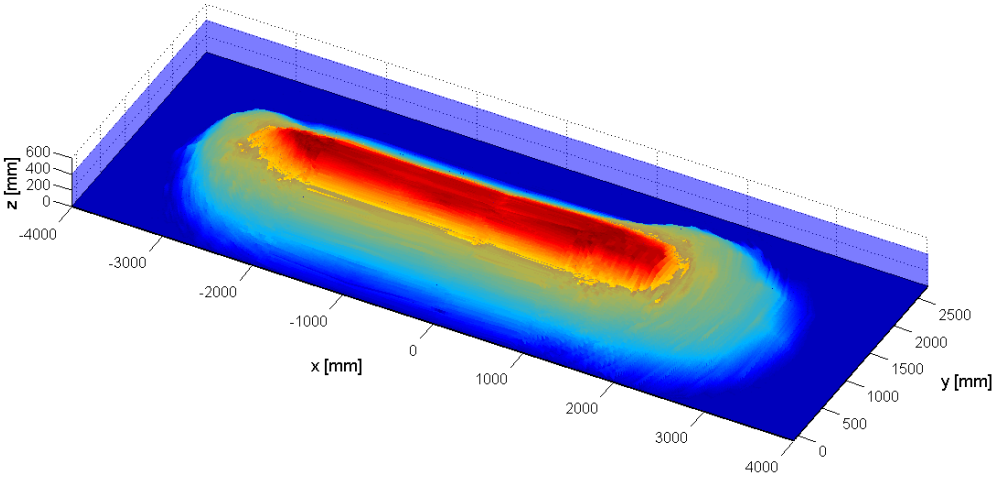

Figure 15 Example of overall breakwater control volume final condition (W-45-10 Final)

4.3 Overwash control volume

In this report, overwash is defined as the amount of material that is deposited on the lee side of the breakwater after the test is completed. The lee side of the structure (region opposite to the area of wave attack) comprises the lee side of the trunk exclusively; this includes the material deposited on the trunk slope (see Figure 16). Moreover, the right and left hand side overwash areas were evaluated separately. The overwash control volume is considered an open system since sediment material can enter the system. The physical model tests were scaled is such fashion that was to minimize the overwash material thus; small overwash amounts were expected for all tests.

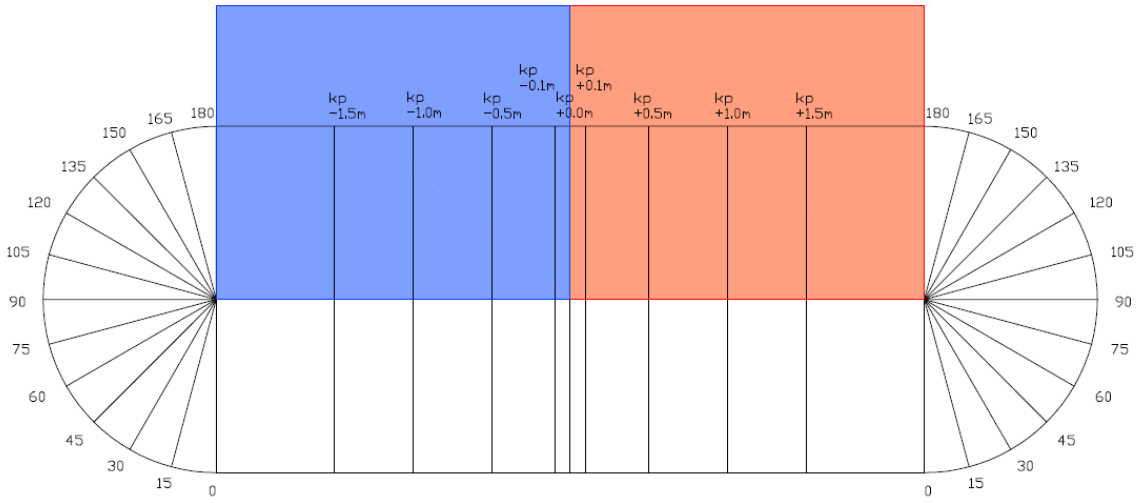

Figure 16 Plan view of left and right overwash control volumes in blue and red, respectively

4.4 Roundhead control volume

The core of this research lies on the roundhead deformation. The left and right hand side roundheads (see Figure 17) were analyzed separately for each of the twelve tests. Because three-dimensional flow patterns dominate the roundhead region, two different methods of sectioning (further explained below) were employed in order to fully analyze volumetric changes: radial and angular cuts. The radial sectioning method represents the cross shore sediment transport (radially outward sediment displacement) while the angular sectioning method showcases the longshore sediment transport (sediment displacement along a circular arc). Moreover, the roundhead control volumes are open systems because depending on the breakwater orientation with respect to the waves, the material may enter or leave the system.

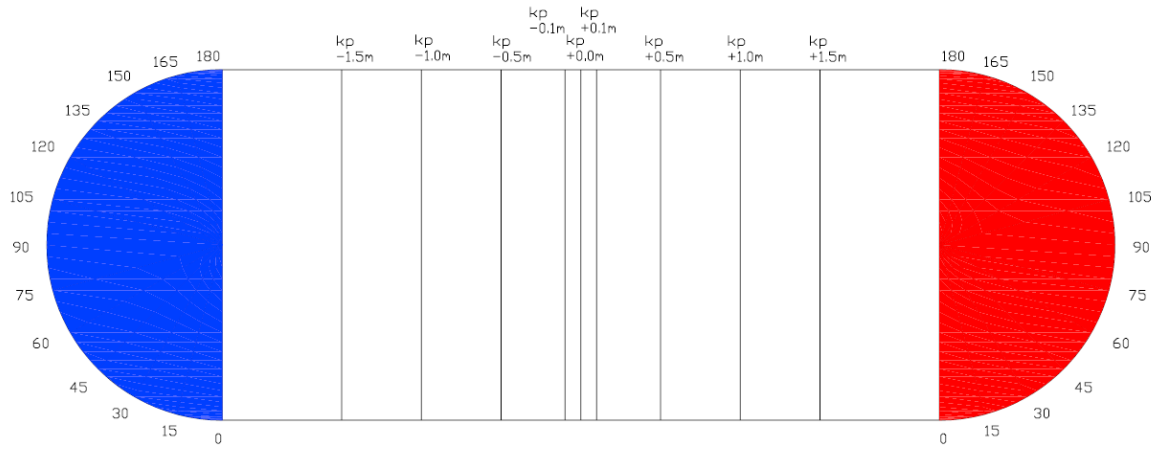

Figure 17 Plan view of left and right roundheads control volumes in blue and red, respectively

4.4.1 Radial Sectioning Method

To analyze the radially outward spread of material, concentric circular sections were taken from the center of the right and left roundheads; this method of sectioning has been defined as “radial.” Two types of radial sections were employed: “cumulative radial” and “radial sector” ranging from a radius (r_i) of 100mm to 1800mm in increments of 100mm (i.e. r_1=100mm, r_2=200mm, r_{18}=1800mm). Cumulative radial (Figure 18) comprises the roundhead region from its center to a given radius, r_i, spanning 0° to 180° whereas; the radial sectors (Figure 19) cover the area bounded in between two consecutive r_i radii with a span of 0° to 180°. To further clarify, the radial sectioning methods are presented in the figures below.

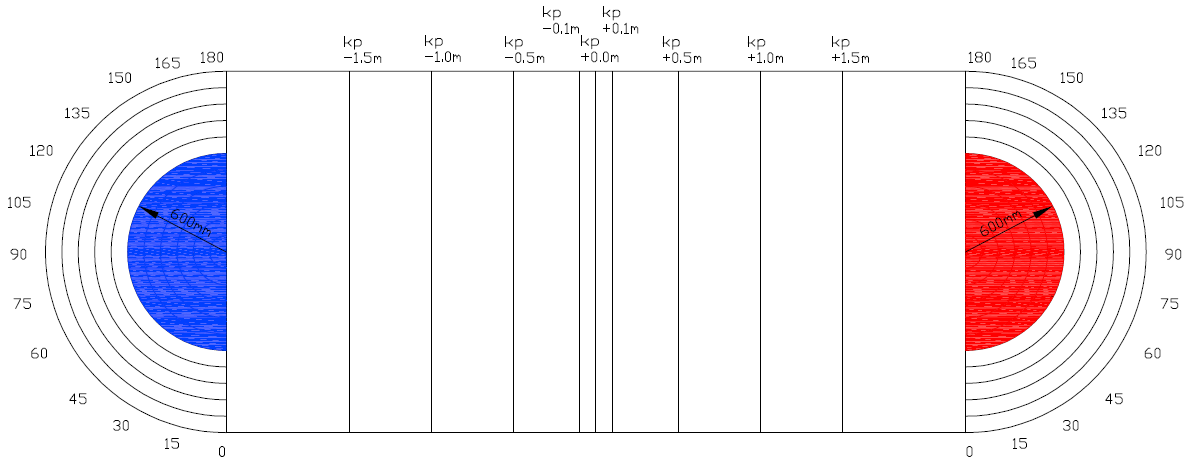

Figure 18 Example plan view of r =600mm cumulative radial sections for left and right roundheads (blue and red)

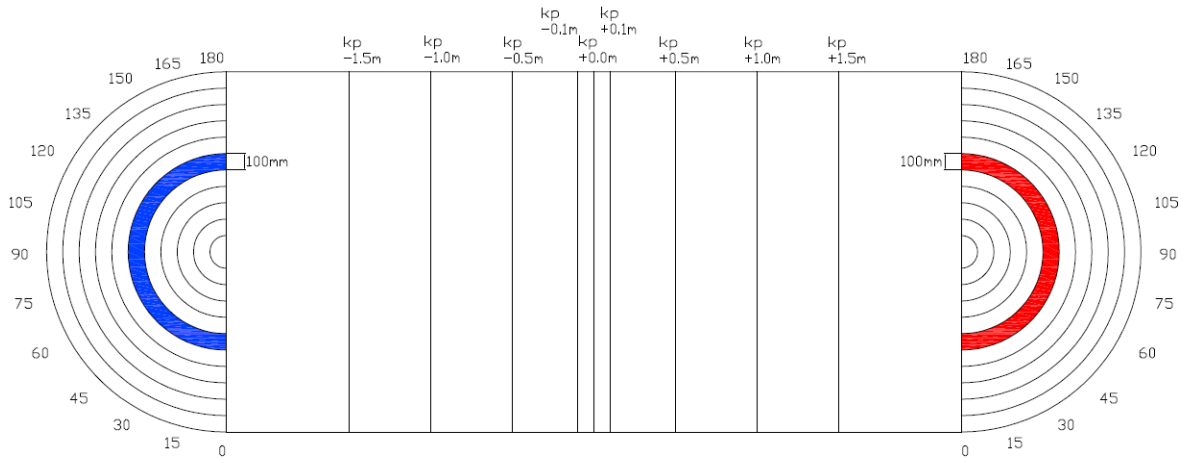

Figure 19 Example plan view of r =600mm radial sectors for left and right roundheads (blue and red)

Since the volumetric changes in the radial sections are an indicator of the radially outward displacement of material (Figure 20), the results should relate to the typical S-curve deformation profile (Figure 3) specifically, at the S-curve inflection point. Thus, the aim of this sectioning method is to investigate at what radius the roundhead stops loosing and starts gaining volume, which portrays a deforming mechanism of the structure.

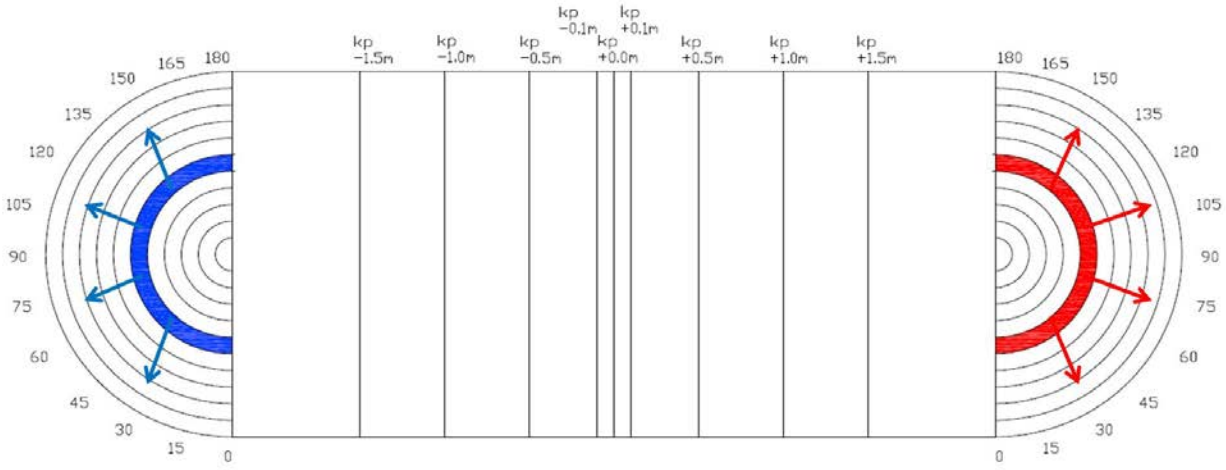

Figure 20 Schematization of potential radially outward displacement of material at roundheads

4.4.2 Angular Sectioning Method

To analyze the angular displacement of material, concentric angular sections of equal radii were taken from the center of the right and left roundheads; this method of sectioning has been defined as “angular.” Similar to the radial sectioning, two types of angular sections were considered: “cumulative angular” and “angular sector” ranging from 0° to 180° in increments of 15° (i.e. α_1=15°, α_2=30°, α_{12}=180°). Cumulative angular (Figure 21) comprises the roundhead region from 0° to a given angle, α_i, with a fixed radius of 1200mm; whereas, the angular sectors (Figure 22) cover the area bounded in between two consecutive angles α_i with 1200mm as a fixed radius. To be conservative and minimize errors, 1200mm was chosen over 1100mm for the radius (see Figure 1) in order to

account for the material which has reached beyond the initial breakwater physical model. To further clarify, the angular sectioning method is presented in the following figures.

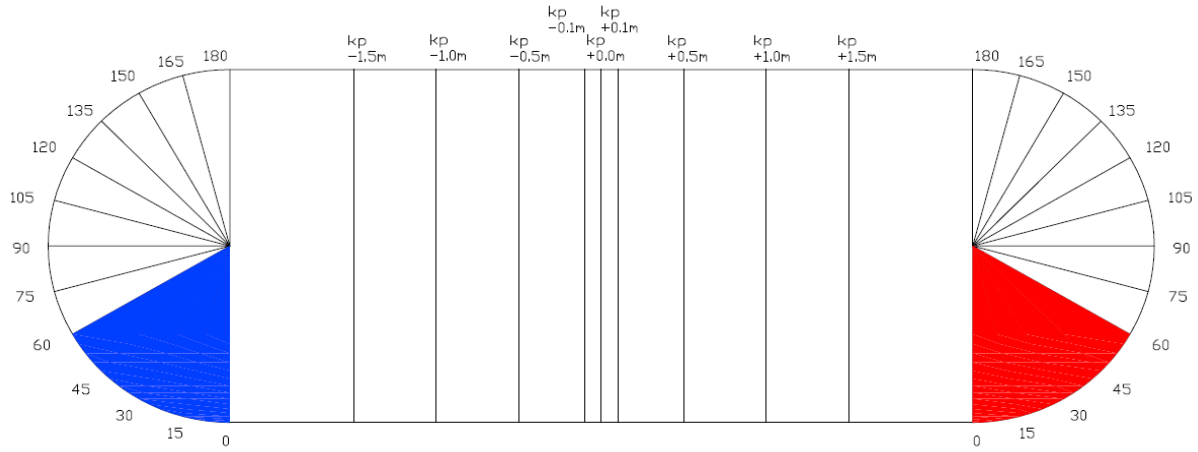

Figure 21 Example plan view of 60° cumulative angular sections for left and right roundheads (blue and red)

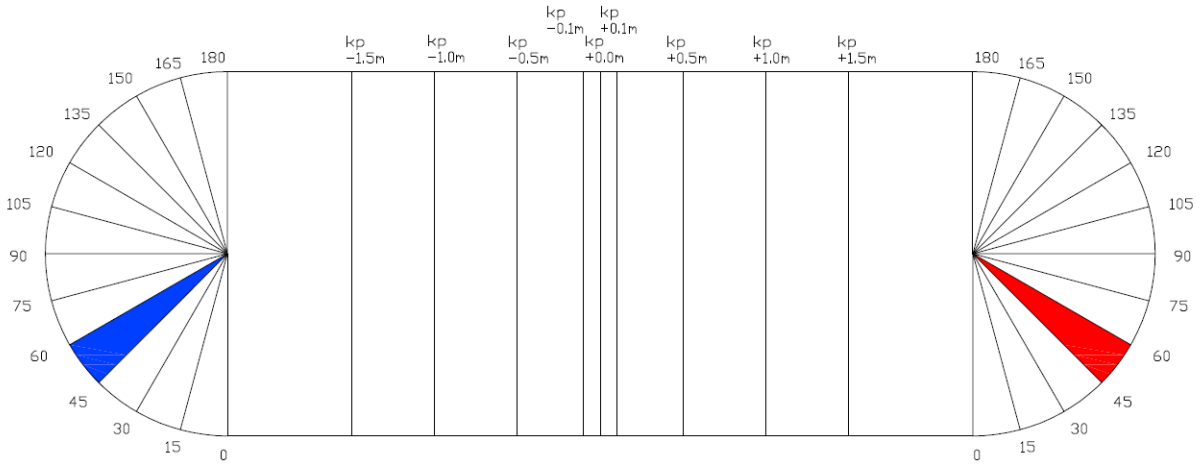

Figure 22 Example plan view of 60° angular sectors for left and right roundheads (blue and red)

Since the volumetric changes in the angular sections are an indicator of the angular displacement of material (Figure 23) and therefore longshore transport, the influence of wave attack angle, if any, should reflect on these results. The aim of this sectioning method is to investigate at what angle the roundhead stops loosing and starts gaining material, which is another mechanism of deformation.

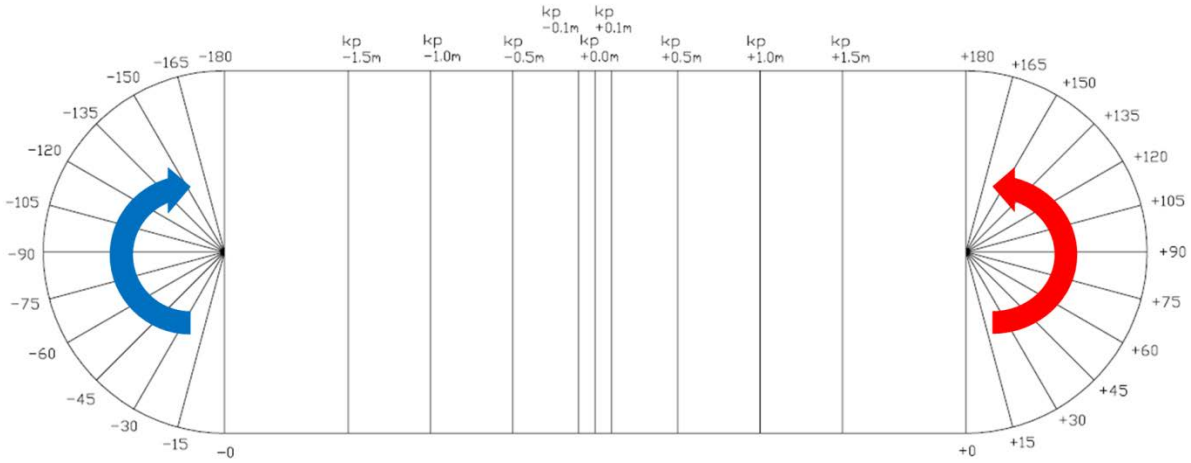

Figure 23 Schematization of potential angular displacement of material at roundheads

4.5 Model limitations

Because the results presented hereto are based on the volume changes which in turn are calculated from the experimental topographical data, the model limitations and its associated errors are strongly related to the accuracy of the collected data sets. As pointed out by Mulders (2010), the laser beam profiling standard error has been considered negligible ($\pm 5 \times 10^{-5}$m); however, the shifting of the frame where the beam is mounted does introduce errors to the system since it was manually shifted. Also, the distances in between cross-sections were measured using a conventional measuring tape: “placing this frame both prior and after every test could lead to slight deviations; especially as the frame had to be shifted again from the original location due to extensive deformation of the roundhead.”

5 Results and Analysis

As previously explained, the structural deformation analysis has been accomplished by means of comparing the calculated volume for a given control volume before and after testing. In this study, structural damage has been defined as the loss of volume (or negative percent change) with respect to its original configuration; thus, the larger the negative percent change, the larger the damage. It is important to point out volumetric percent change will be referred to as "percent change." This chapter is divided into three sections covering the overall breakwater deformation, overwash amounts, and roundhead behavior. The main focus of this study lies on roundhead deformation at section 5.3.

5.1 Overall breakwater

Table 3 shows the results corresponding to the initial and final overall breakwater volumes and their respective percentage change. The before and after surveys were performed in such a way that all the material was accounted in the laser profiling domain; meaning, the percentage change in mass should be equal to zero. However, the percentage change in volume may not necessarily be zero since changes in soil packing and porosity are expected to take place.

Table 3 Overall breakwater volume results

	Test	Initial volume [x10^9 mm^3]	Final volume [x10^9 mm^3]	% change
Narrow	N-0-8	4.368	4.341	-0.6218
	N-0-10	4.464	4.459	-0.0943
	N-30-8	4.481	4.478	-0.0654
	N-30-10	4.485	4.481	-0.0825
	N-45-8	4.493	4.492	-0.0330
	N-45-10	4.521	4.521	-0.0003
Wide	W-0-8	4.536	4.546	0.2216
	W-0-10	4.545	4.546	0.0220
	W-30-8	4.532	4.536	0.0891
	W-30-10	4.535	4.541	0.1183
	W-45-8	4.522	4.517	-0.1041
	W-45-10	4.498	4.501	0.0760

When looking at Table 3, it can be noted the percentage change for all tests are less than one percent. Even though small variations in the percent change magnitude were obtained, consistent tendencies can be found, aside from the W-45-8 test data point. A clear distinction is observed between the narrow and wide grading: narrow grading exhibits a loss in volume while wide grading displays an increase in volume. Since all the material was accounted in the measurements (closed control volume), these volumetric changes are not only dependent on sediment transport mechanisms but they are also the result of material sorting and changes in packing density.

Porosity is defined as the ratio of the volume of the pore space to the total volume of the soil; “when the porosity is small the soil is called densely packed, when the porosity is large it is loosely packed” (Verruijt, 2010). It was expected for the wide grade material to have a large porosity before testing. When the porosity is high, the voids can be filled with the finer material; therefore, a more densely packed soil configuration (negative volume change) was expected for the wide graded material. Counterintuitively, after testing the volumes increased for the wide graded tests indicating an evidence of a sorting or segregation mechanism.

Mulders (2010) described in a conceptual model the sediment transport based on segregation due stone displacement: “during the tests with the wide grading a clear segregation of the mixture occurred for transverse direction as well as the longitudinal direction. In the initial phase the coarsest fractions proved to be the most unstable thereby dominating the transport as result of gravity in mainly transverse direction. [...] For smaller fractions a different situation occurred. In this case stones were transported in the direction of wave run-up and run-down resulting in a large transverse displacement as well as a longer transport distance in longitudinal direction. […] The finer the material, the larger the scale on which this process occurred.”

Table 3 results quantitatively prove Mulders’ conceptual model where non-uniform sorting mechanisms take place throughout the structure and they are dependent on the material grading. The wide grading material is characterized by the coarsest fraction which causes an increase in volume due to the transverse movement of the coarsest fraction. On the other hand, the narrow grading, which is associated with the finer fraction, decreases in volume indicating a soil compaction and therefore a porosity reduction. A plausible explanation concerning the deviation of W-45-8 test could potentially be attributed to measurement errors.

5.2 Overwash

As previously explained, the overwash refers to the material deposited on the lee side of the breakwater trunk due to 3D flows taking place at and around the roundheads.

Table 4 presents the overwash results which include the left and right overwash percent volume with respect to the initial overall breakwater volume. As shown, the overwash amounts are quite low having 1.95% volume as the highest value corresponding to the W-45-10 test. Small overwash percent volumes are expected because the physical tests had been set up in such a way for the overwash to stay at a minimum; nonetheless, the calculated values are indeed indicators of the direction of sediment transport.

Table 4 Overwash volume results

Narrow		Overwash [x10^{4}mm^3]	% volume	Wide		Overwash [x10^{4}mm^3]	% volume
N-0-8	Right	908.3	0.21	**W-0-8**	Right	717.1	0.16
	Left	240.1	0.05		Left	650.2	0.14
N-0-10	Right	2387.9	0.53	**W-0-10**	Right	1635.6	0.36
	Left	4168.9	0.93		Left	3375.6	0.74
N-30-8	Right	1951.2	0.44	**W-30-8**	Right	1741.2	0.38
	Left	2.3	0.00		Left	-189.6	-0.04
N-30-10	Right	8254.9	1.84	**W-30-10**	Right	4052.5	0.89
	Left	66.7	0.01		Left	-801.2	-0.18
N-45-8	Right	2643.2	0.59	**W-45-8**	Right	4375.6	0.97
	Left	-274.8	-0.06		Left	101.8	0.02
N-45-10	Right	8669.8	1.92	**W-45-10**	Right	8754.9	1.95
	Left	-336.9	-0.07		Left	185.6	0.04

A somewhat symmetrical response between the left and right overwash was observed for tests with 0° angle of wave incidence; in such cases, both left and right overwash volumes are greater than zero as expected. For the tests where the angle of wave incidence was 30° and/or 45°, the right roundhead (highest exposure to wave action) overwash volumes were always larger than zero with increasing percent volume as the hydrodynamic loading increased (angle of incident and have height) with the exceptions of the N-30 tests.

On the other hand, the tests corresponding to the left roundhead for oblique waves, which was the most sheltered roundhead from wave action, produced values close to zero as well as negative values. Because the left roundhead is sheltered and the sediment transport occurs along the direction of wave incidence, the left overwash should be close to zero. This situation has been reflected on tests N-30-8, N-30-10, W-45-8, and W-45-10. Negative volumes are considered physically impossible thus; for the remaining tests, negative values can be potentially explained through measurement errors or with the possibility of lee side glued material detaching from the breakwater during testing.

Overall, the tests with the largest wave heights produced the largest overwash volumes and no clear trend could be assessed concerning the relation between the wide and narrow grading material. Finally, as expected for the oblique wave attack, the right and left overwash tests exhibit positive and zero volumes, respectively.

5.3 Breakwater roundheads

The main focus of this study lies on roundhead deformation; such analysis has been accomplished by means of comparing a variable of interest —wave height, angle of wave attack, or grading, while keeping the other ones constant for different test results. This section presents a detailed analysis regarding the influence each variable has on the deformation of roundheads. The sub-chapter has

been divided into three parts: symmetry considerations, deformation analyses based on radial, and deformation analyses based on angular methods of sectioning.

5.3.1 Symmetry considerations

A nearly symmetric behavior with respect to the deformation of left and right roundheads was expected for the tests having 0° as the angle of wave attack. Nonetheless, small percent change differences between left and right roundheads were observed when the angle of wave attack was indeed 0°; thus, a fully symmetric response did not characterized any of test. The response was however considered nearly symmetric for 0° because the variations between left and right roundhead are negligible when comparing them to the roundhead responses for 30° and 45° wave attack angles — in such cases a clear distinction between left and right roundheads dominates.

In the case of radial sectioning, a higher percentage change was observed on the left than on the right roundheads as seen on Figure 24 (left and right roundheads indicated with respective by dashed and solid lines); the overall greatest difference in percent change was (left minus right percentage change) 4.63% from the W-0-10 test. By the same token with regards to the angular sectioning (Figure 25), similar behaviors were observed for left and right roundheads deformation. In this case however, the variations in percentage change between left and right roundheads were noticeably higher compared to the radial sectioning method; the greatest observed difference between left and right roundheads was 11.86% corresponding once again to the W-0-10 test.

Overall, a quasi-symmetrical behavior is seen between the left and right roundheads for an angle of wave attack equal to 0°. The left roundhead does however exhibit an overall greater percentage volume change when compared to the right roundhead in the radial as well as angular sectioning methods. The cause of this difference is unknown but since it was consistent throughout all the tests, it might be attributed to uneven wave impacts possibly originating from the wave maker.

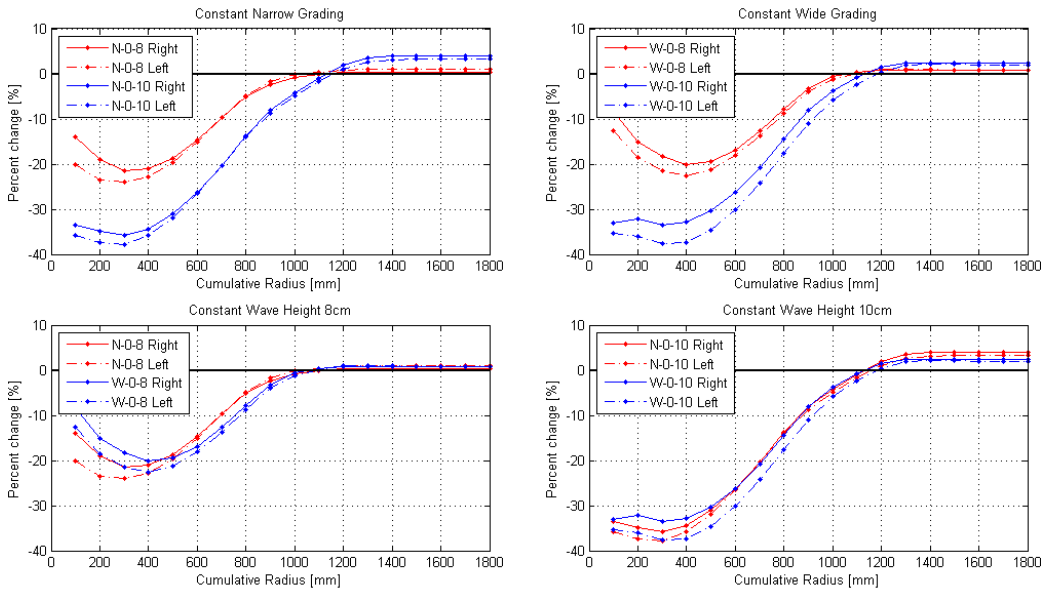

Figure 24 Symmetry considerations for left and right roundhead - radial sectioning

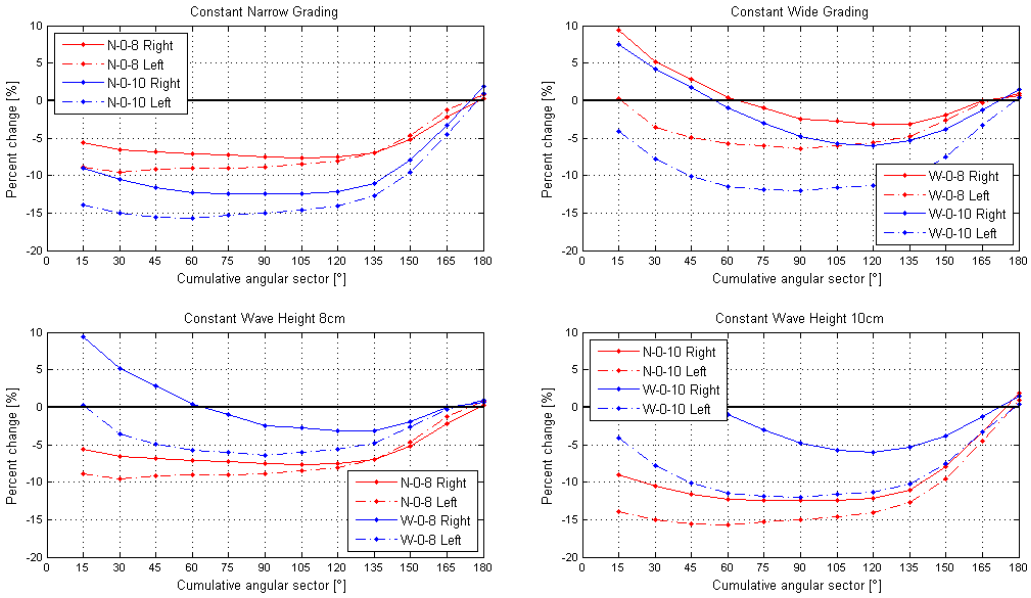

Figure 25 Symmetry considerations for left and right roundhead - angular sectioning

5.3.2 Radial Sectioning Method Results

This section is dedicated to the radial sectioning method results with an emphasis on the oblique angle of wave attack tests since symmetry considerations have already been discussed. Cumulative radial results were used to assess the overall roundhead behavior while radial sectors indicated the outward radial spread of material. Since this analysis aims at the volume loss, and the initial breakwater roundheads covered a radius of 1100mm (Figure 5), for conservative purposes the results presented hereto will adhere to an upper limit radius of 1200mm. Appendix 7.2 shows the results corresponding to radii larger than 1200.

A key indicator in this analysis is the “transition radius” which has been defined as the radial sector where the roundhead transitions from losing to gaining volume (from negative to positive percent change).

Influence of wave load - radial

In Figure 26, for the right roundheads the percentage change for the low (8cm) and high (10 cm) wave height are compared in red and blue lines, respectively. To isolate the wave load (or wave height) influence, the grading and angle of wave attack have been kept constant.

It is clearly evident for all tests, the higher wave load caused a greater volume loss (negative percent change) at the same 300mm radial sector. Also, with the exception of N-45-8/10 tests (lower left panel), a higher wave load produced larger volume gains at the outer radii. Moreover, similar percentage losses were observed for narrow and wide grading test while the percentage gain increased for wide grading material. This observation is in line with the sorting mechanism described in section 5.1.

With regards to the transition radius, the wave load did have an impact: as the wave load increased, the transition radius also increased. This increment in transition radius was more noticeable for narrow than for wide grading. Remarkably, this transition could be considered a parallel phenomenon to the S-curve reshape occurring at the breakwater trunk (see Figure 3); consequently, larger transition radii would relate a wider S-curve.

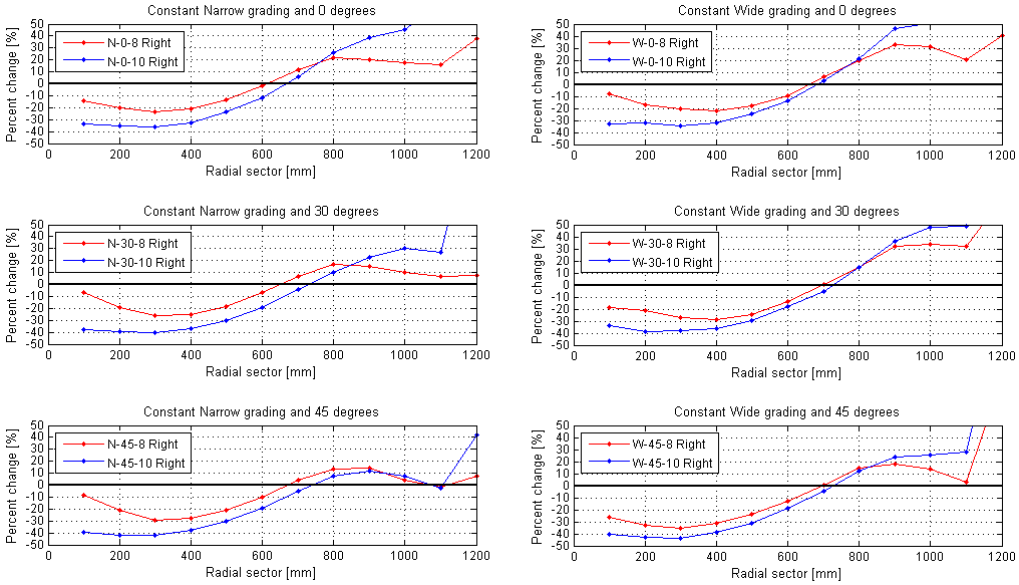

Figure 26 Wave load influence on right roundhead - radial sectioning

Referring to Figure 27, the left roundhead is sheltered since it is the least exposed to wave action due to its orientation. In general, higher wave loads caused a larger deformation either by volume gain or loss. On the other hand, the wave load did not seem to influence the transition radius location to a large extent; only a slight increase in transition radius was seen for larger wave loads but not comparable to the right roundhead results.

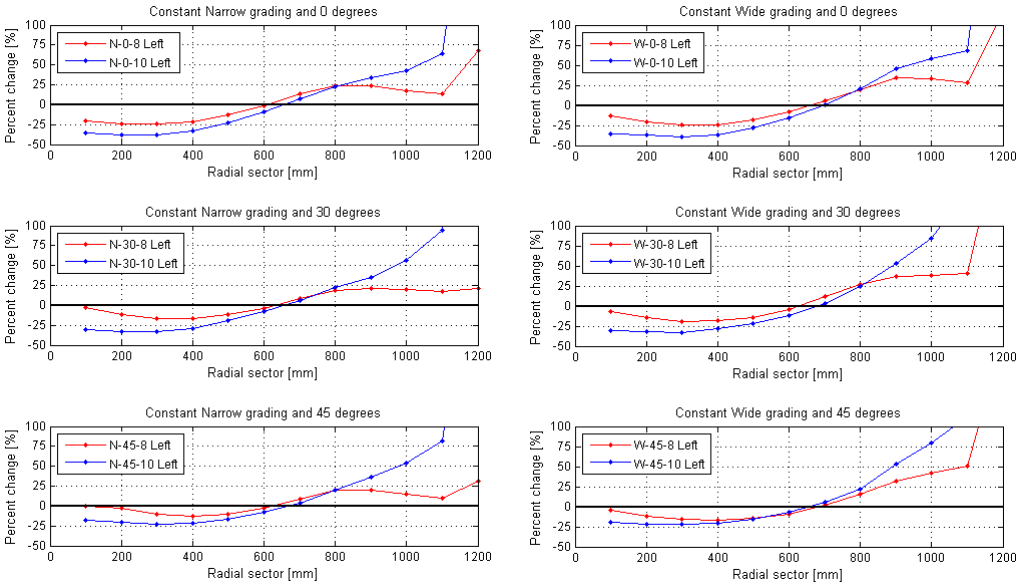

Figure 27 Wave load influence on left roundhead - radial sectioning

Influence of angle of wave attack - radial

Since the angle of wave attack determines the direction of sediment transport, the main distinction between the right and left roundheads is given by such angle. Table 5 gives a summary of the overall left and right roundhead behaviors based on the angle of wave attack independently of grading and wave load. For further considerations, refer to percent changes in cumulative volume shown on Appendix 7.2.

Table 5 Angle of wave attack summary

Angle of wave attack	Left roundhead	Right roundhead
0°	Gain	Gain
30°	Gain	Loss
45°	Gain	Loss

As shown, the left roundhead always accreted while the right roundhead eroded for oblique wave attacks. Since both roundheads had a positive percent change at the outer most radius while exposed to head-on waves; the volume increase could have originated at the trunk. This observation is also supported by Mulders' longshore transport results (2010). The eroded material from the right roundhead could have either been deposited at the trunk, at the left roundhead, or outside the control volume (radius greater than 1200mm). At this point, it is not feasible to assess the origin of the accreted left roundhead material, and pertinent recommendations are made in the next chapter.

In Figure 28, the right roundheads percentage change for the 0°, 30°, and 45° angles of wave attack are compared in green, red, and blue lines, respectively. To isolate the angle of wave attack influence, the wave load and grading have been kept constant. As the angle of wave impact increased, so did the percent loss; in parallel, the largest percent gain occurred for head-on waves (with the exception of 30°, wide grading, 8cm wave height test). Also, the percent gain magnitudes were higher than the percent loss. Thus, it can be inferred the percentage loss at the roundhead is proportional to the angle of wave attack since oblique waves generate longshore transport.

The transition radius seemed to be nearly constant for oblique wave attack occurring in between 700mm and 750mm (with the exception of narrow grading and low wave load). However, for head-on wave attack, the transition radius reduced. Overlapping result plots indicated identical radial response independent of wave attack between the radii of 500mm to 800mm.

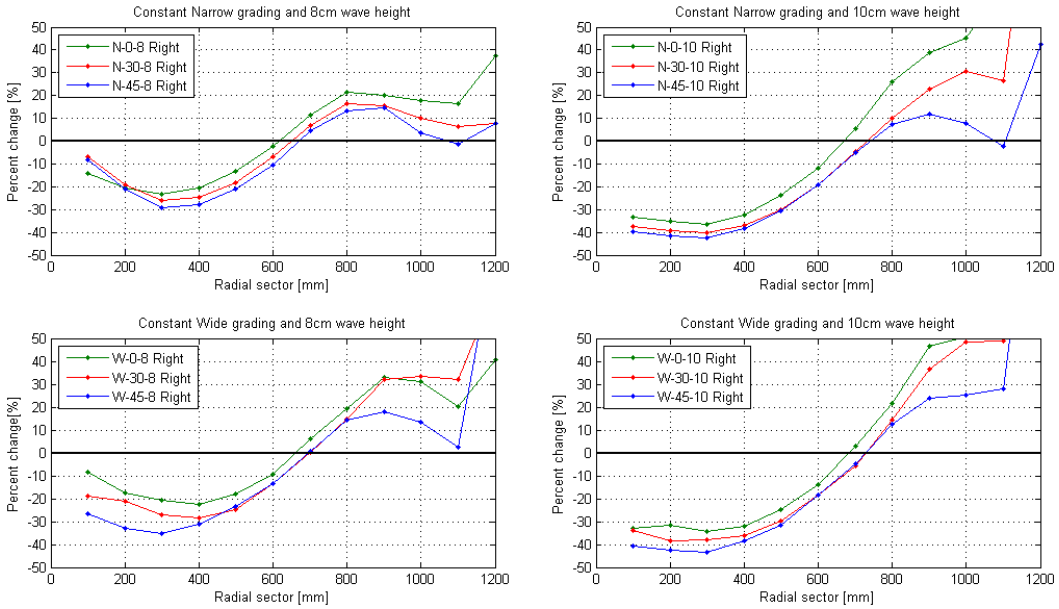

Figure 28 Angle of wave attack influence on right roundhead - radial sectioning

Figure 29 exhibits the difference in behavior between the left and right roundheads. For the left roundheads, as the angle of wave impact increased, so did the percent loss. However from the test results, no clear influence of wave impact angle on accretion can be found. For higher wave loads, the 30° tests appear to accrete more than the 45° followed by the 0°; this result is in line with Mulders' findings at the trunk (2010). It is difficult to draw conclusions regarding the transition radius but similar responses were obtained when comparing the higher wave load tests. In such cases, the plots overlap close to the 0 percent change which could be interpreted as a constant transition radius for a fixed set of conditions.

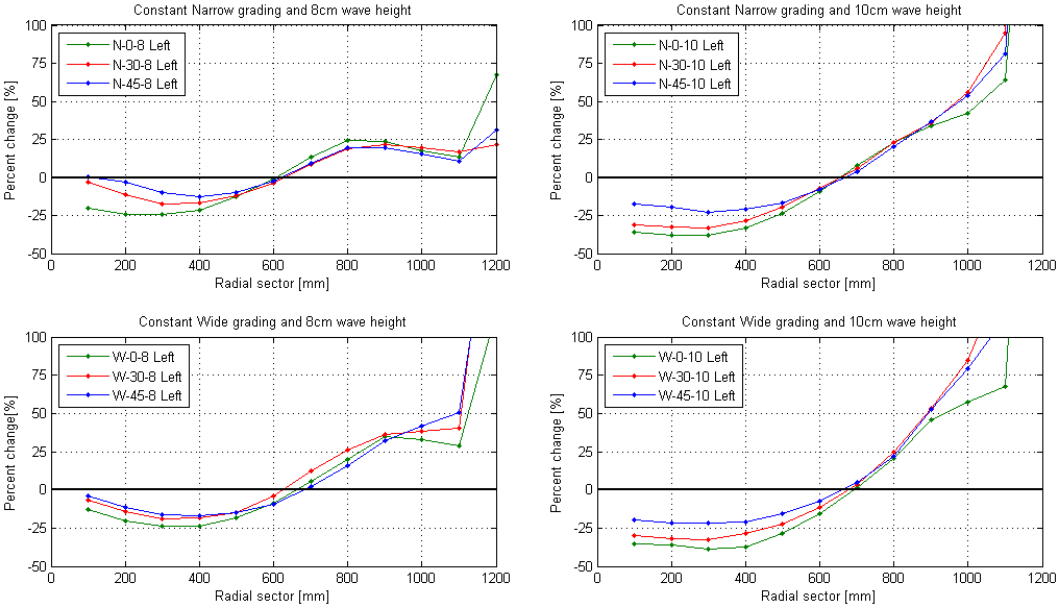

Figure 29 Angle of wave attack influence on left roundhead - radial sectioning

Influence of grading - radial

In Figure 30, for the right roundheads the percentage change for narrow and wide are compared in red and blue lines, respectively. To isolate the grading influence, the wave load and angle of wave attack have been kept constant.

Strikingly similar plots are observed for higher wave loads. In these cases (the panels on the right), a nearly identical behavior was observed from radii 100mmm to 700mm, which included the transition radii. Thus, for higher wave loads, grading did not have an impact on volume loss but rather on volume gain. In the outer breakwater radial sectors, the wide graded material gained more volume than narrow grading which is an indicator of the coarse fractions rolling radially outward and therefore downwards on the right roundheads. This apparent material gain, which is in fact an increase in volume, could be interpreted as a decrease in packing density —instead of the finer fractions filling the gaps form the coarse fractions, the coarse fractions rolled down slope increasing the radial sector volume.

Looking at the low wave loads (panels on the left), a volume loss trend did not seem evident. Higher volume gains were observed for wide than for narrow material starting from the 800mm radial sector (in the same vicinity for the higher wave load). In general for all tests, the wide grading roundheads had a higher volume increase than the fine grading.

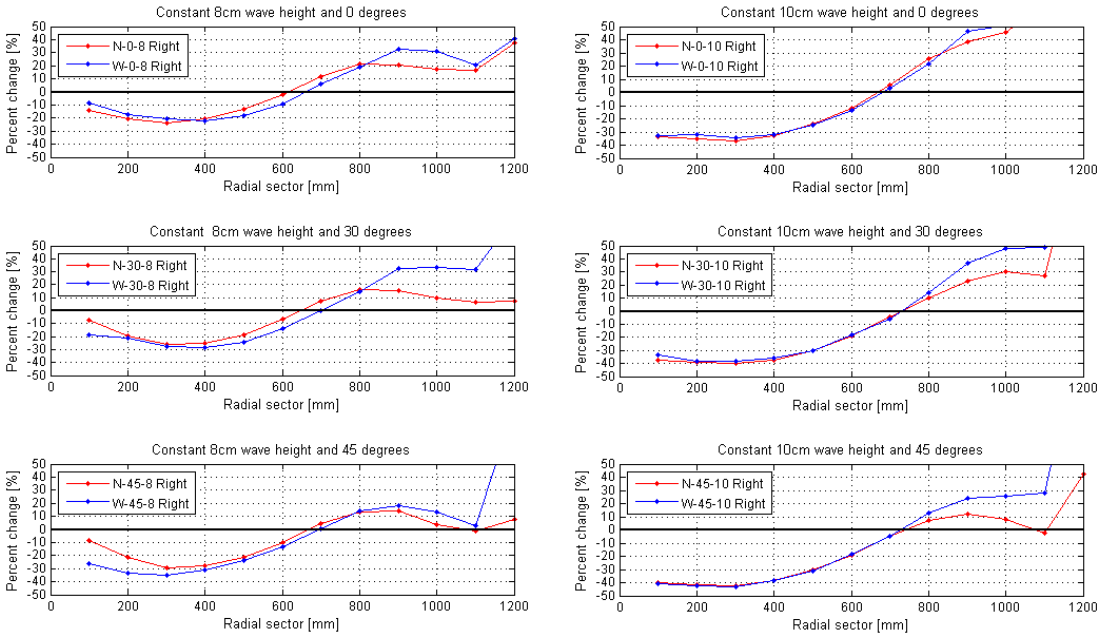

Figure 30 Grading influence on right roundhead - radial sectioning

Figure 31 presents the left roundhead results and for all tests, and it shows a similar pattern to the right roundhead tests results with high wave load (right panels): similar, if not equal, percent loss for narrow and wide grading, and more accretion at the outer radial sectors for wide graded material. These results once again confirm the non-uniform sorting mechanism in which coarser fractions are displaced downslope potentially decreasing in packing density. Lastly, no clear trend is visible with regards to the left roundhead transition radii.

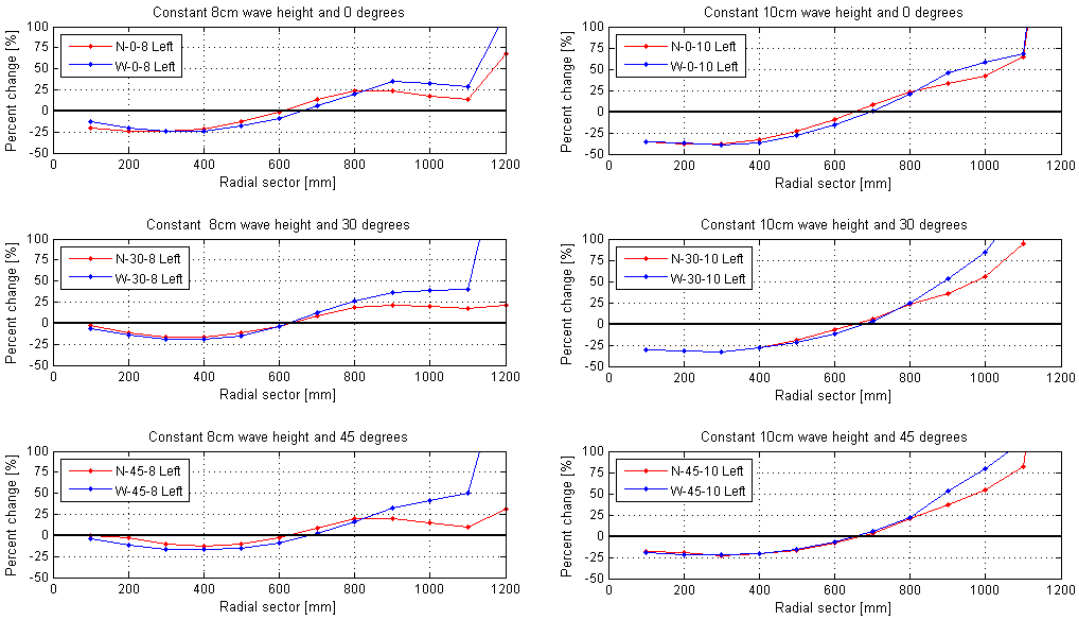

Figure 31 Grading influence on left roundhead - radial sectioning

5.3.3 Angular Sectioning Method Results

This section is dedicated to the angular sectioning method results with an emphasis on the oblique angle of wave attack tests since symmetry considerations have already been discussed. The results presented hereto refer to the angular sectors rather than the cumulative results since individual sectors are more pertinent to damage analysis. Both result sets are shown on Appendix 7.3. Since the analysis aims at the volume loss with respect to the initial breakwater roundhead configuration (Figure 5), a fixed conservative radius of 1200mm was used throughout the calculations.

A key indicator in this analysis is the “transition angle” which has been defined as the angular sector where the roundhead transitions from losing to gaining volume (from negative to positive percent change).

Influence of wave load – angular

In the figures below, roundhead percentage change for the low (8cm) and high (10 cm) wave loads are compared in red and blue lines, respectively. To isolate the wave load (or wave height) influence, the grading and angle of wave attack have been kept constant.

As anticipated, Figure 32 shows an uneven distribution of volume changes for the right roundhead over the angular sectors where, volume losses were followed by volume gains. In general, the larger wave loads caused slightly higher percentage losses. However, this characteristic is clearer for narrow grading in other words; the percentage loss difference between high and low wave loads is more pronounced for narrow grading. The plots on the left panels show similar behaviors with respect to one another: nearly parallel plots for low and high wave loads are observed until before reaching the transition angle. On the other hand, no clear or definite trend was seen for the wide

grading tests since the percent change across the radial sectors fluctuated; it is believed these fluctuations were inherited from the physical testing and topographic measurements.

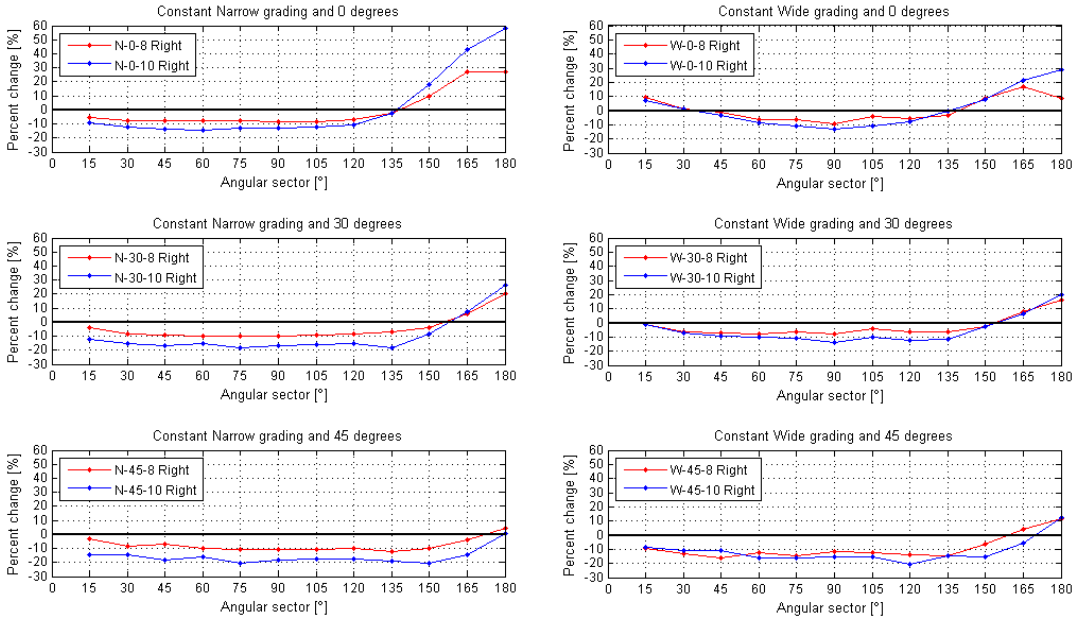

Figure 32 Wave load influence on right roundhead - angular sectioning

For the left roundhead (Figure 33), somehow clearer trends were observed on the narrow grading tests, and wide grading tests displayed less uniformity. In narrow grading cases, higher wave loads caused larger percentage gains and losses (with W-45-10 as an exception). It is evident that higher wave loads did have a larger impact on accretion than on erosion; recalling the left roundhead is an open control volume with an incoming source of sediment.

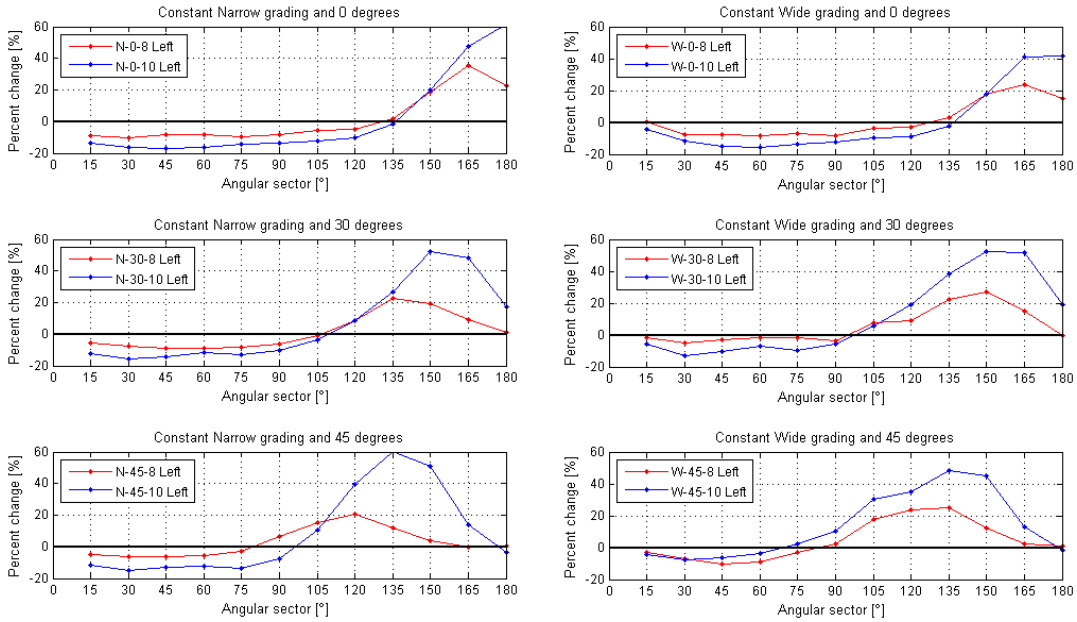

Figure 33 Wave load influence on left roundhead - angular sectioning

Influence of angle of wave attack – angular

In Figure 34 and Figure 35, the roundheads percentage change for the 0°, 30°, and 45° angles of wave attack are compared in green, red, and blue lines, respectively. To isolate the angle of wave attack influence, the wave load and grading have been kept constant.

Over the right roundhead (Figure 34), larger angles of wave impact appeared to have slightly larger percentage losses, and smaller wave impact angles had considerably larger volume gains when comparing their magnitudes. Keeping in mind the volume changes were calculated with respect to the initial roundhead layout (open control volume with a conservative radius of 1200mm), the head-on wave collision tests did a better job at keeping the sediment within the control volume. Head-on waves shifted the volume to an angular sector starting from 135°; whereas, the oblique wave attack tests pushed the it further having a volume gain starting from 150° and 165° angular sectors corresponding to the 30° and 45° wave impacts. In general, accretion occurred at the lee side of the roundhead starting from 135°$\pm$5° angle with respect to the wave direction.

What is truly remarkable about Figure 34 as well as Figure 35 is there was no angular sector with a maximum percent loss for any angle of wave impact (perhaps excluding W-0-10 Right). This observation is counterintuitive since higher percentage losses were in fact anticipated at the angular sectors with maximum wave loading meaning, 0° relative to the wave direction or the “front side.” However, the results are consistent and a solid, reassuring conclusion can be drawn from such: even though there is a component of longshore transport, it is not the dominant sediment transport mechanism at the roundheads; the dominant mechanism is transverse transport or radially outward as shown on Figure 28. The radial sectioning results do show a clear minimum and maximum percent change across the radial sectors.

If longshore transport effects were dominant, clear noticeable differences would show on the angular sectors, and this was not the case. Instead, rather constant percentage losses, particularly for the narrow grading tests, were observed throughout the angular sectors indicating the angle of wave impact did not influence the volume losses. The plots display some variability which is considered to be inherited from the physical tests as well as profile measurements.

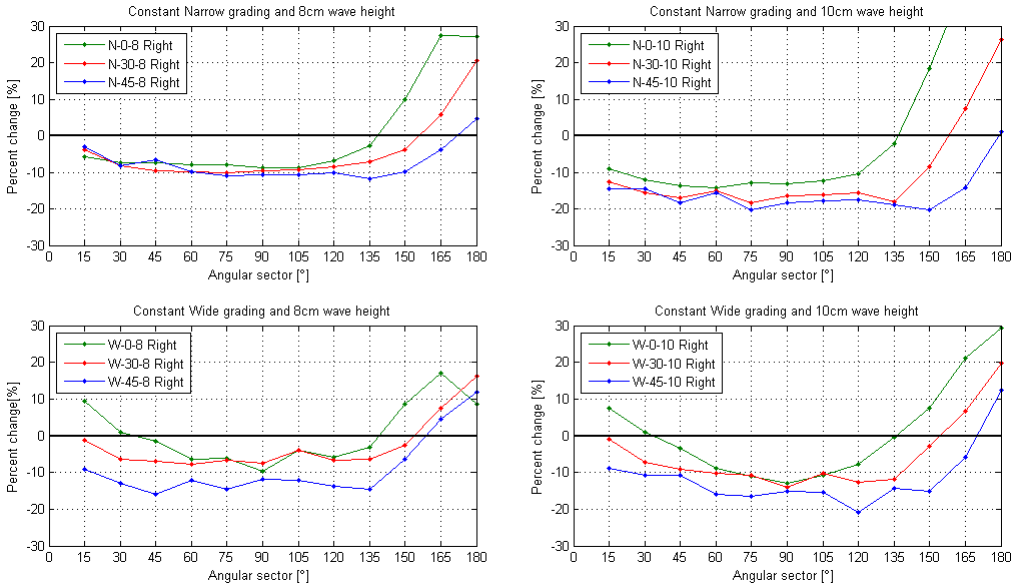

Figure 34 Angle of wave attack influence on right roundhead - angular sectioning (peaks were omitted)

The left roundhead (Figure 35) showed the same behavior to the right roundhead with regards to longshore transport; no maximum percentage loss defined the roundhead behavior which confirms the previous conclusion. On the other hand, the overall effect of wave incidence angle was reflected on the percentage gain. Independently of grading and wave load, the volume gain magnitude was considerably larger than the volume loss. As expected, larger accretion areas correspond to larger angle of wave impact: 45°, 30°, and 0° angle of wave attack tests accreted between 75° and 95°, 105°, and 135° radial sectors, respectively. This pattern has been attributed to how sheltered the left roundhead was – the more oblique the wave attack, the more sheltered the roundhead, and the higher volume gain.

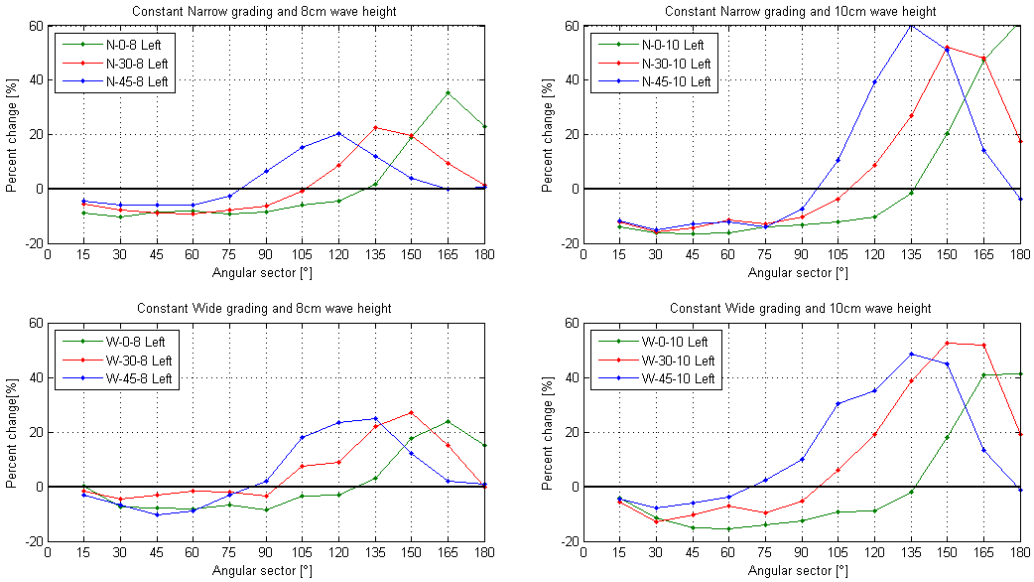

Figure 35 Angle of wave attack influence on left roundhead - angular sectioning

Influence of grading – angular

In Figure 32 and Figure 33, the right and left roundheads percentage changes for the narrow and wide grading are compared in red and blue lines, respectively. To isolate the grading influence, the wave load and angle of wave attack have been kept constant.

In general, no clear distinction could be found in the angular sectioning results between narrow and wide grading. Nonetheless, some differences were visible for both left and right roundheads; such differences have been attributed to the accuracy of the physical testing including topographic measurements. Some remarks can be made: the narrow grading tests showed slightly more constant percentage losses than wide grading, and some test combinations such as, N/W-30-8 Right, N/W-0-8 Left, and N/W-0-10 Left displayed similar results with respect to wide and narrow grading. But overall, the differences between wide and narrow grading were not distinctive enough to draw conclusions.

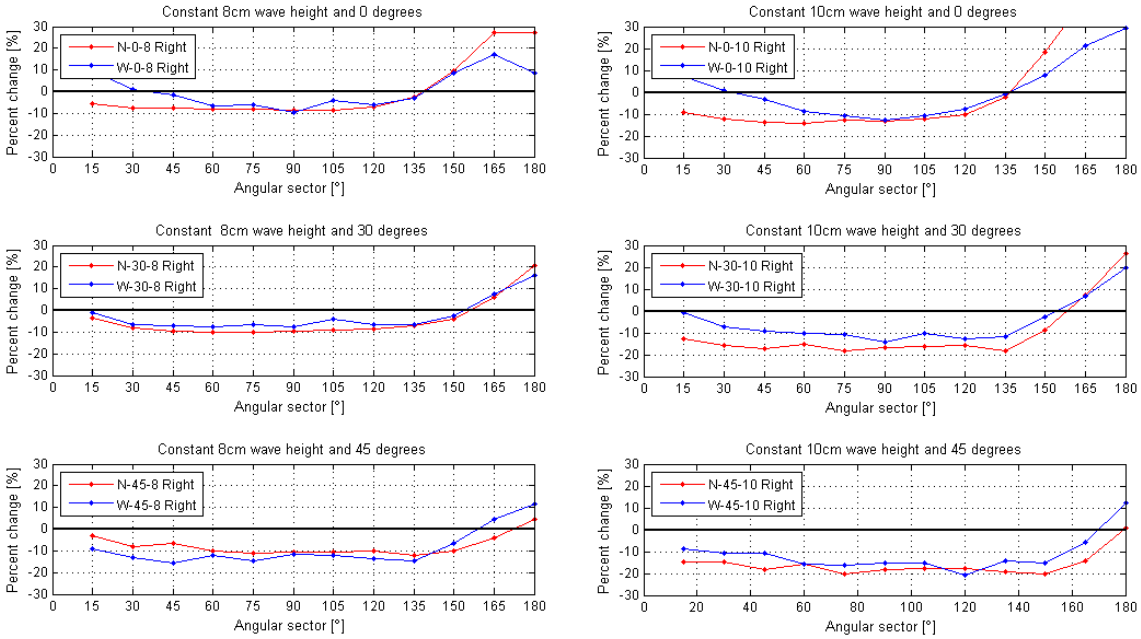

Figure 36 Grading influence on right roundhead - angular sectioning

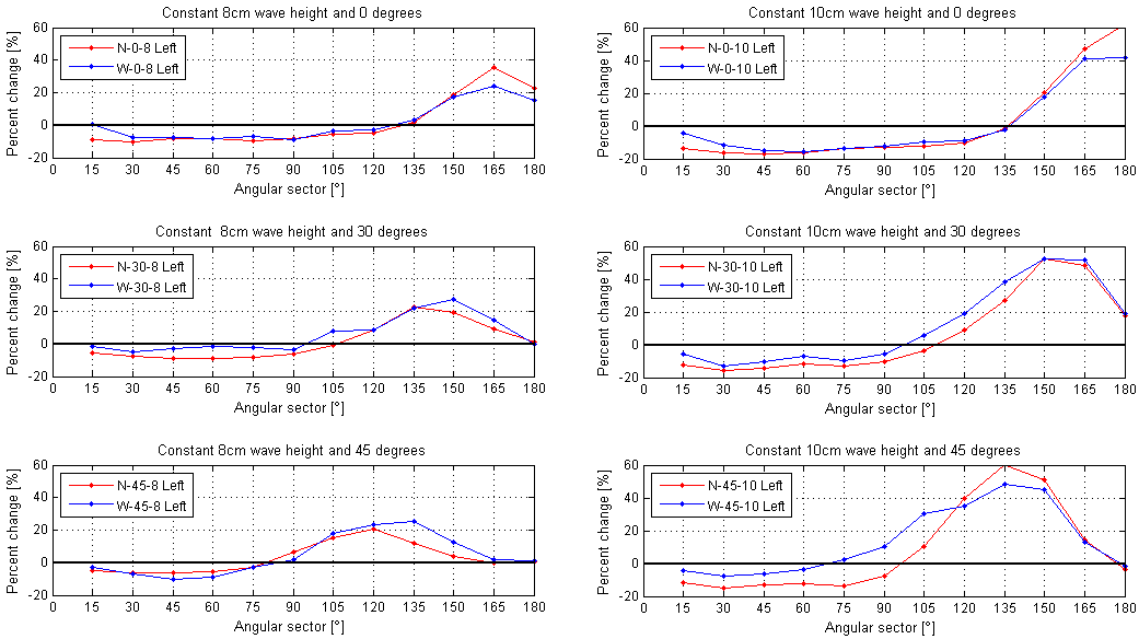

Figure 37 Grading influence on left roundhead - angular sectioning

6 Conclusions and Recommendations

6.1 Conclusions

Previous studies have been carried out to understand the breakwater behavior when exposed to hydrodynamic loading; such studies comprise the complete breakwater structure including the armoring layer which prevents the core material from deforming. Few studies have aimed at the behavior of the core material; breakwater cores can suffer larger deformation during construction since it designed to withstand moderate or severe wave loading. Mulders (2010) performed physical tests for breakwaters under construction (or core material) exposed to wave attack, and he dedicated his study to the analysis of the trunk response. The present study is targeted at the understanding of the deformation mechanisms of rubble mound breakwater roundheads under construction following the data obtained from Mulders' physical tests.

To investigate the influence of hydrodynamic loading, which includes wave height and angle of wave incidence, and the influence of grading on roundheads under construction, twelve scaled physical model tests were performed varying the wave height (8cm for low and 10cm for high wave heights), wave angle (0°, 30°, and 45°), and grading (f_g= 1.3 for narrow and f_g=6 for wide grading).

The deformation analysis was accomplished via volume percent change for a given control volume; these volumes were estimated using the filtered and interpolated (when needed) experimental three dimensional data along with the trapezoidal rule for calculations. The control volumes consisted of the overall breakwater, the overwash, and the roundheads, where the main focus of the study lays on. For the breakwater roundheads, two different control volume approach were taken: radial and angular sectioning.

Radial sectors covered the area bounded by "semi-rings" with a thickness of 100mm centered at the roundhead center point; angular sectors covered the area bounded by 15° and a radius of 100mm centered at the roundhead enter point. What is relevant about these two sectioning methods is what sediment transport mechanism they represent. The radial sector depicts the cross-shore transport or radially outwards while the angular sectors illustrate the longshore sediment transport at the roundhead; the results have indeed reflected so.

Overall roundheads under construction

A clear distinction was observed between the narrow and wide grading material volume changes for the overall breakwater (closed control volume). Narrow grading exhibited a loss in volume while wide grading displayed a volume increase; these volumetric changes are not only dependent on sediment transport mechanisms but they are also the result of material sorting and changes in packing density.

After testing, the finer fractions were expected to fill the voids of the wide grading material which should have resulted in a volume decrease and therefore, larger packing densities. Counterintuitively, after testing the volumes increased for the wide grading tests indicating evidence of a sorting or segregation mechanism. These results quantitatively proved Mulders' conceptual

model where non-uniform sorting mechanisms take place throughout the structure and they are dependent on the material grading.

To sum up, wide graded material caused a volume increase due to the transverse movement of the coarsest fraction while the narrow grading associated with the finer fraction, decreases in volume indicating a soil compaction and therefore, a larger packing density.

Overwash under construction

The calculated overwash values were an indicator of the direction of sediment transport even though small overwash percent volumes were obtained. Small overwash volumes were expected and obtained because the physical model had been designed for the overwash to stay at a minimum.

In general, a fairly symmetrical response between the left and right overwash was observed for tests with 0° angle of wave incidence. For oblique wave incidence, the right roundhead (the most exposed to wave action) overwash volumes were always larger than zero with increasing percent volume as the hydrodynamic loading increased (angle of incident and have height). Overall, the tests with the largest wave heights produced the largest overwash volumes, and no clear trend could be assessed concerning the relation between the wide and narrow grading material. For oblique wave attack, the right and left overwash tests exhibited positive and zero volumes, respectively.

Roundheads under construction

A quasi-symmetrical behavior was detected between left and right roundheads for an angle of wave attack equal to 0°. The left roundheads did exhibit greater percentage volume than the right roundheads for radial and angular sectioning results. The cause of this difference is unknown but it could be attributed to uneven wave impacts potentially originating from the wave maker.

Radial sectioning method

For the radial sectioning, a distinctive maximum percent loss was seen in all test results; thus, the cross shore or radially outward sediment transport was found to be the dominant deformation mechanism for roundheads under construction.

In general, the higher wave loads caused greater material losses at the 300mm radial sector; higher wave loads also produced larger volume gains at the outer radii. Moreover, narrow and wide grading tests gave similar percentage losses thus; volume losses were indifferent to grading. On the other hand, the wide grading produced larger percentage gains compared to the narrow grading; this observation is in line with the sorting mechanism described by Mulders (2010) where coarser fraction rolls down slope to the outer radii. The wave load also influenced the transition radii because as the wave load increased, the transition radius also increased. This transition is considered a parallel phenomenon to the S-curve occurring at the breakwater trunk consequently; larger transition radii would point towards a wider S-curve.

With regards to wave direction, both roundheads had a positive percent change at the outer most radii when exposed to head-on waves; therefore and also based on Mulders' longshore transport results (2010), the additional volume causing these increments could have originated at the trunk. As expected, the left roundheads always accreted while the right roundheads experienced volume

losses for oblique wave attacks. In addition, when comparing different incidence wave angles, larger angles caused a slight increase in percentage loss at the radial sectors which could be attributed to a potential increase in longshore transport. The transition radius seemed nearly constant approximately at 700mm for oblique wave attack (wide S-curve); however, for head-on wave attack, the transition radius reduced (narrow S-curve).

With regards to the influence of grading, strikingly similar results were obtained for narrow and wide graded material especially for the high wave load tests as well as the left roundheads. In the radial sectors where the breakwater is losing volume, nearly identical behaviors (overlapping results) were attained between narrow and wide grading; on the other hand, at the radial sectors where the breakwater gained volume, the wide grading volume gain was larger than the narrow grading. This result is confirmation of the coarse fractions rolling downwards and radially outwards. This apparent material gain might be interpreted as a decrease in packing density for the coarse fractions due a volume increase; this observation is in line with the conclusion presented for the overall breakwater control volume.

Based on the findings in the radial direction, it can be concluded the grading does not influence the roundhead volume losses but it does affect the volume gains due to a non-uniform sorting mechanism where coarser fraction are displaced downslope possibly decreasing the packing density.

Angular sectioning method

For the angular sectors, no distinctive percent loss was found in the test results; thus, the longshore sediment transport was not the dominant deformation mechanism for roundheads under construction.

When looking at the wave load influence, an expectedly uneven distribution of volume changes was observed at the angular sectors. In general, volume losses occurred from 0° to 135°±5° with respect to the wave direction followed by volume gains. Generally, the larger wave loads caused slightly higher percentage losses than the lower wave loads; this characteristic was clearer for narrow grading tests. Also, for the left roundhead, the higher wave loads had a considerably larger impact on volume gains than on volume losses because of the open control volume with an incoming sediment source.

Concerning the angle of wave incidence, higher percentage losses were anticipated at the angular sectors with maximum wave loading (0° relative to the wave direction) however; the wave incidence angle did not impact the volume percent loss over the different angular sectors. Instead, rather constant percentage losses, particularly for the narrow grading tests, were observed. Even though this conclusion seems counterintuitive, the results are consistent and solid: a longshore component did exist at the roundheads but did not dominate the sediment transport mechanisms; cross shore transport was found as the dominant transport mechanism.

Also at the left roundheads, the volume gain magnitudes were considerably larger than the volume losses as expected, and larger accretion areas corresponded to larger angles of wave impact. Such pattern relates to how sheltered the left roundhead is from wave attack.

Lastly, no clear distinction could be found in the angular sectioning results between narrow and wide grading.

Summarizing the key points

- Overall, wide graded material caused a volume increase due to the transverse movement of the coarsest fractions while the narrow grading (finer fraction) decreases in volume increasing the packing density
- Overwash volumes were proportional to wave load and angle of wave attack
- At the roundheads, distinctive percentage volume losses (radial sectors with low resistance) were clearly present; thus, transverse (radially outward) sediment transport was the dominant deformation mechanism over longshore transport.
- Longshore transport did contribute to roundhead deformation; however, no maximum losses were found since the volume losses were nearly equal throughout the angular sectors. As a result, the angle of wave incidence did not affect the volume losses in the angular direction.
- Wide graded material caused a volume increase at the outer radii due to the transverse movement of the coarsest fraction (sediment sorting) indicating a reduction in packing density
- Grading did not influence the roundhead negative percent change in the radial direction; thus, grading appeared to be indifferent to volume losses but relevant for volume gains
- High wave loads caused greater volume losses particularly in the radial direction
- Higher wave loads enlarged the transition radius indicating a wider S-curve like profile for higher wave heights
- The angle of wave incidence caused volume losses I angular sectors from 0° to 135°±5° with respect to the wave direction and volume gains from 135°±5° to 180°

6.2 Recommendations

The results of this research study give an insight into the deformation of breakwater roundheads under construction (core material). The analyses presented hereto are based on twelve physical tests exclusively which include variations of wave height, angle of wave incidence, and grading. Having said that, the following recommendations are proposed to enrich the understanding of roundhead deformation mechanisms.

Further analysis of existing physical test data

A volumetric study into the deformation of the trunk similar to the analysis presented in this report is recommended since such calculations fell out of this scope of work. It would beneficial to perform volumetric change analysis in the trunk in order to assess the roundhead retreat; in other words, how the breakwater trunk is shrinking due to roundhead deformation

Also, a third method of sectioning the roundheads in longitudinal cuts parallel to the x-y plane is highly recommended. These results should reflect the influence of water surface elevation was well as weave run up/run down on roundhead deformation.

This study aimed at analyzing the deformation based on a control volume for the initial roundhead configuration; however, there are results and raw data available to further analyze the direction/locations at which the sediment has been deposited. This kind of analysis would be beneficial if the goal of the study is to analyze the sediment deposition in the lee side of the structure such as, the blockage of an entrance channel.

Rerun current test configurations

Since these analyses were completed using volume calculations, the results cannot indicate where the sediment originated or to what location it was displaced. Therefore, it is recommended to rerun the current physical tests using tracers (colored aggregates) in order to assess the directionality of the sediment. In addition, using photographs and camera overlay technique (Van Gent & Van der Werf, 2010) it might be possible to perform a mass balance and therefore, density changes.

Expand physical test data

As Mulders (2010) points out, “another way to expand the data set is by conducting tests with different values for grading, angle of wave attack and wave conditions. It is therefore recommended to carry out experiments with gradings in between the currently used gradings and wider gradings, so that relations can be derived which are valid for a wider range. Besides different gradings also additional tests with angles of wave attack in between 30° and 45° are advised as well as smaller angles for exact determination of the relations between wave obliquity and deformation.” The author also recommends varying the water surface elevation along with wave height and breakwater slope in order to assess the effects different wave run ups and run downs might have on roundhead deformation.

7 Appendix

7.1 Roundhead visual schematizations

Scattered data plotted in green dots represents the experimental data which has been filtered and interpolated accordingly. The colored surface is a result of there-dimensional interpolation.

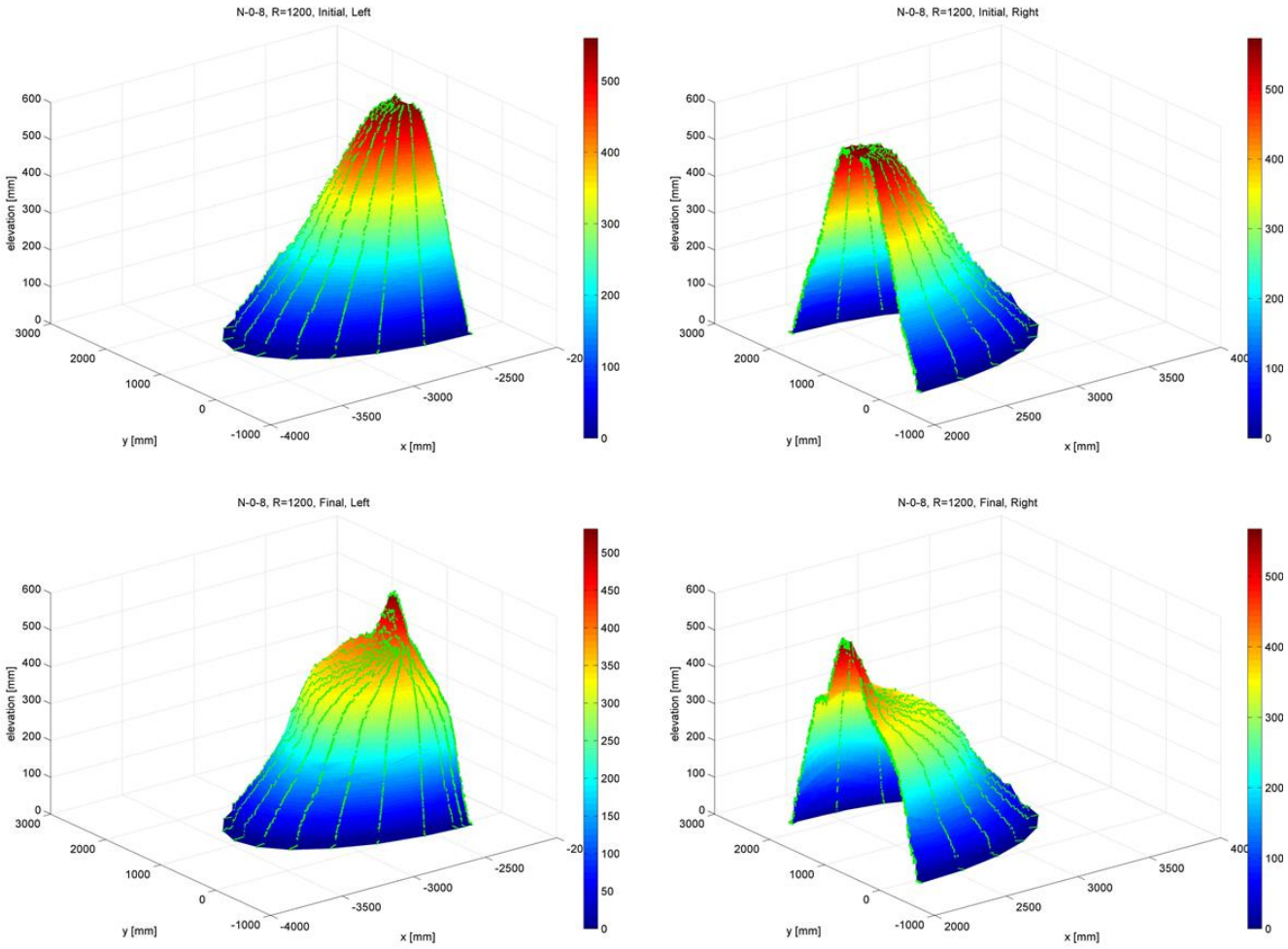

Figure 38 Initial and final condition for left and right roundheads for N-0-8 test

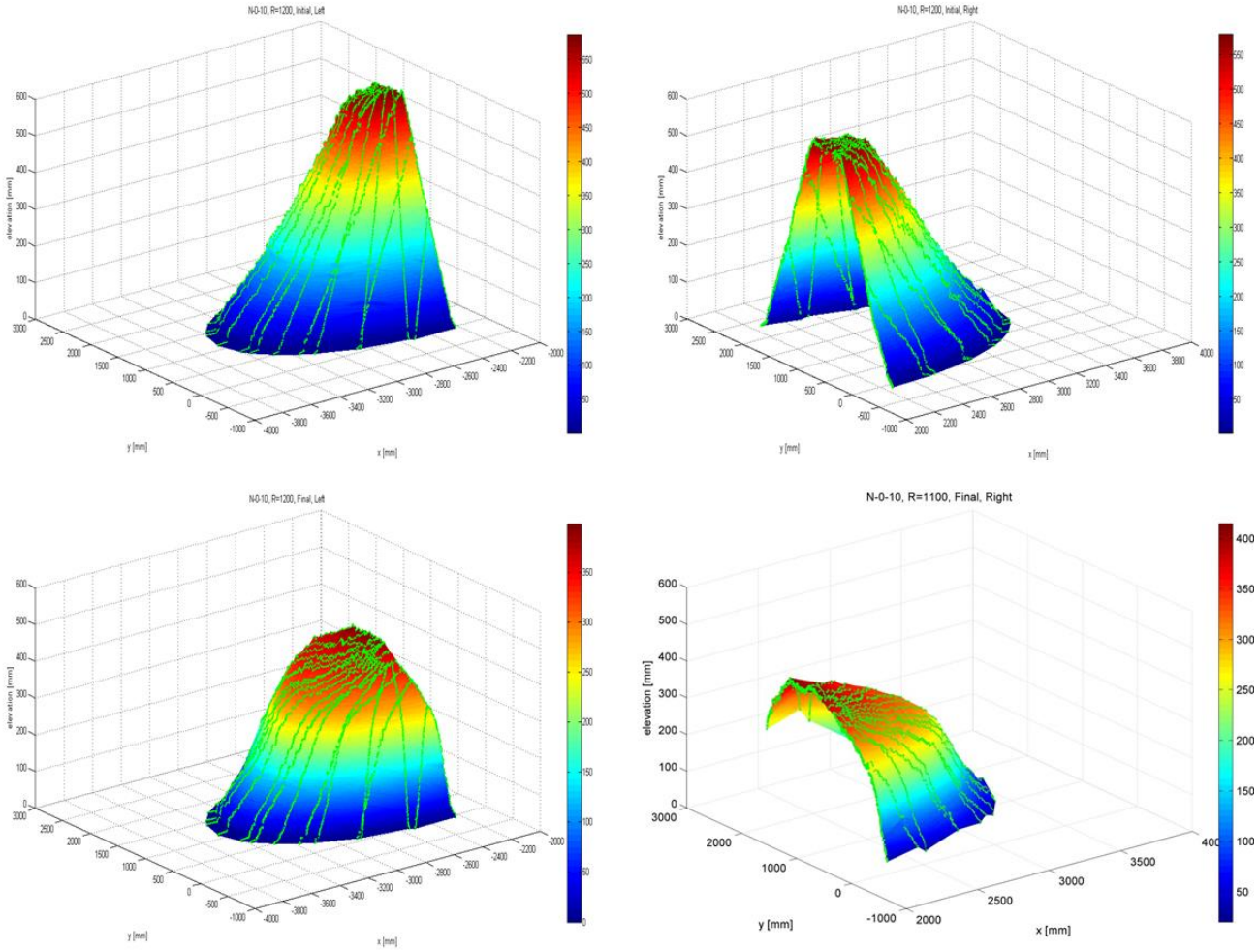

Figure 39 Initial and final condition for left and right roundheads for N-0-10 test

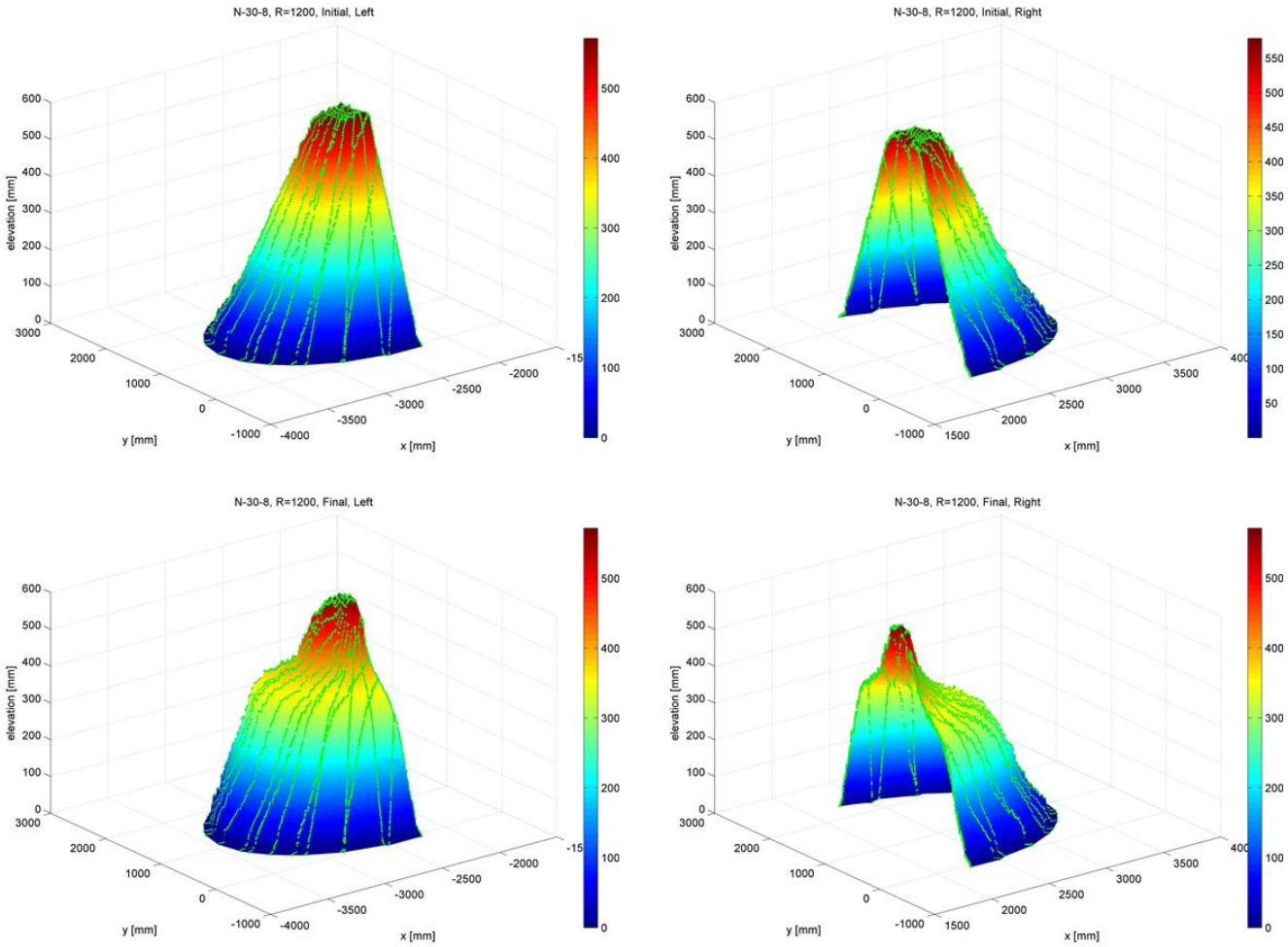

Figure 40 Initial and final condition for left and right roundheads for N-30-8 test

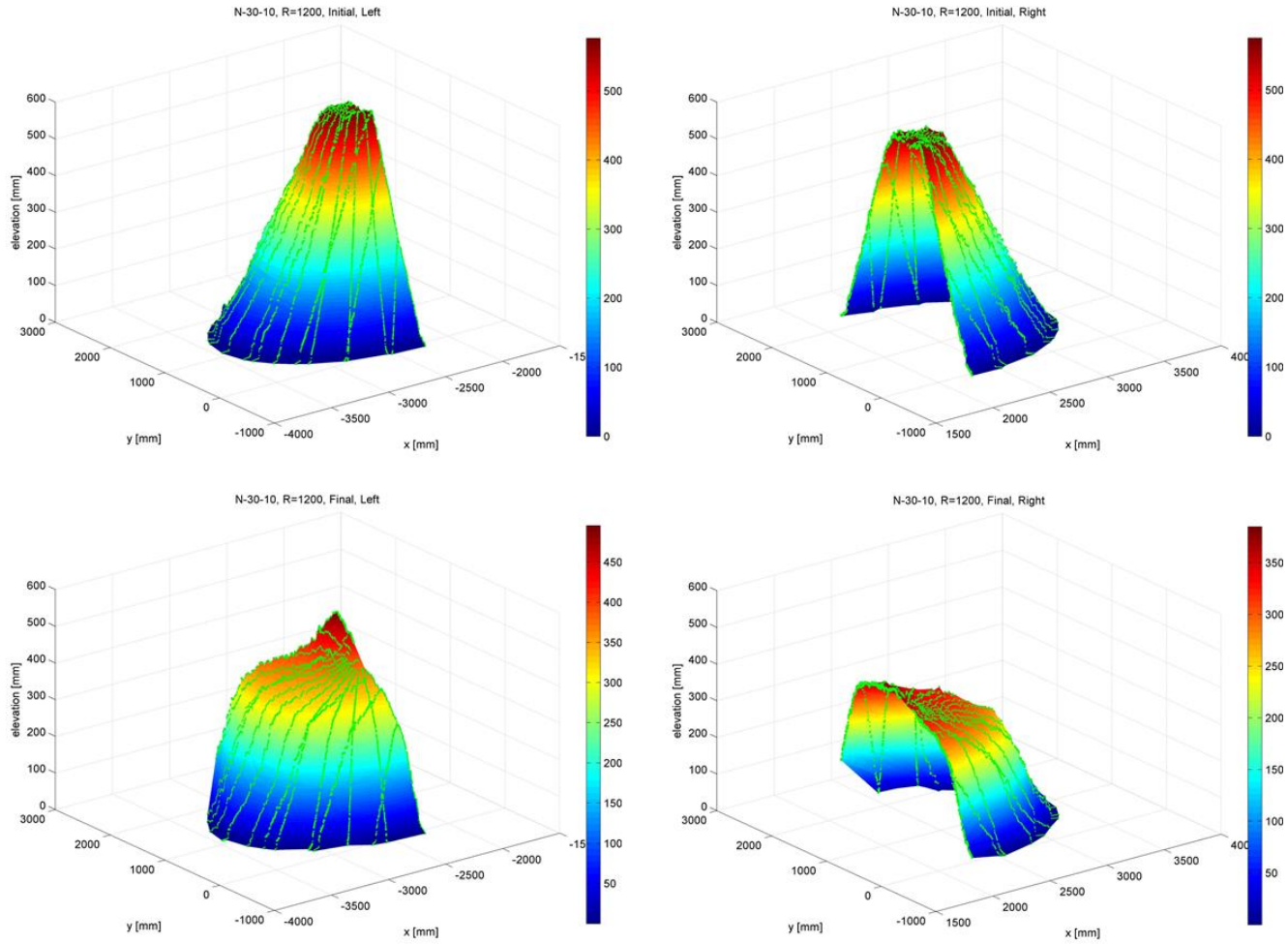

Figure 41 Initial and final condition for left and right roundheads for N-30-10 test

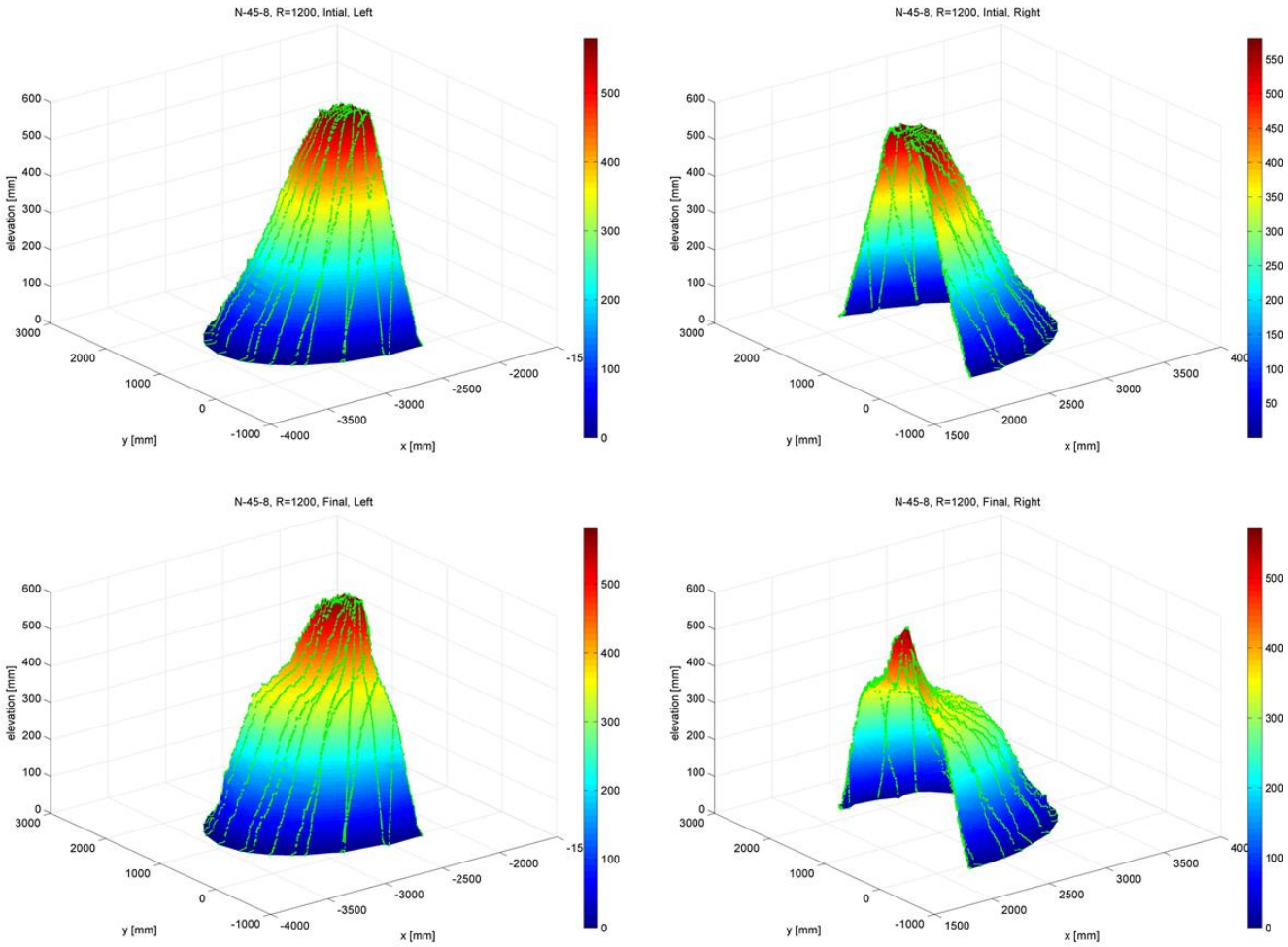

Figure 42 Initial and final condition for left and right roundheads for N-45-8 test

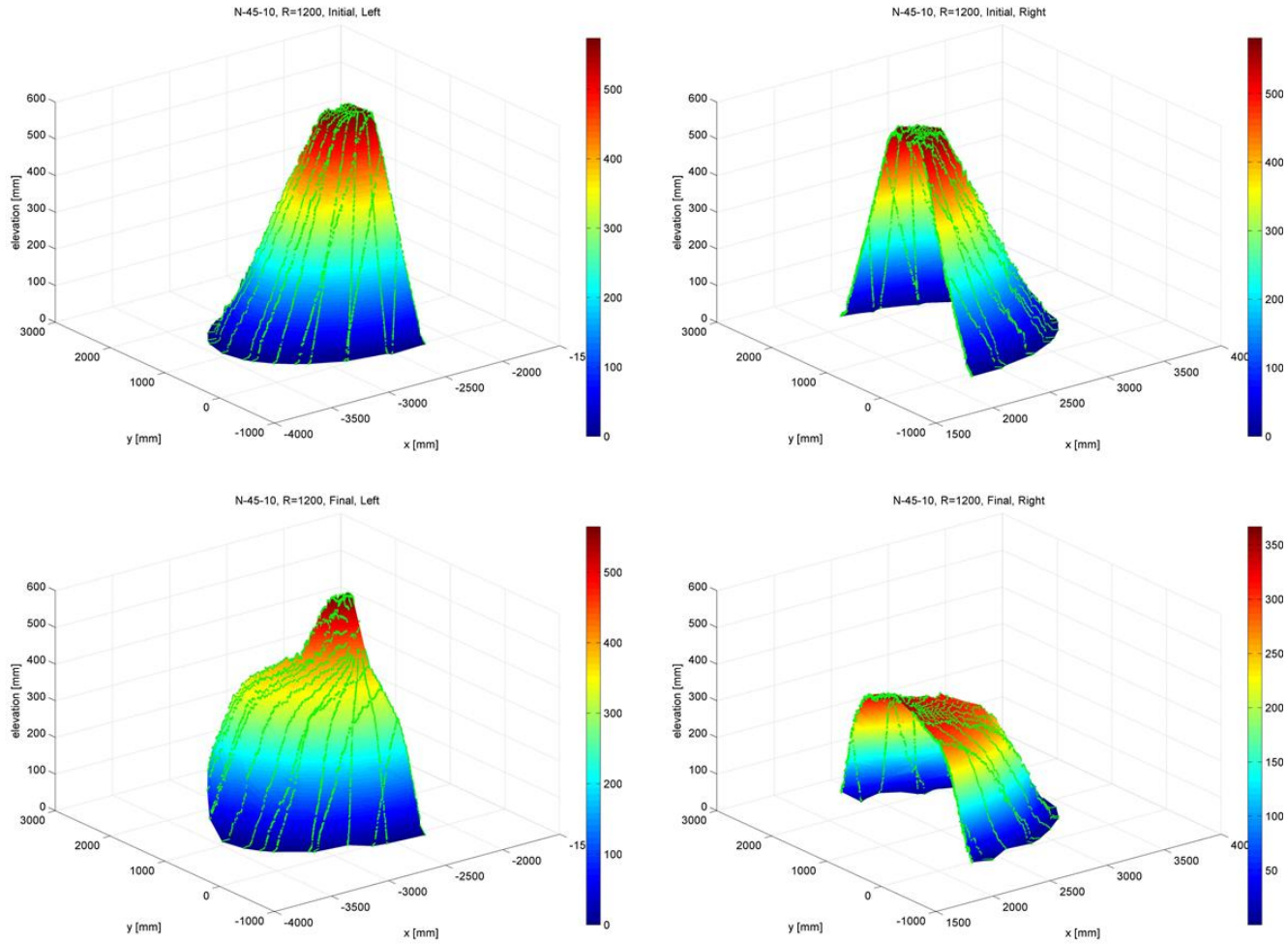

Figure 43 Initial and final condition for left and right roundheads for N-45-10 test

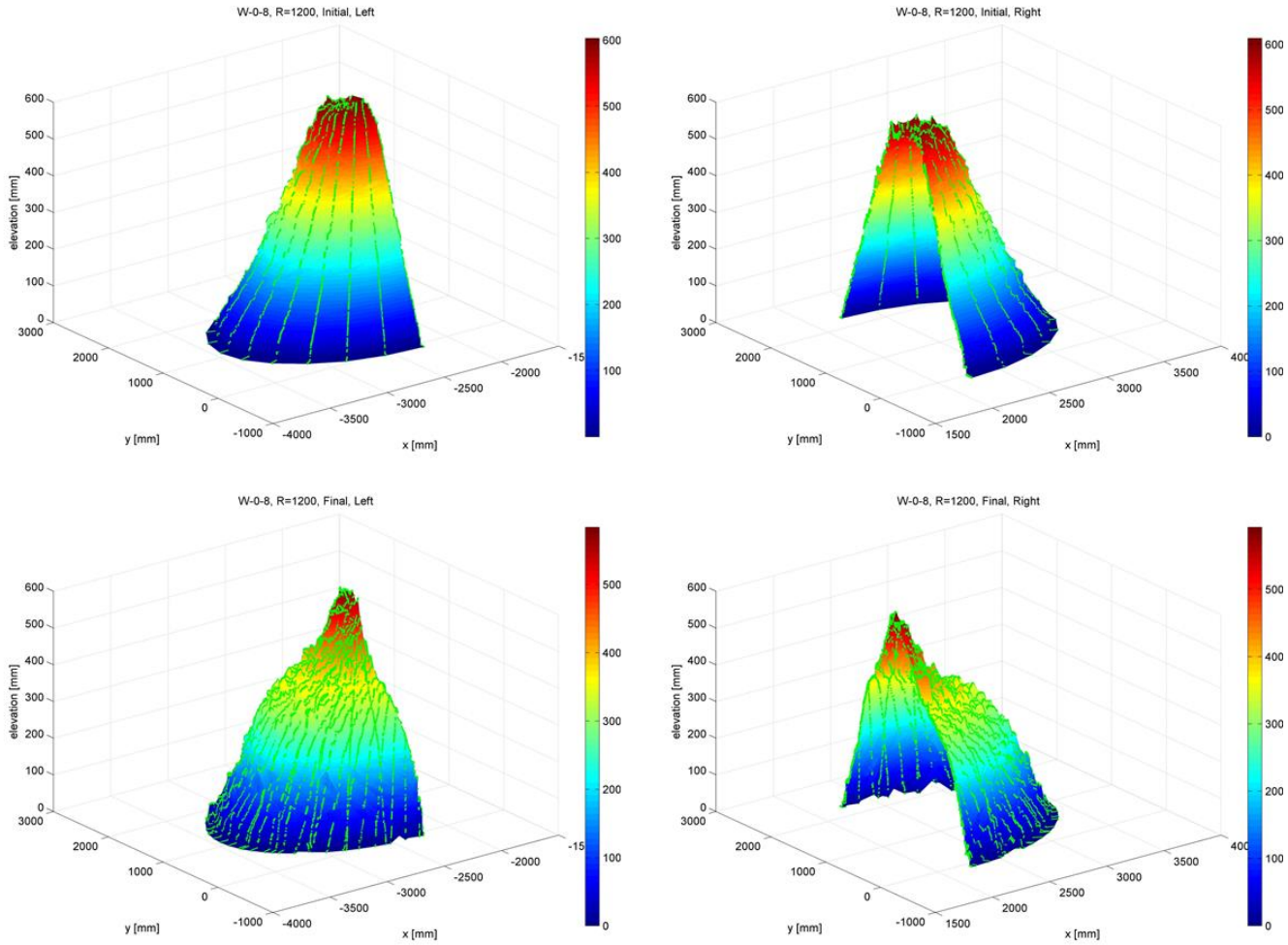

Figure 44 Initial and final condition for left and right roundheads for W-0-8 test

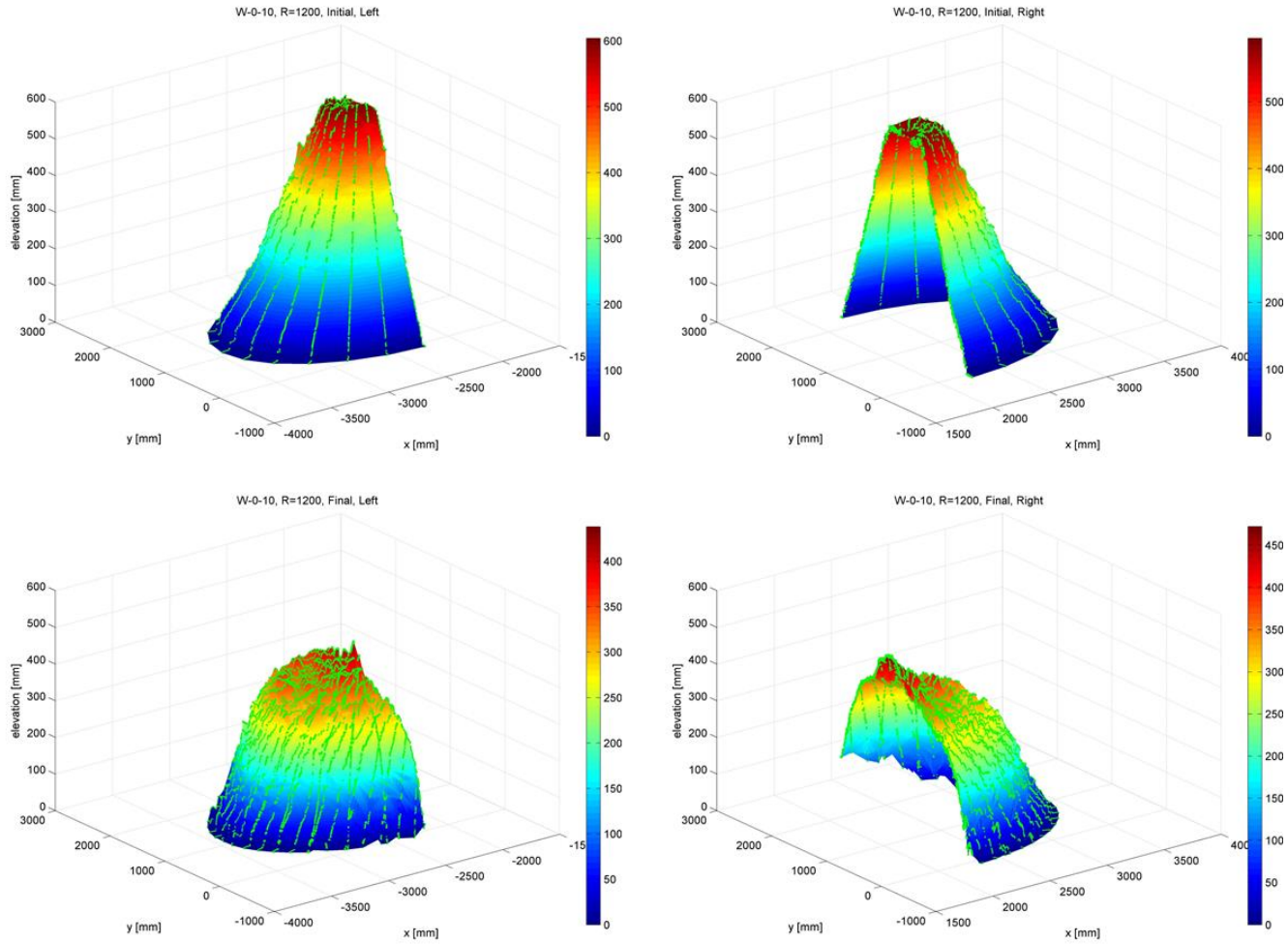

Figure 45 Initial and final condition for left and right roundheads for W-0-10 test

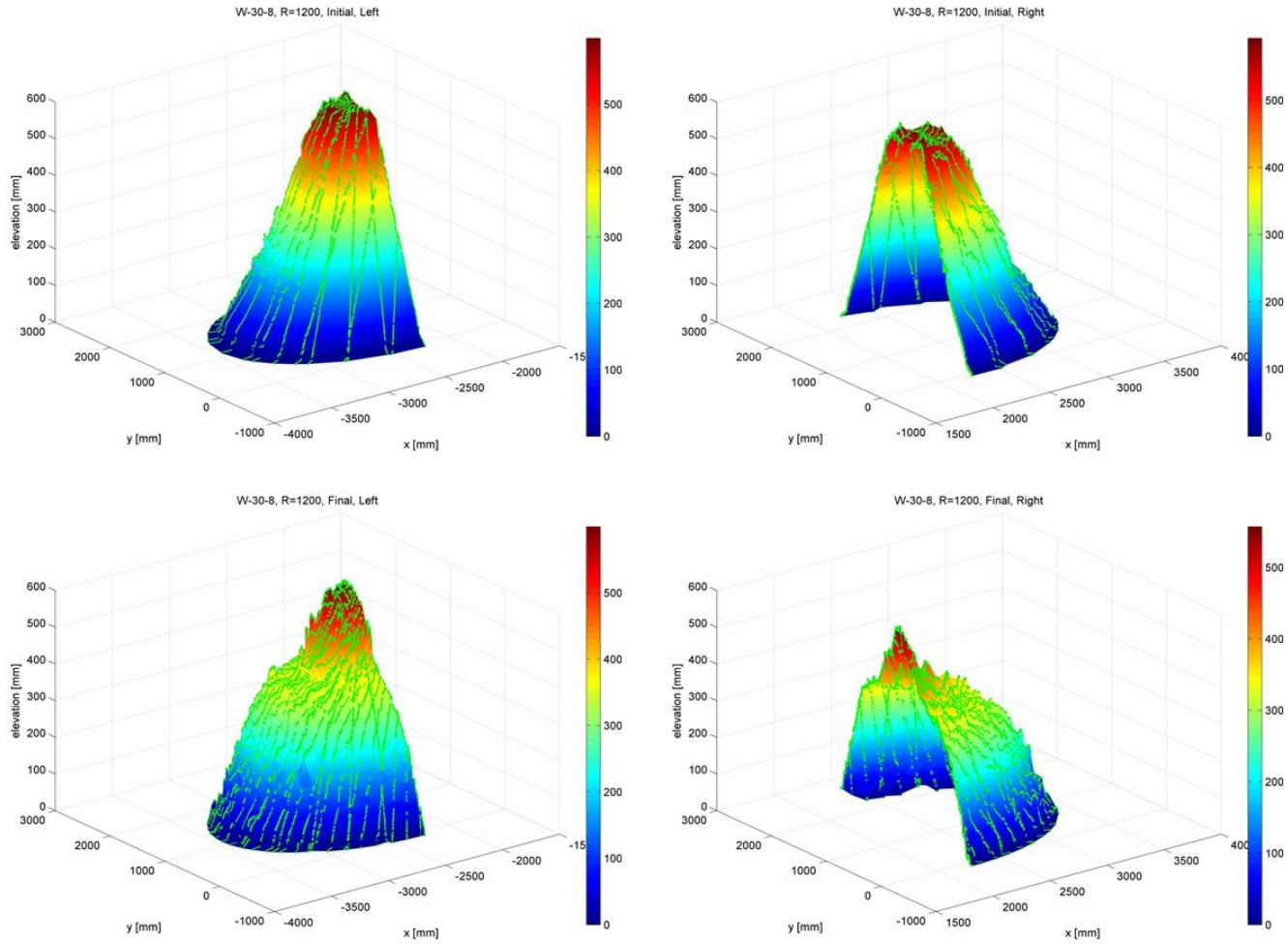

Figure 46 Initial and final condition for left and right roundheads for W-30-8 test

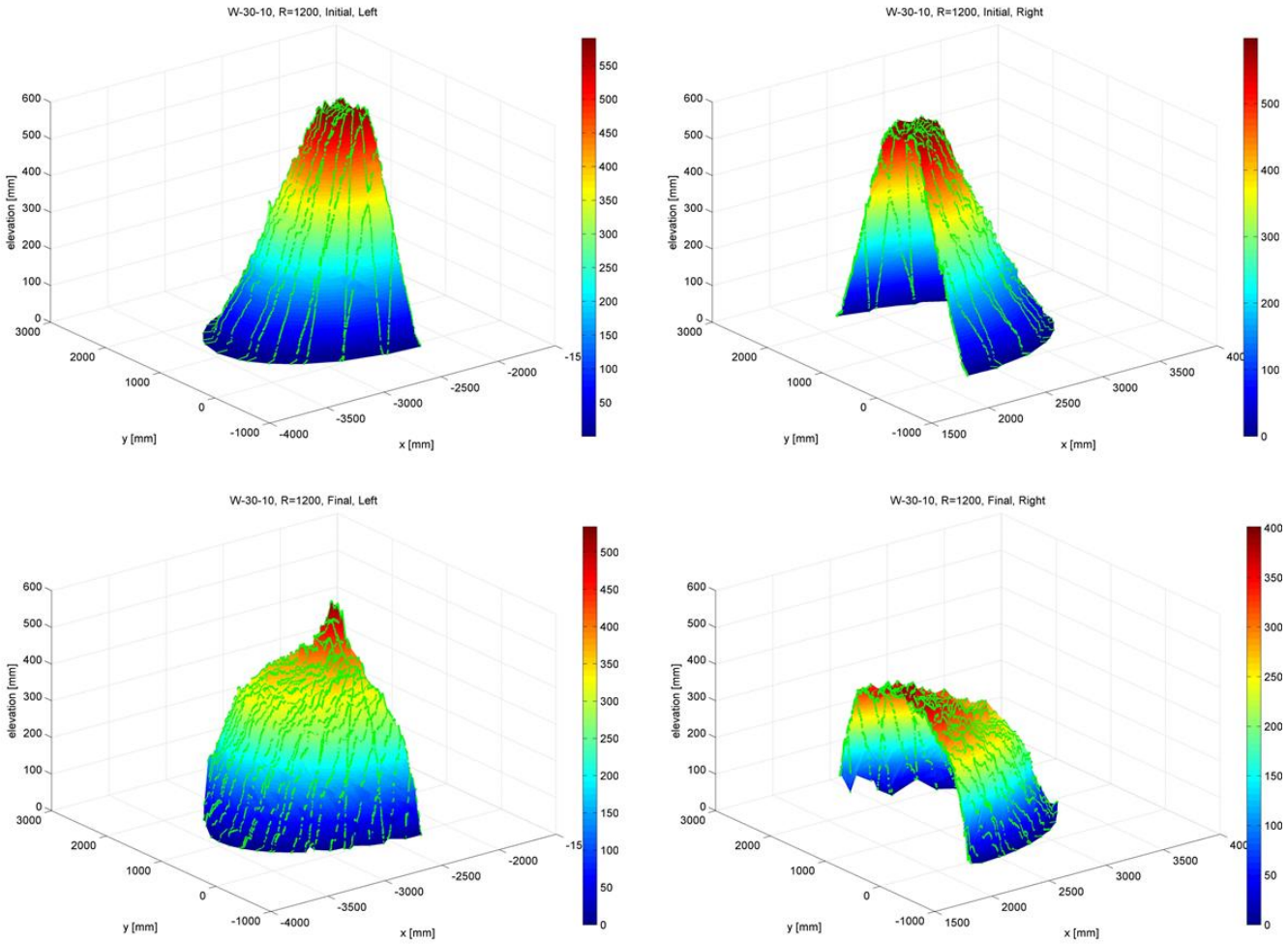

Figure 47 Initial and final condition for left and right roundheads for W-30-10 test

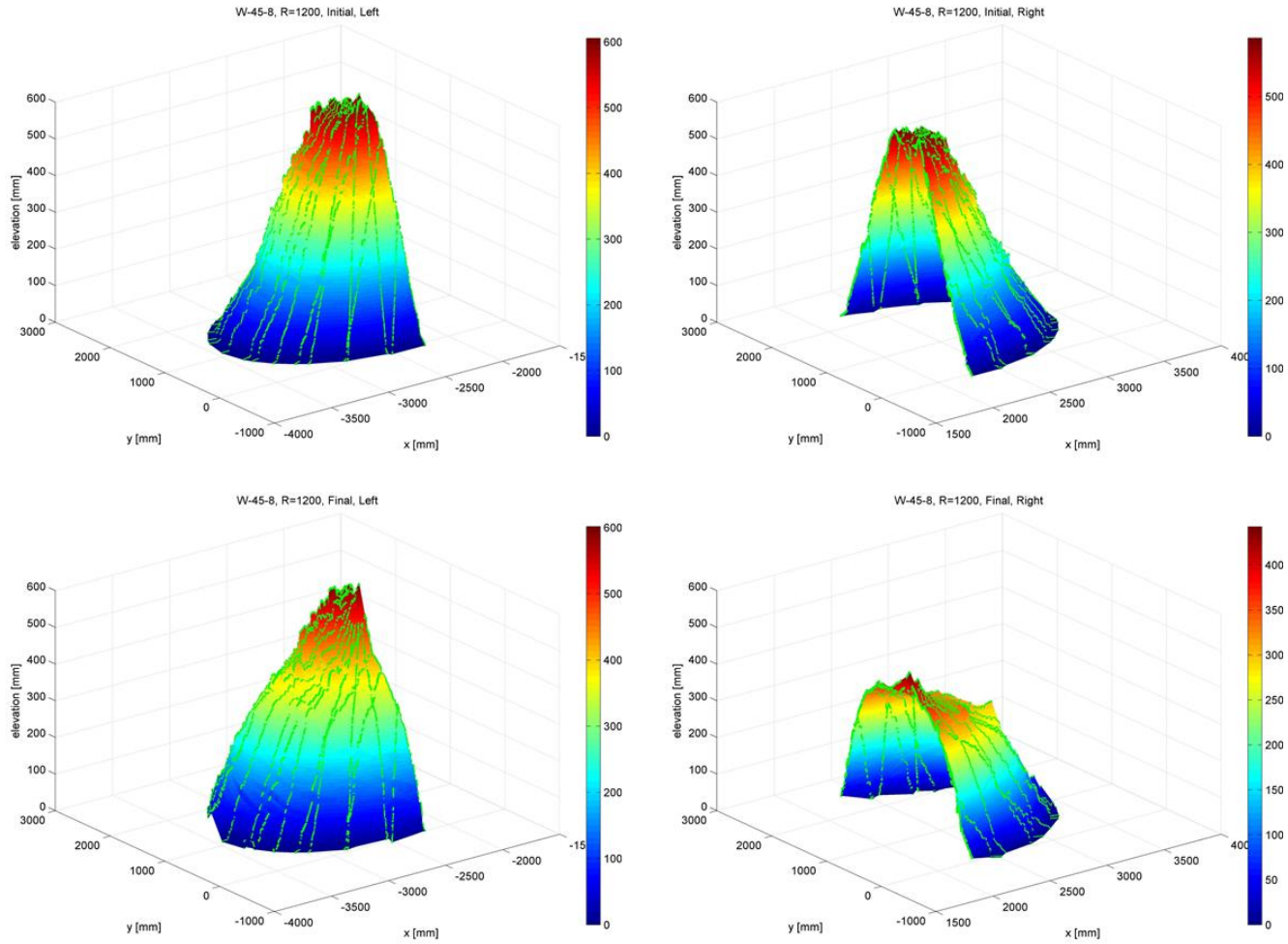

Figure 48 Initial and final condition for left and right roundheads for W-45-8 test

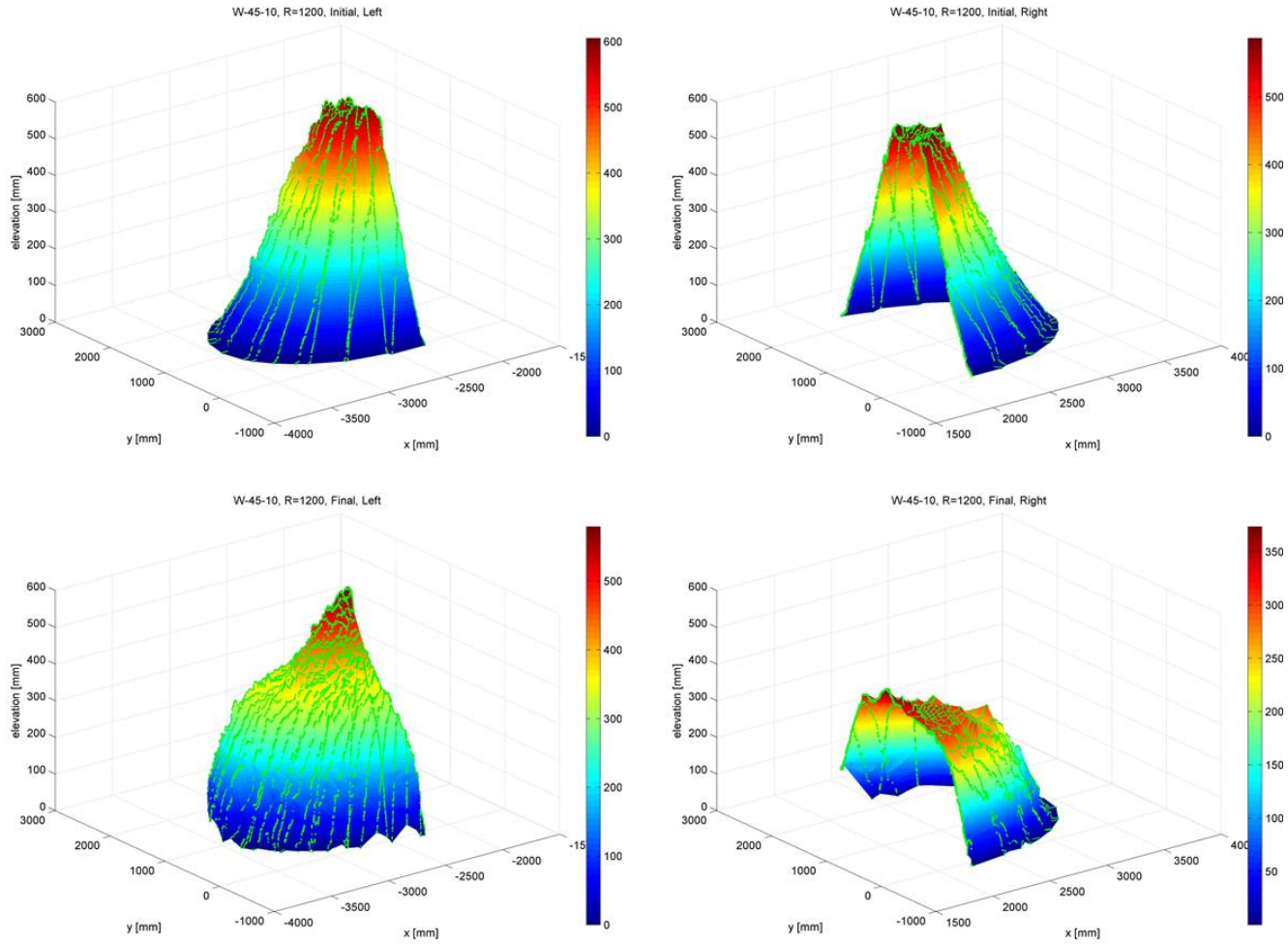

Figure 49 Initial and final condition for left and right roundheads for W-45-10 test

7.2 Radial sectioning method results

The percentage change at radii higher than 1200mm are very sensitive to small variations in volume; thus, such results may fall out of the window plot and were not accounted in the analysis.

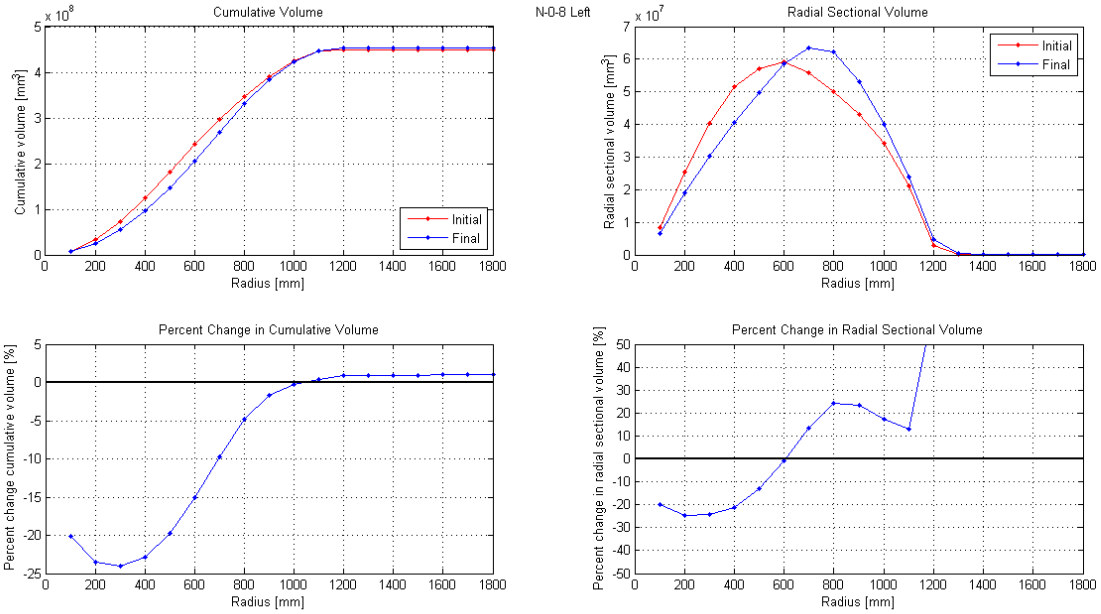

Figure 50 Complete results for N-0-8 Left radial sectioning

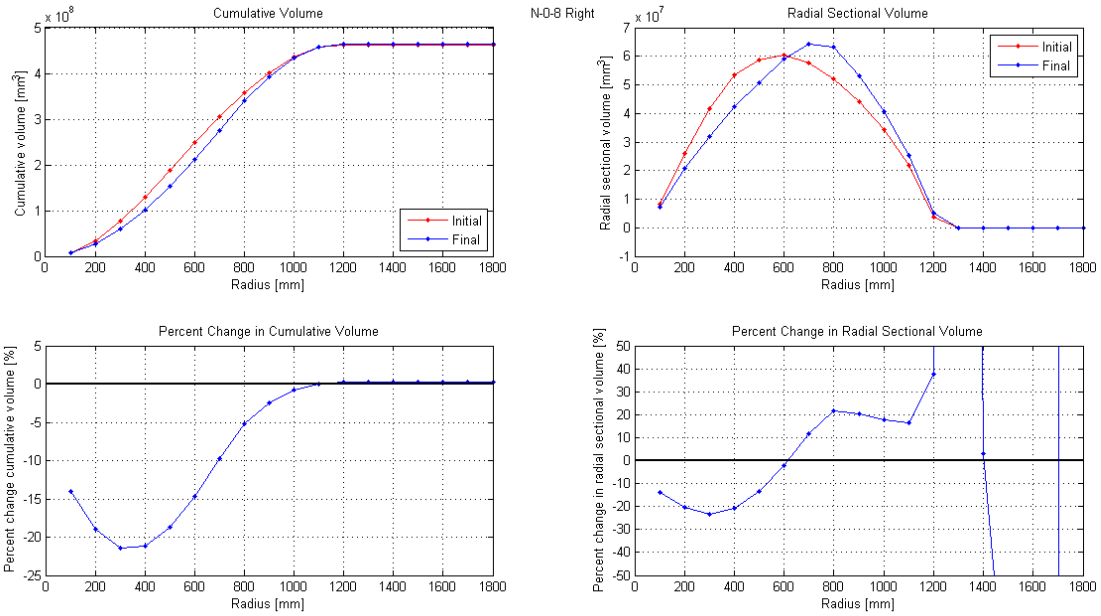

Figure 51 Complete results for N-0-8 Right radial sectioning

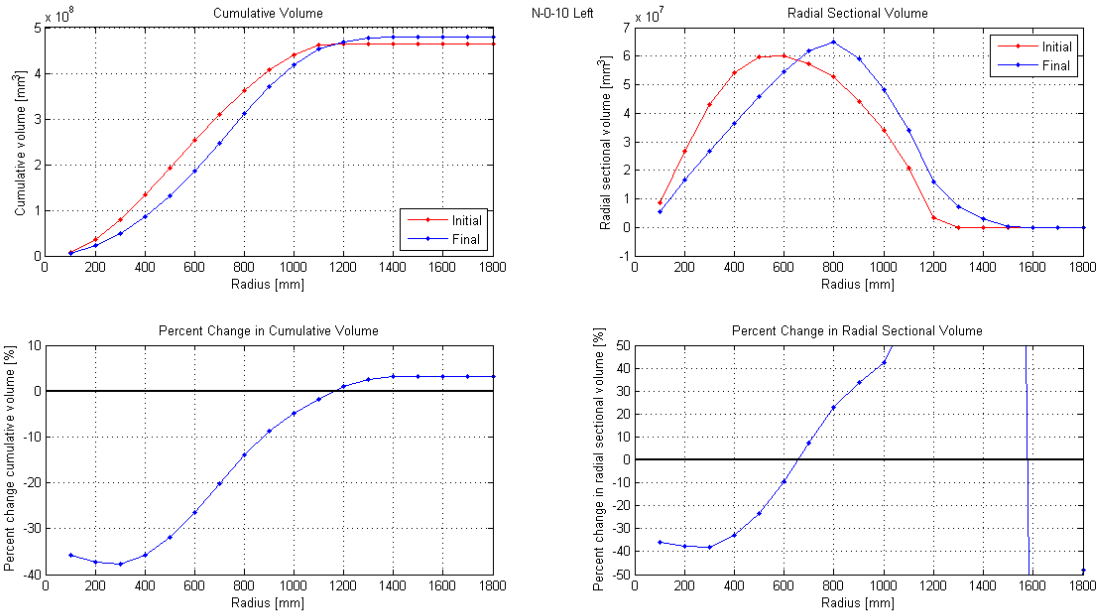

Figure 52 Complete results for N-0-10 Left radial sectioning

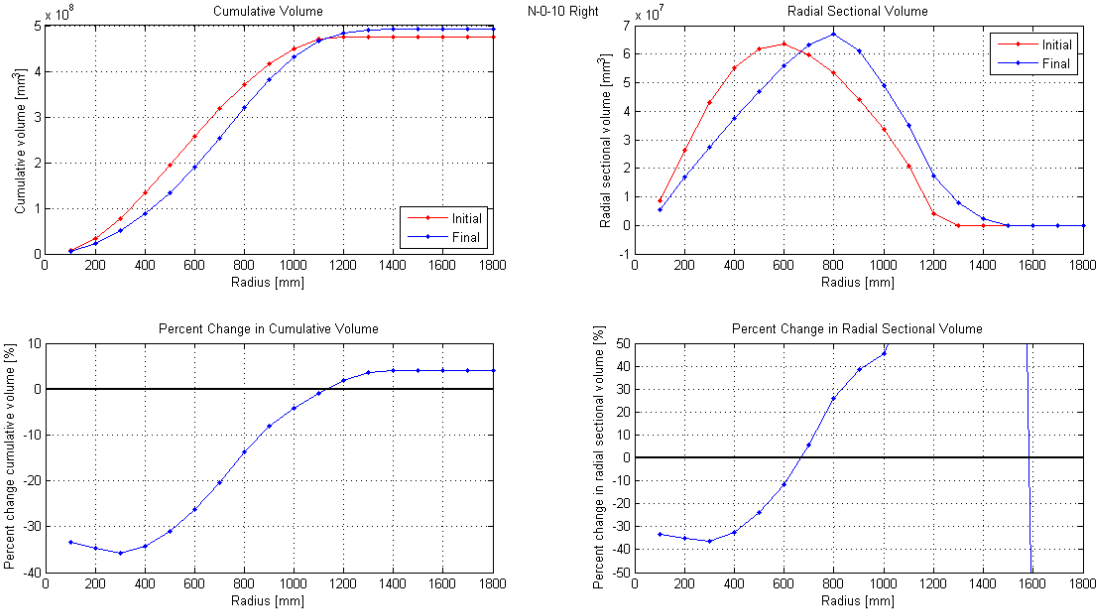

Figure 53 Complete results for N-0-10 Right radial sectioning

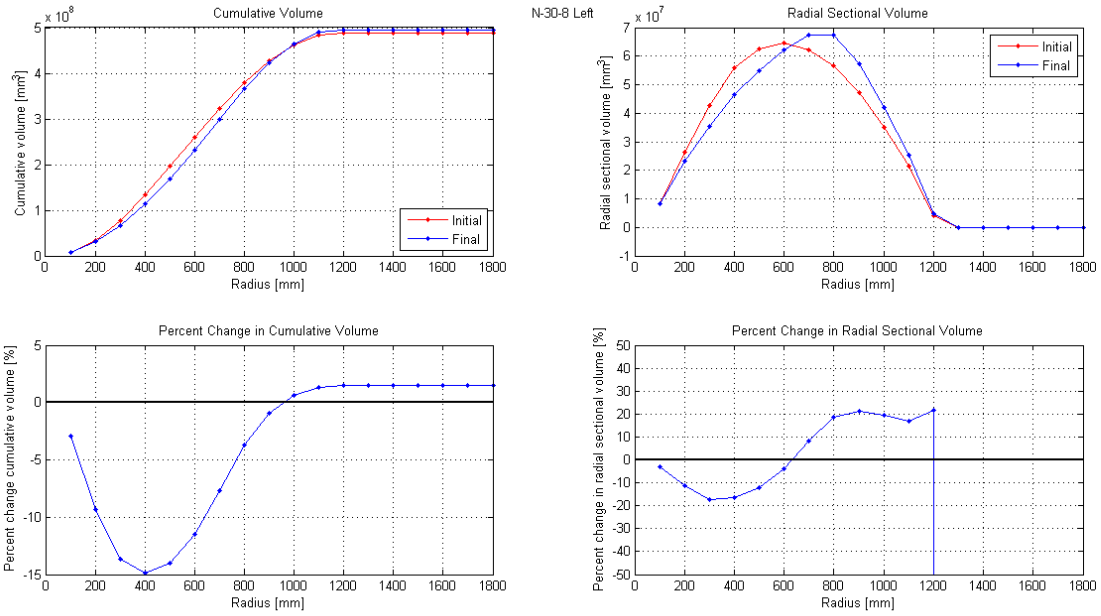

Figure 54 Complete results for N-30-8 Left radial sectioning

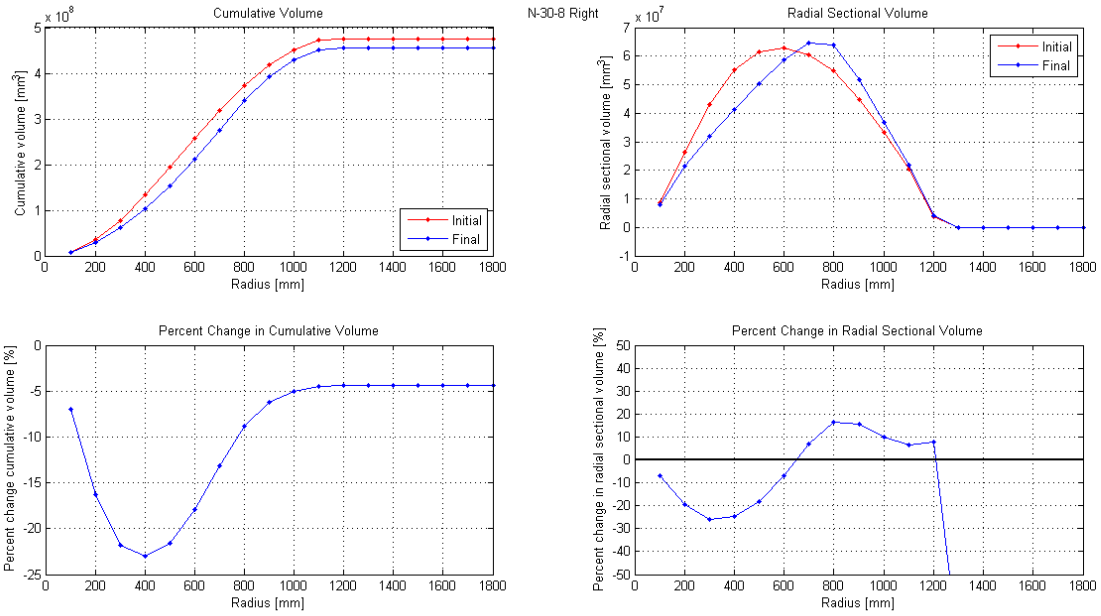

Figure 55 Complete results for N-30-8 Right radial sectioning

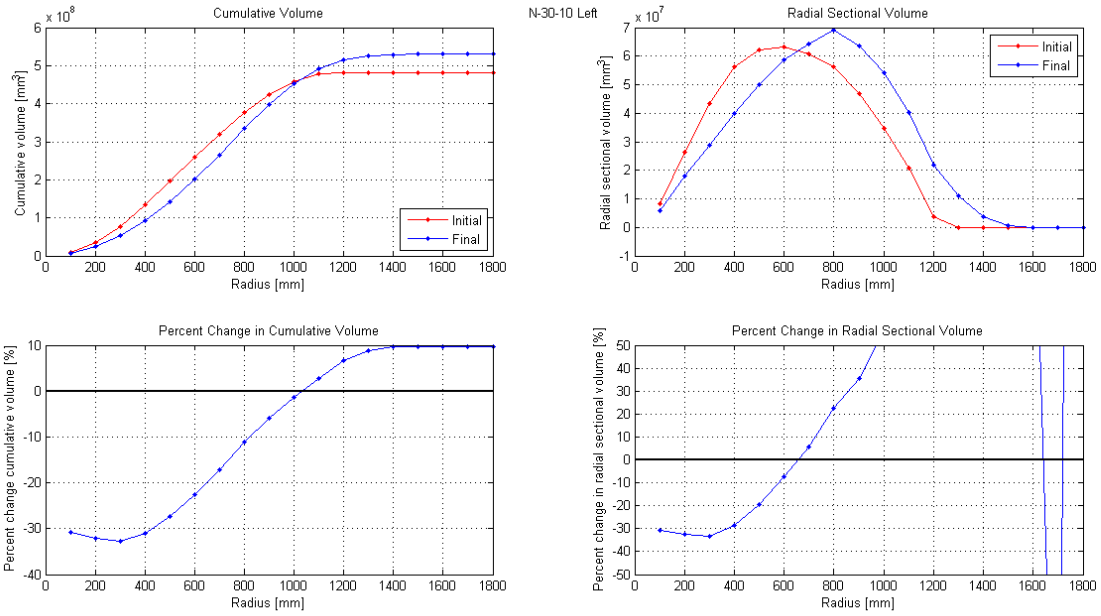

Figure 56 Complete results for N-30-10 Left radial sectioning

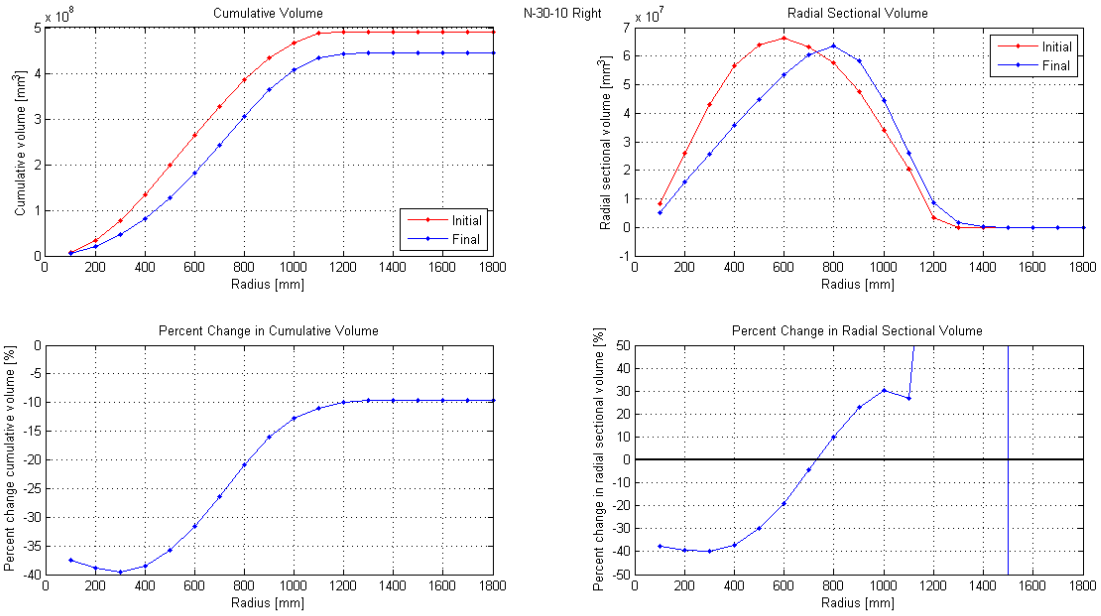

Figure 57 Complete results for N-30-10 Right radial sectioning

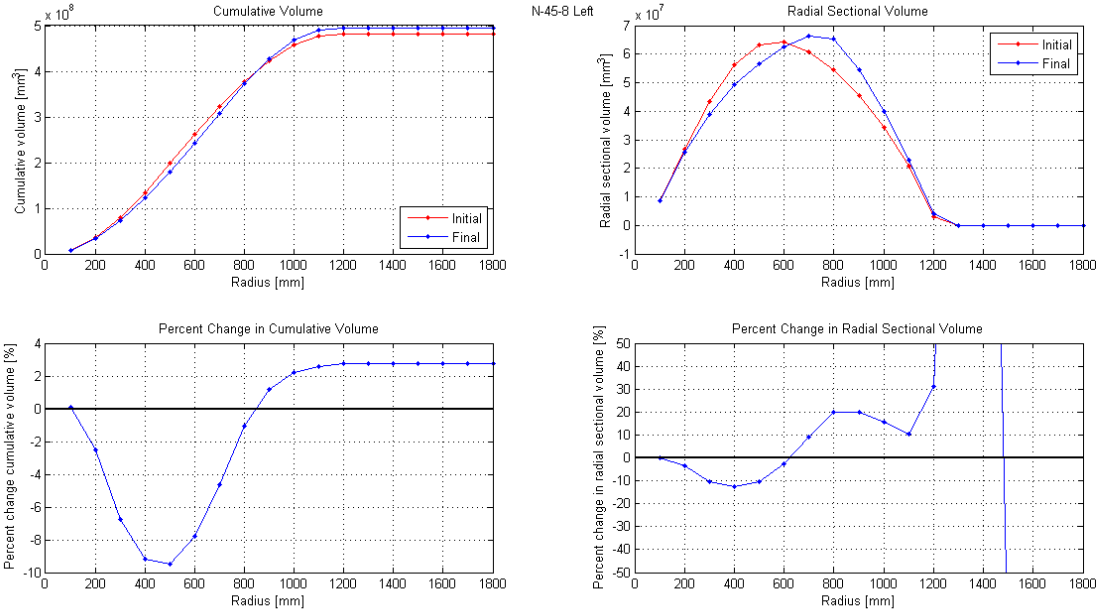

Figure 58 Complete results for N-45-8 Left radial sectioning

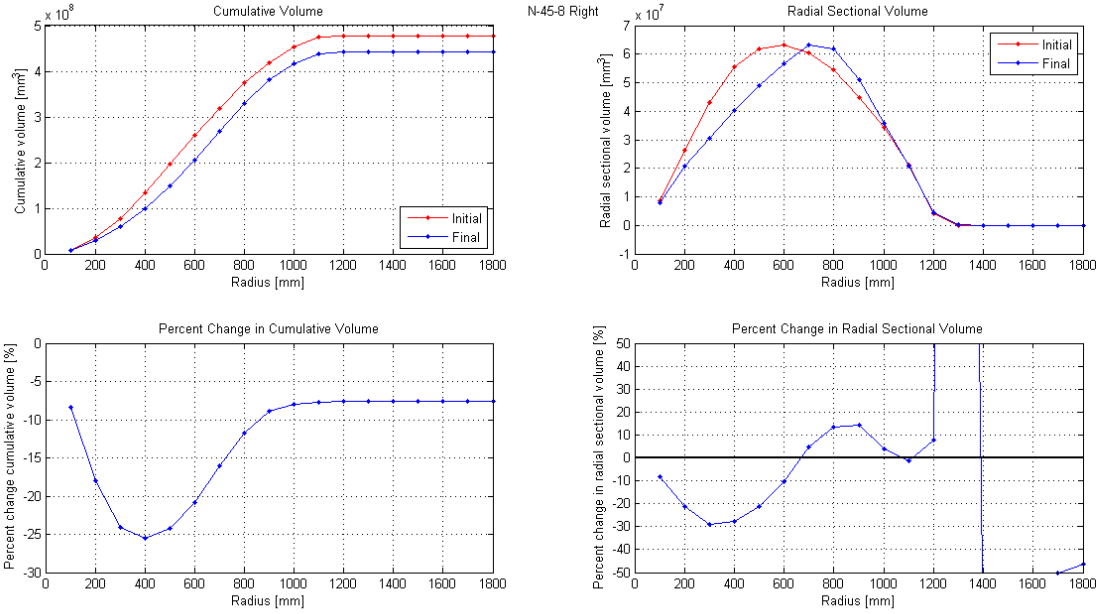

Figure 59 Complete results for N-45-8 Right radial sectioning

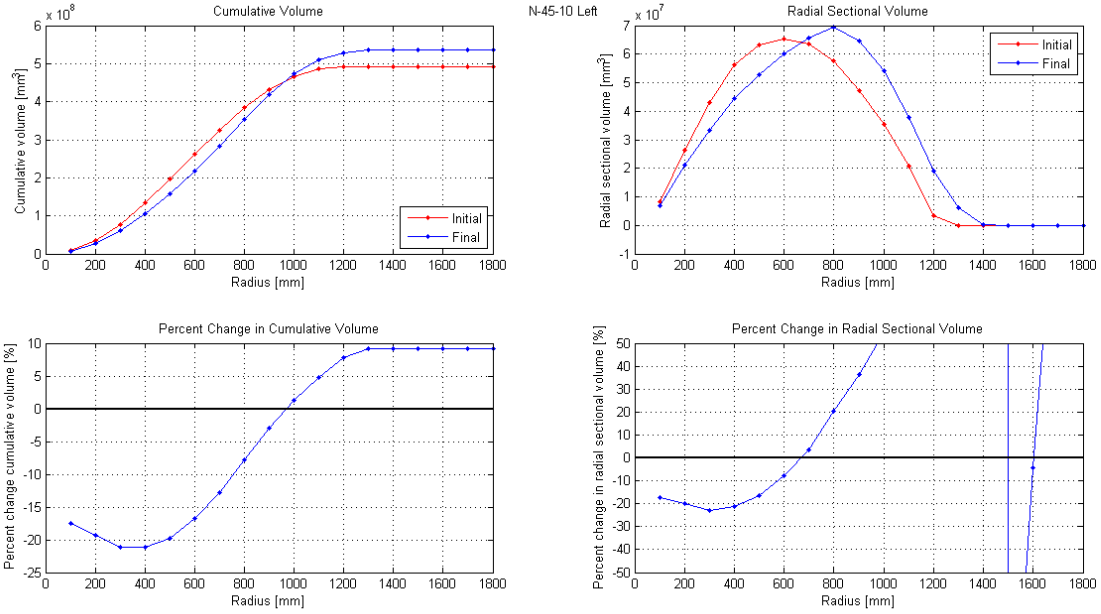

Figure 60 Complete results for N-45-10 Left radial sectioning

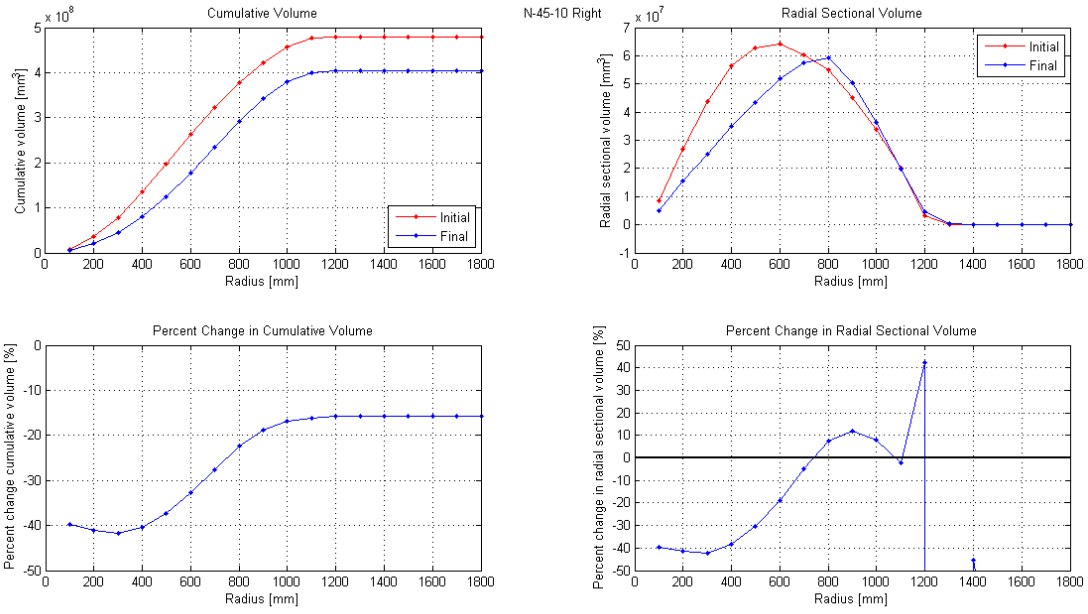

Figure 61 Complete results for N-45-10 Right radial sectioning

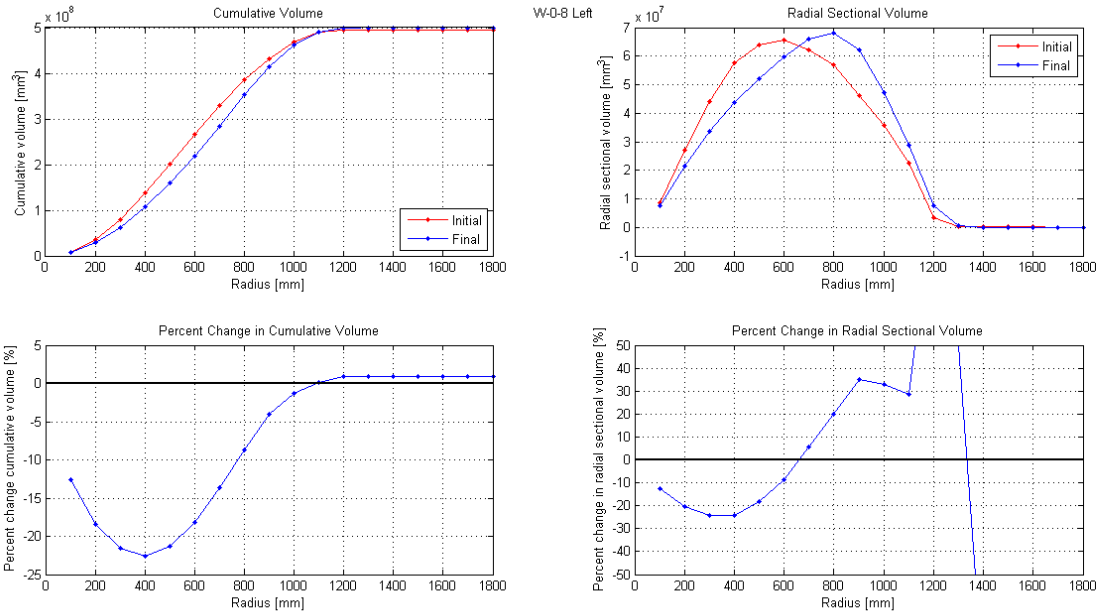

Figure 62 Complete results for W-0-8 Left radial sectioning

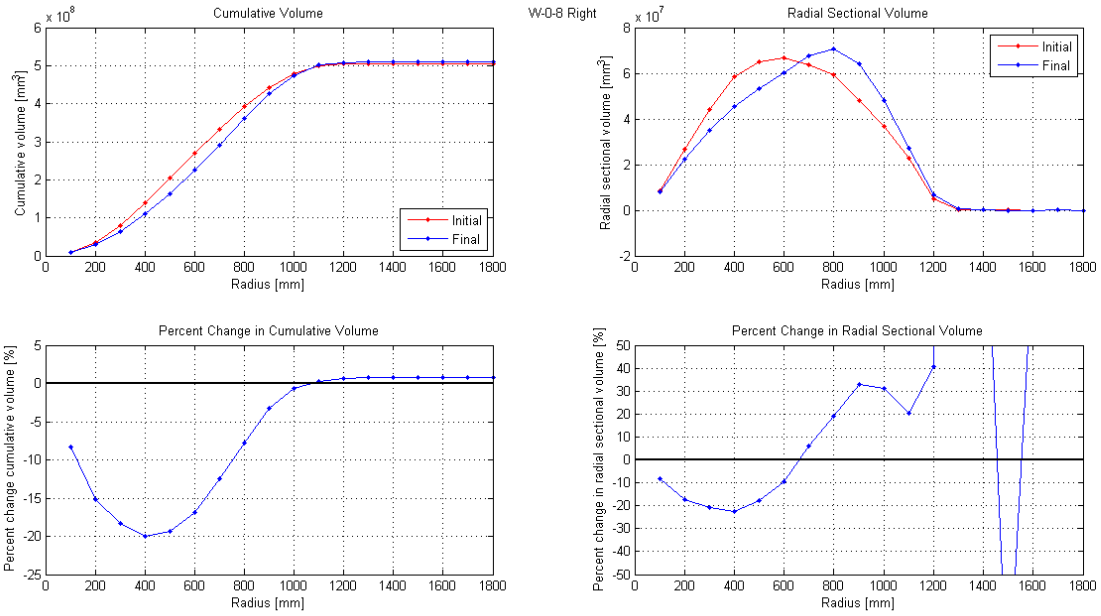

Figure 63 Complete results for W-0-8 Right radial sectioning

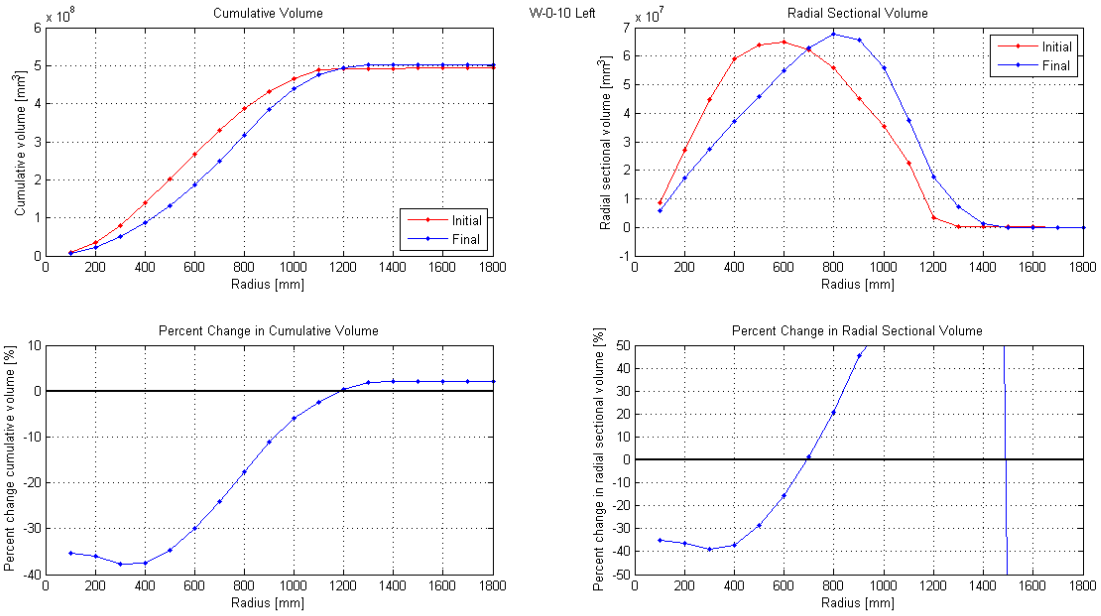

Figure 64 Complete results for W-0-10 Left radial sectioning

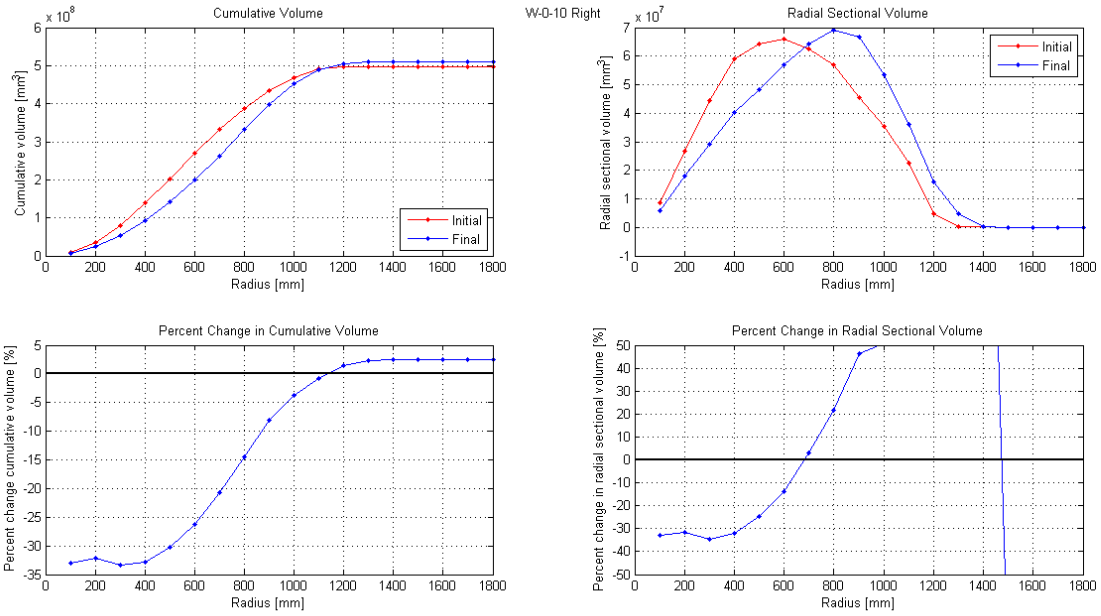

Figure 65 Complete results for W-0-10 Right radial sectioning

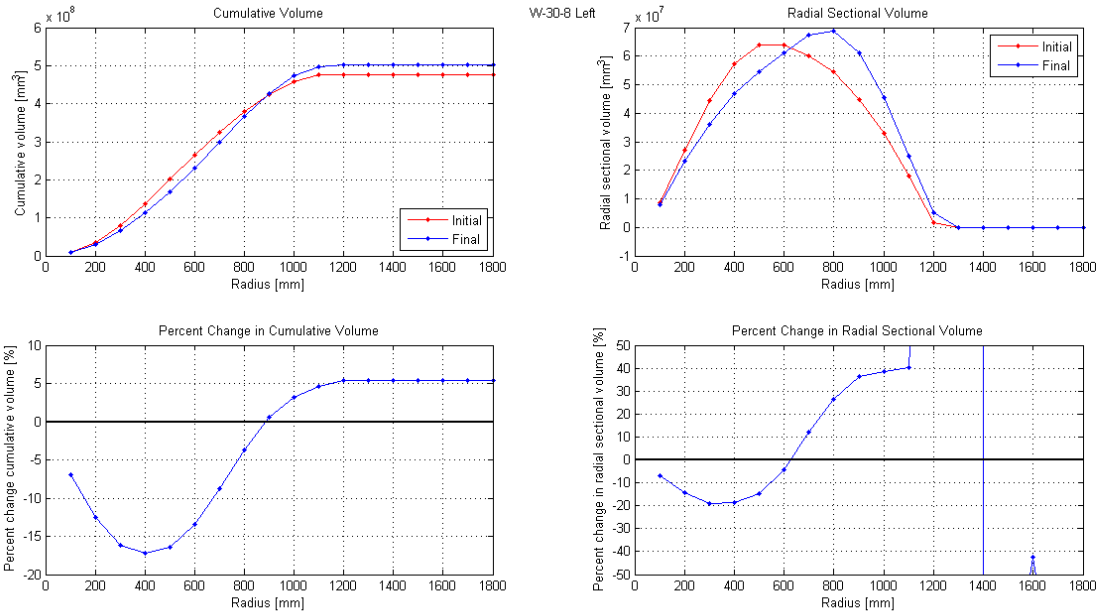

Figure 66 Complete results for W-30-8 Left angular sectioning

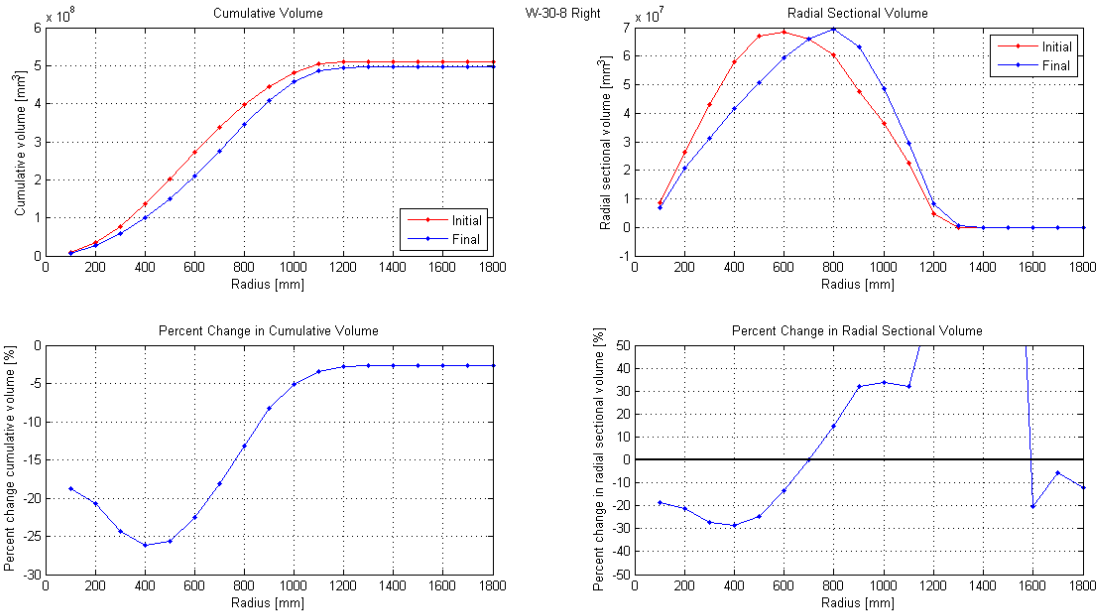

Figure 67 Complete results for W-30-8 Right angular sectioning

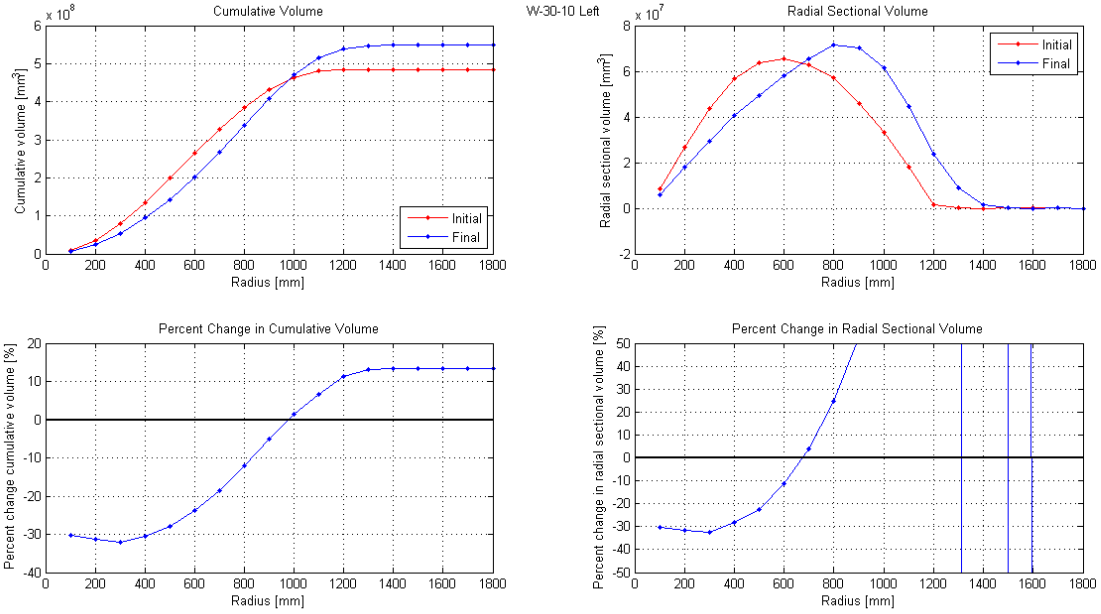

Figure 68 Complete results for W-30-10 Left radial sectioning

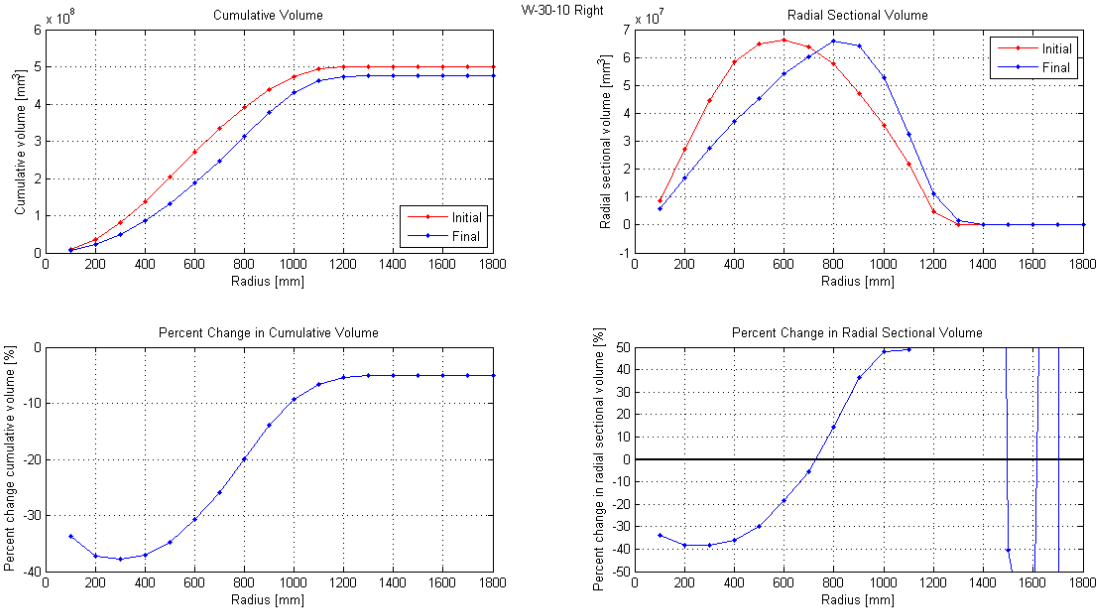

Figure 69 Complete results for W-30-10 Right radial sectioning

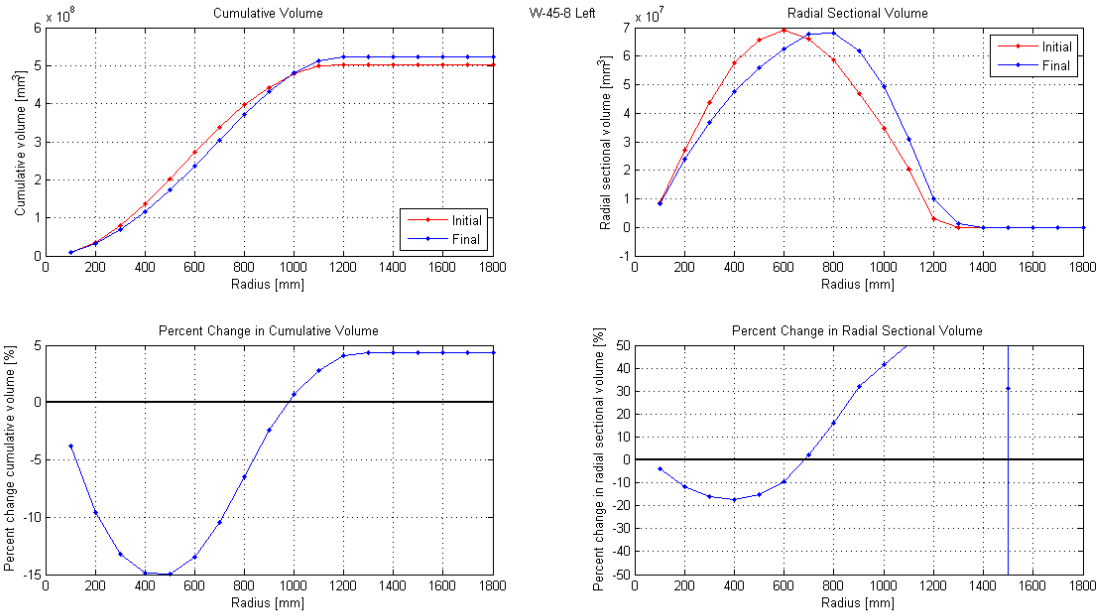

Figure 70 Complete results for W-45-8 Left radial sectioning

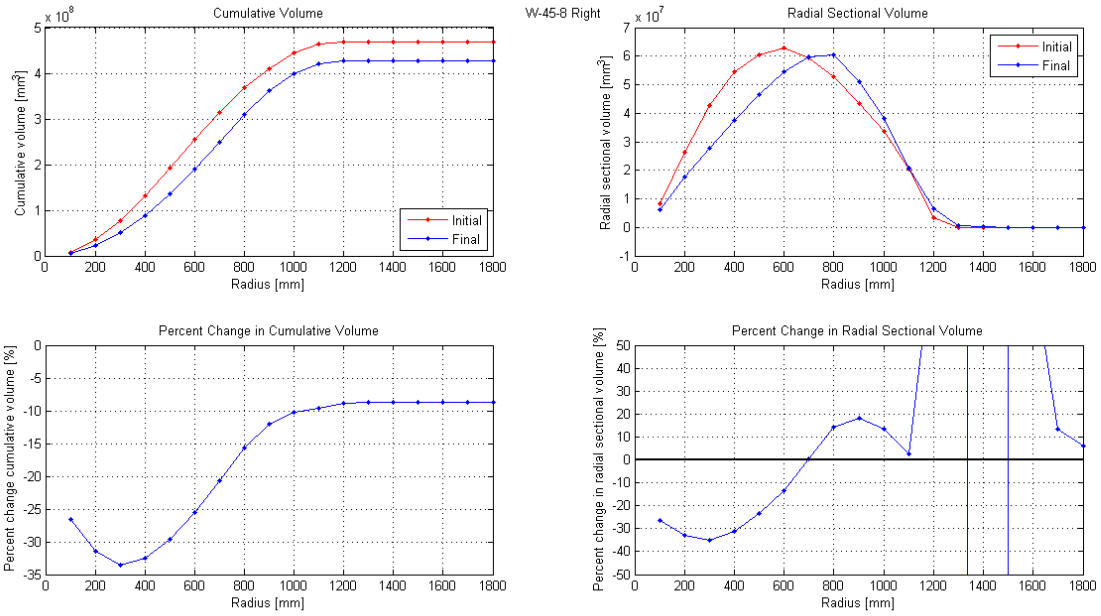

Figure 71 Complete results for W-45-8 Right circular sectioning

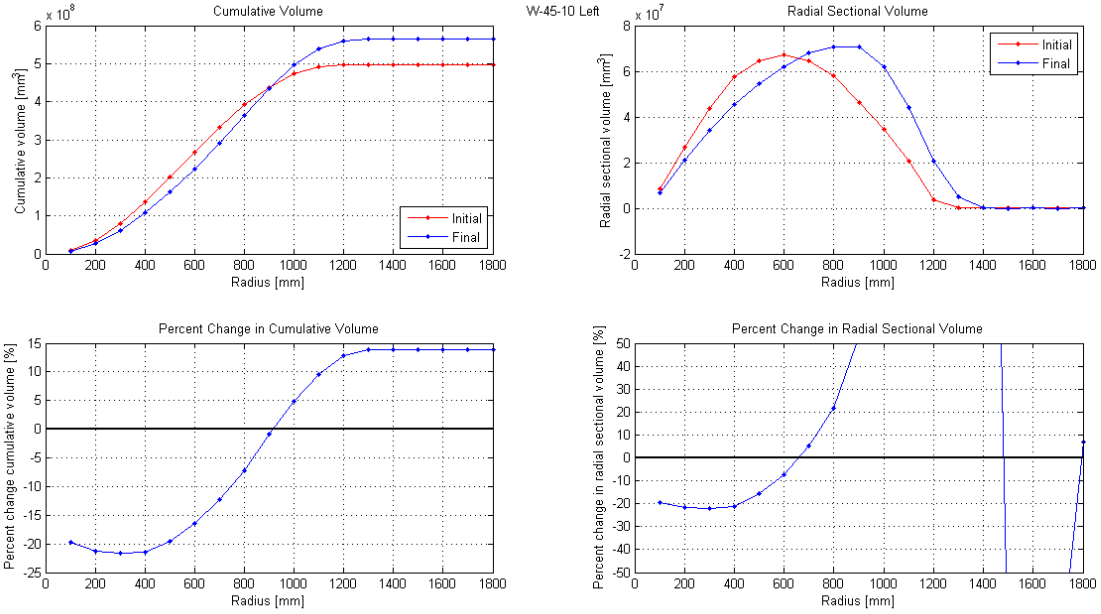

Figure 72 Complete results for W-45-10 Left radial sectioning

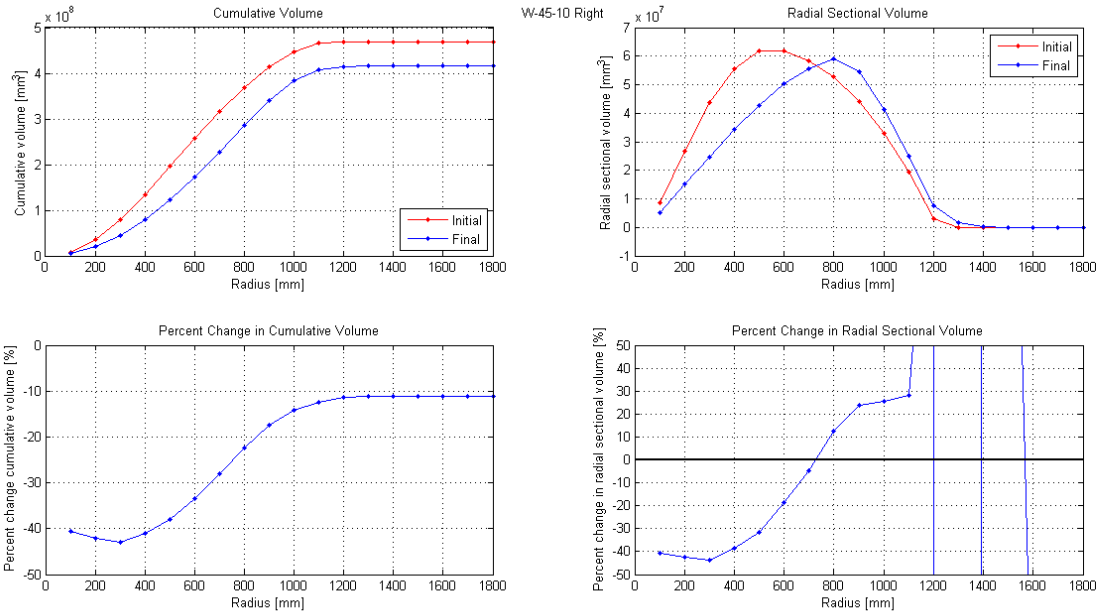

Figure 73 Complete results for W-45-10 Right radial sectioning

7.3 Angular sectioning method results

The percentage changes for all angular sectors were calculated with a fixed radius of 1200mm for all tests.

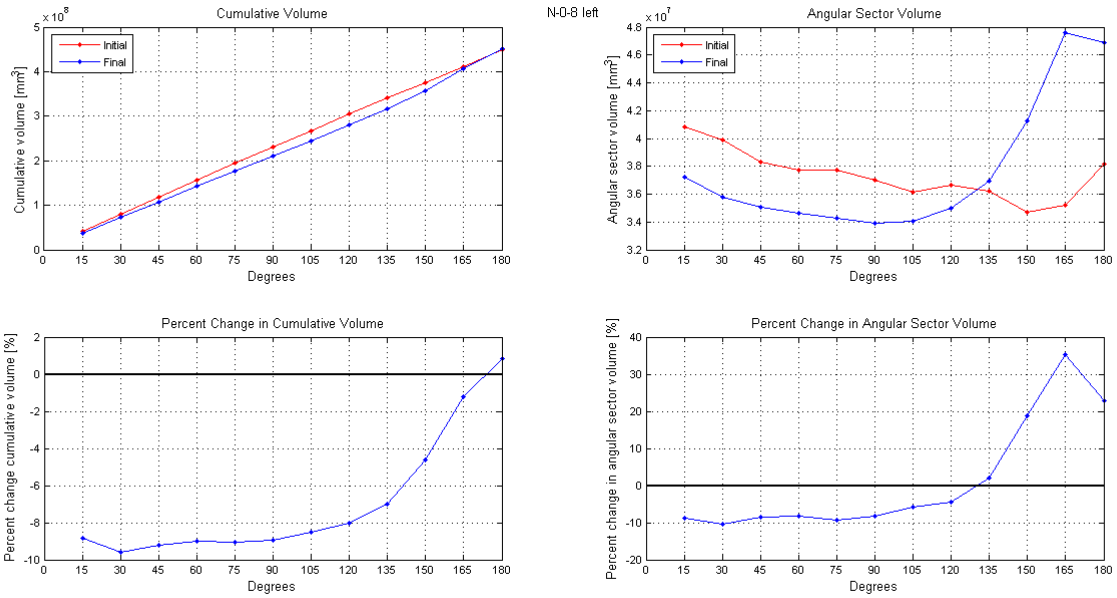

Figure 74 Complete results for N-0-8 Left angular sectioning

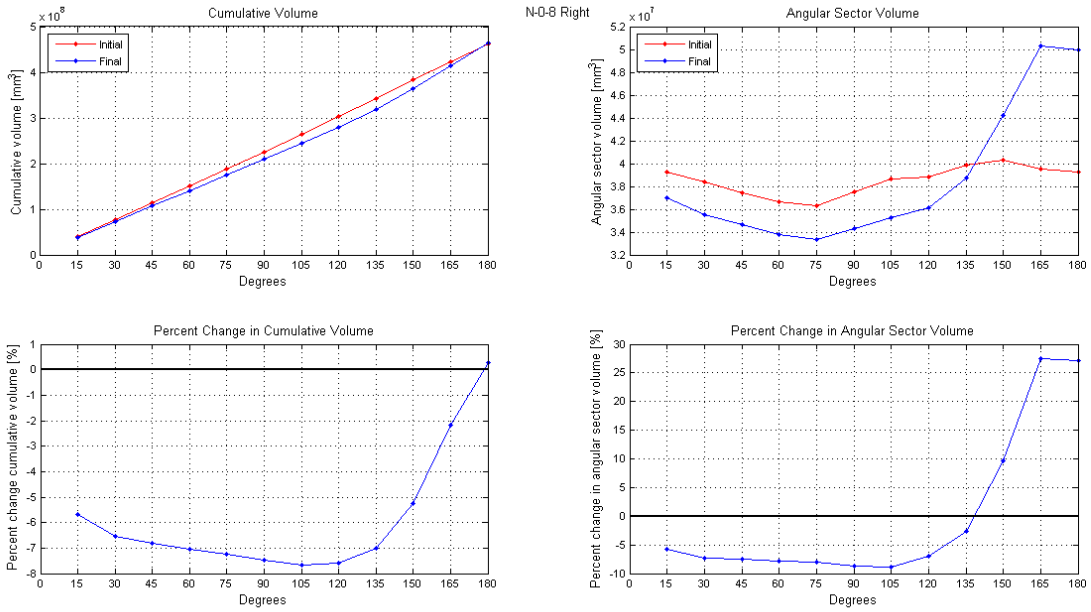

Figure 75 Complete results for N-0-8 Right angular sectioning

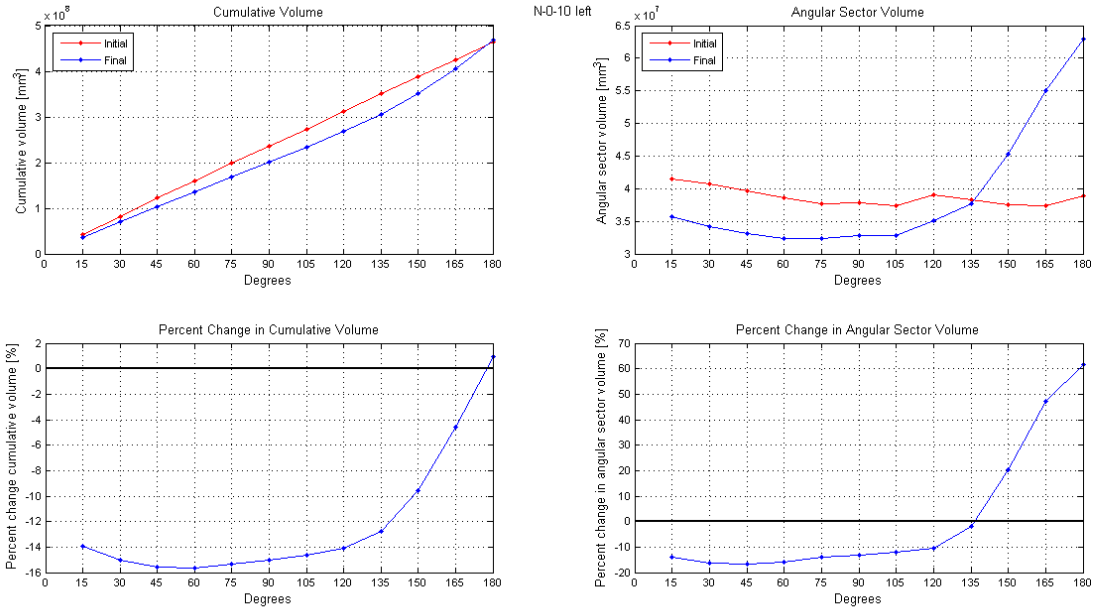

Figure 76 Complete results for N-0-10 Left angular sectioning

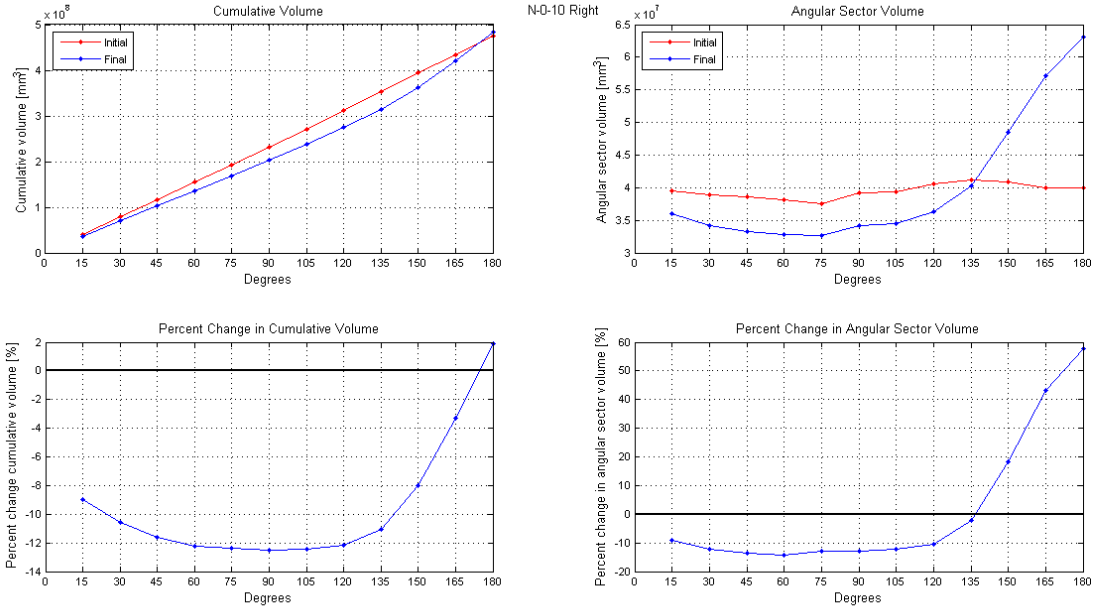

Figure 77 Complete results for N-0-10 Right angular sectioning

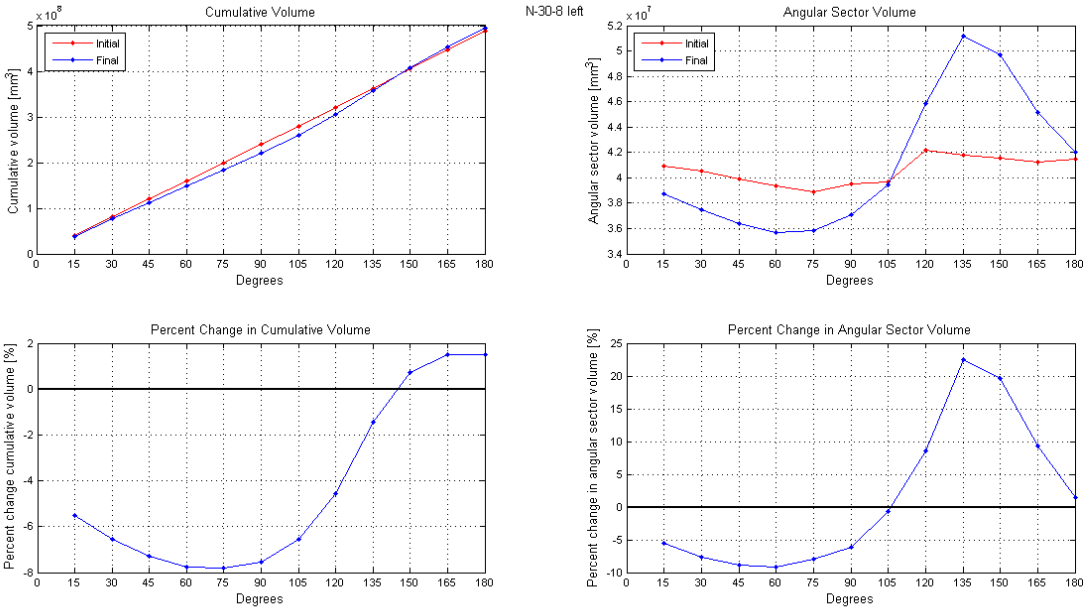

Figure 78 Complete results for N-30-8 Left angular sectioning

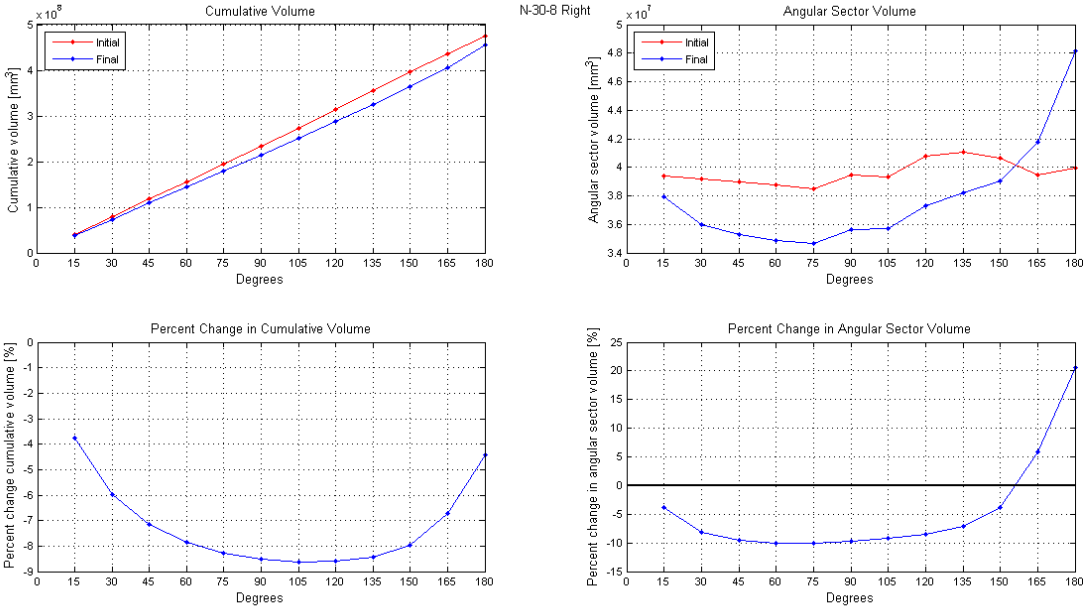

Figure 79 Complete results for N-30-8 Right angular sectioning

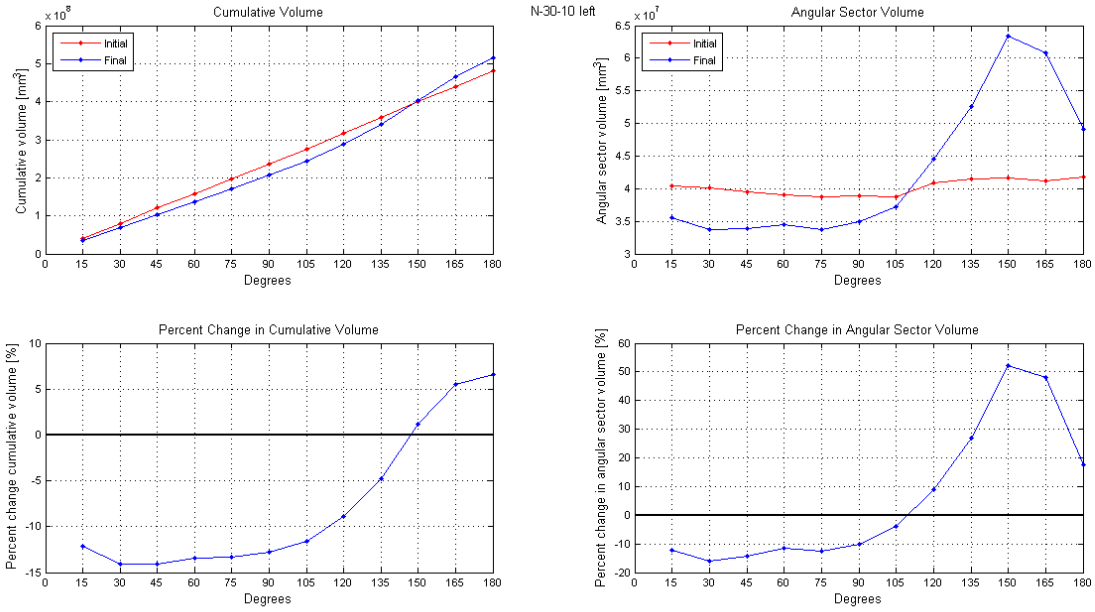

Figure 80 Complete results for N-30-10 Left angular sectioning

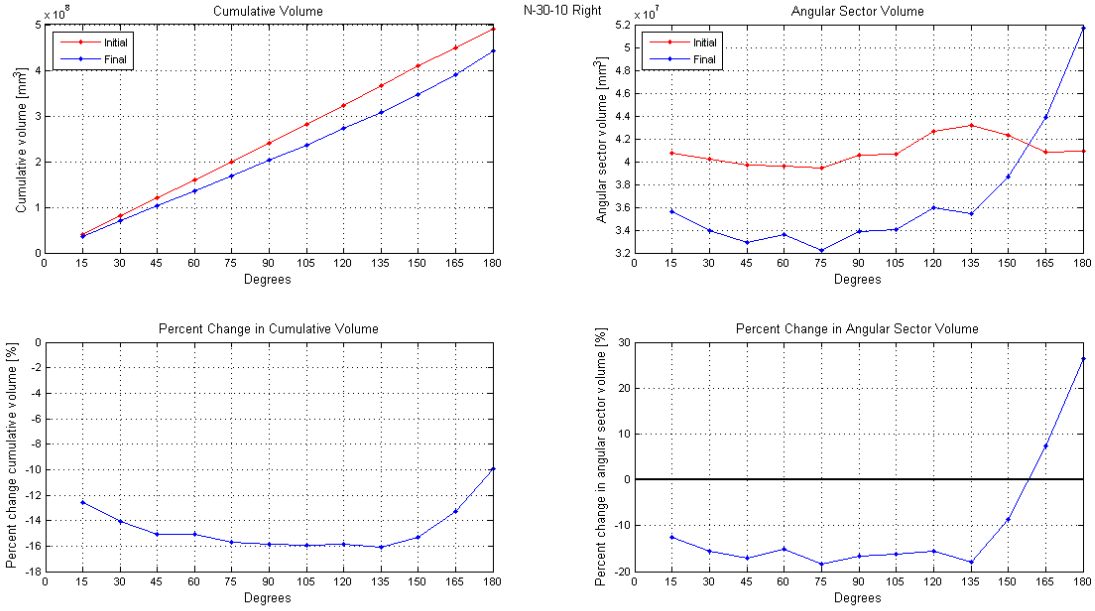

Figure 81 Complete results for N-30-10 Right angular sectioning

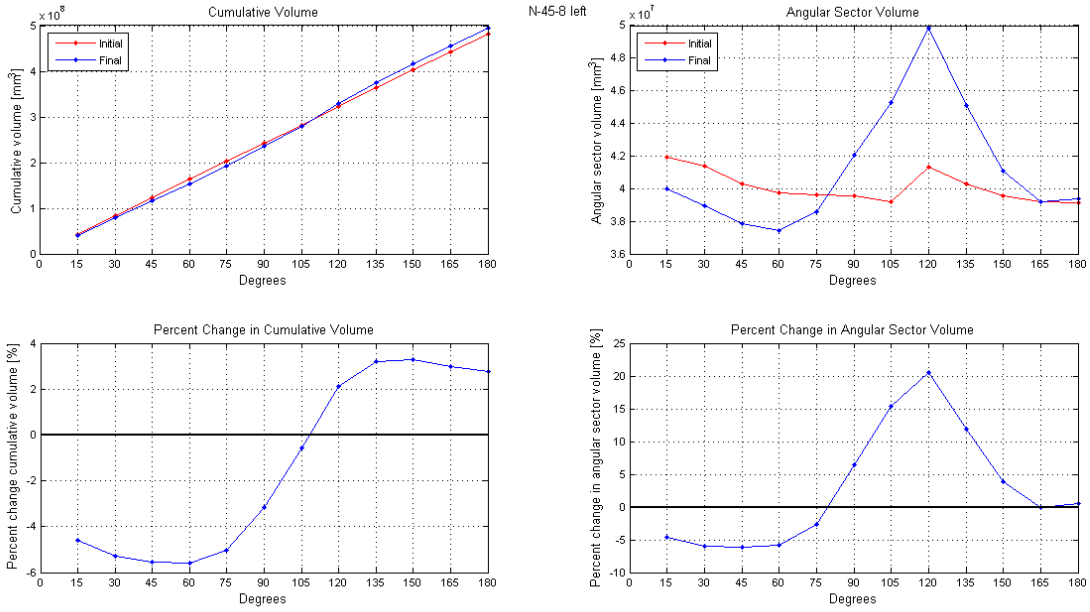

Figure 82 Complete results for N-45-8 Left angular sectioning

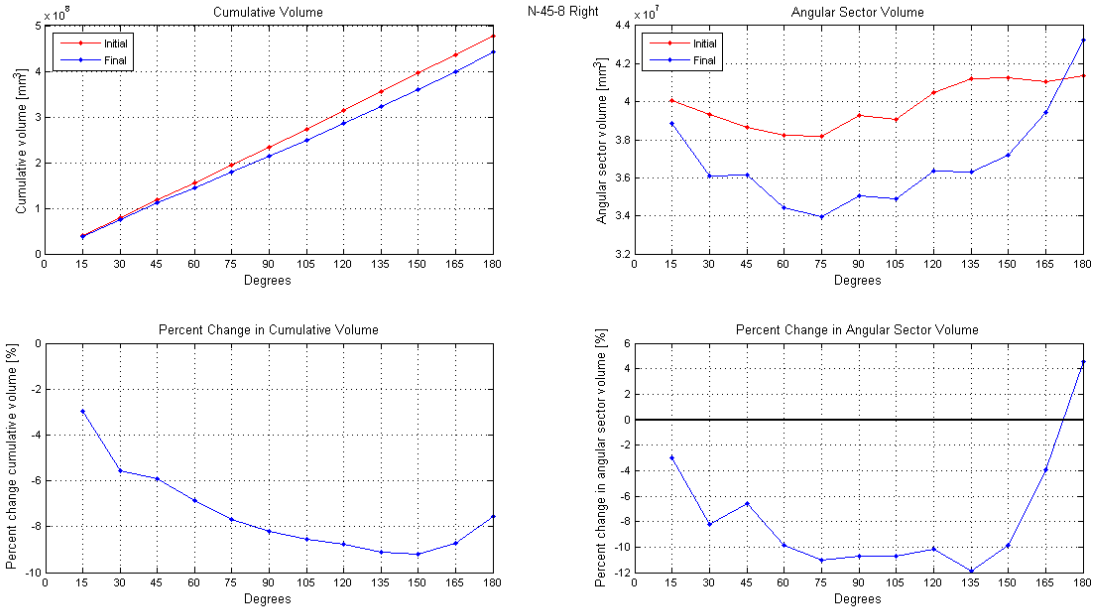

Figure 83 Complete results for N-45-8 Right angular sectioning

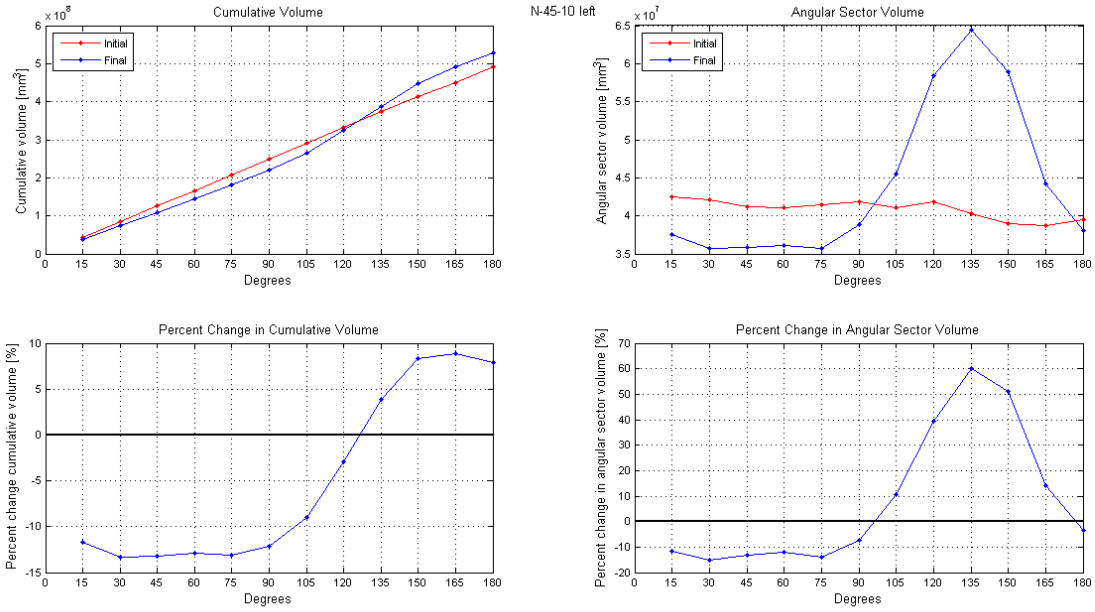

Figure 84 Complete results for N-45-10 Left angular sectioning

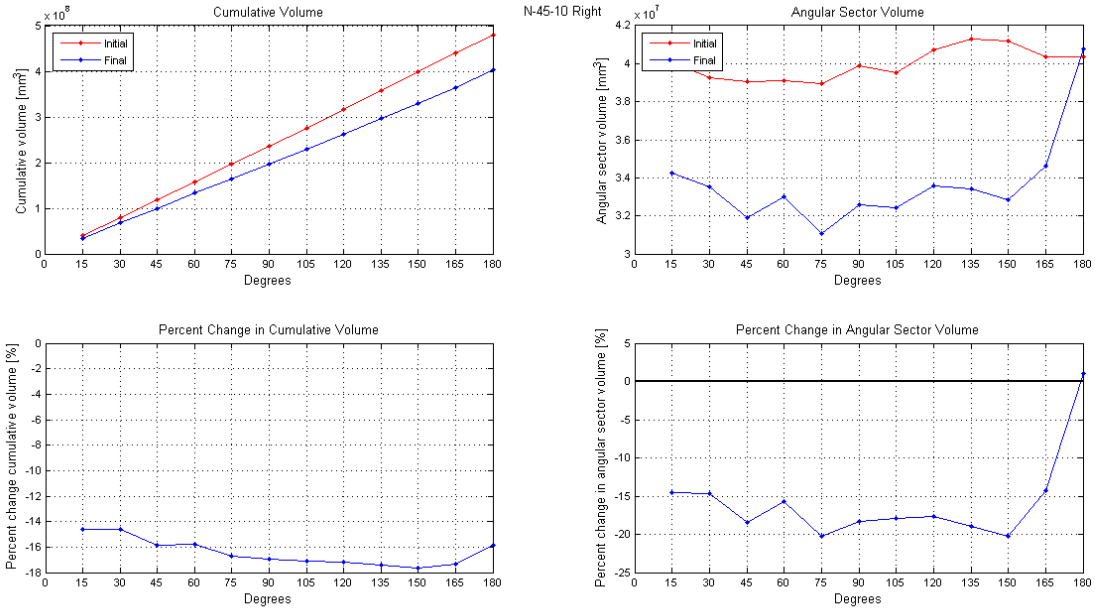

Figure 85 Complete results for N-45-10 Right angular sectioning

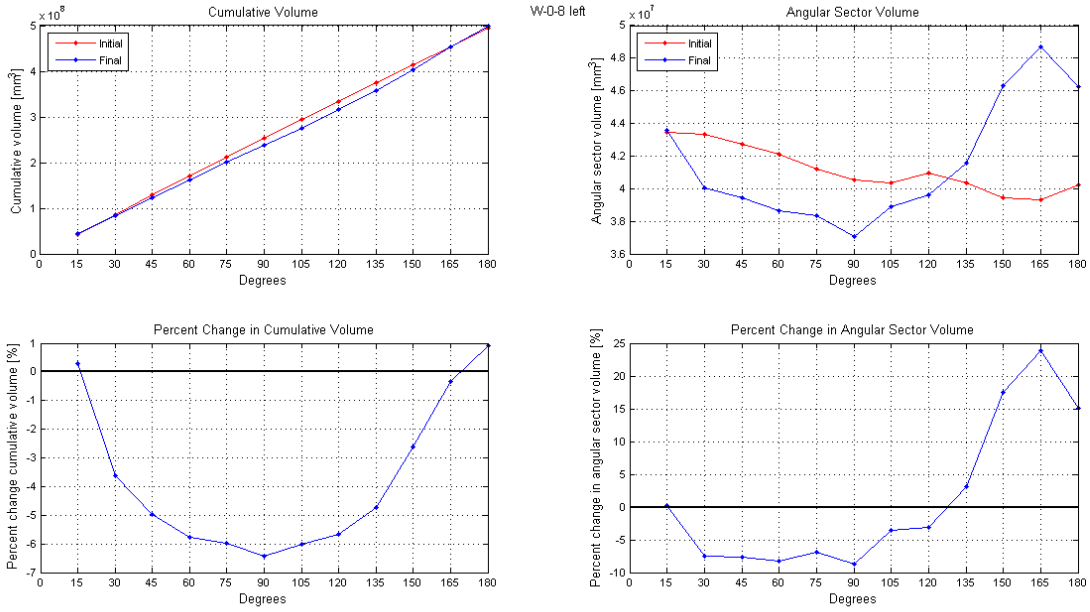

Figure 86 Complete results for W-0-8 Left angular sectioning

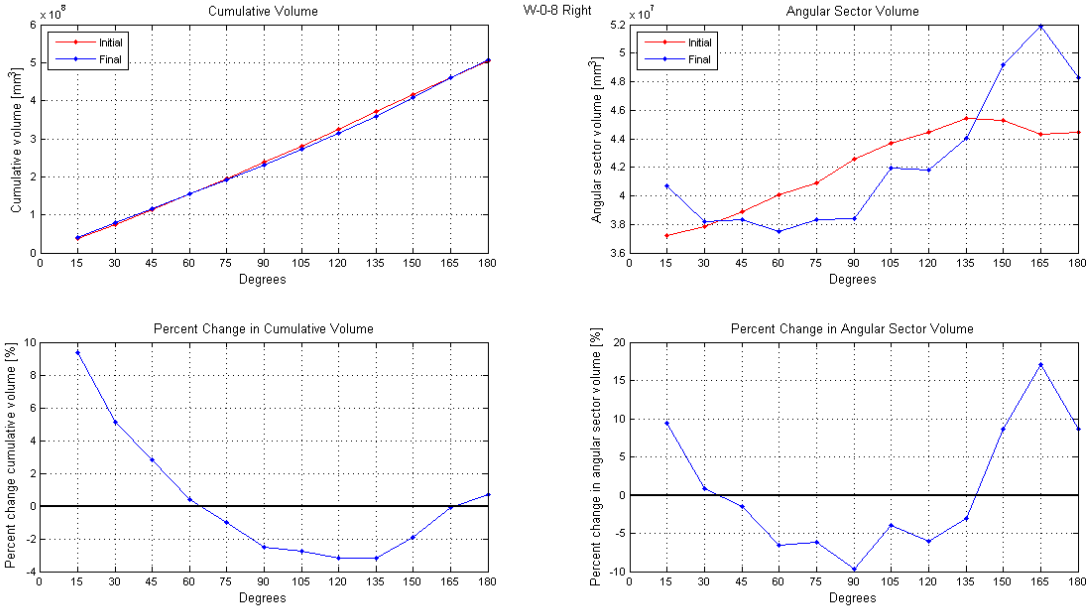

Figure 87 Complete results for W-0-8 Right angular sectioning

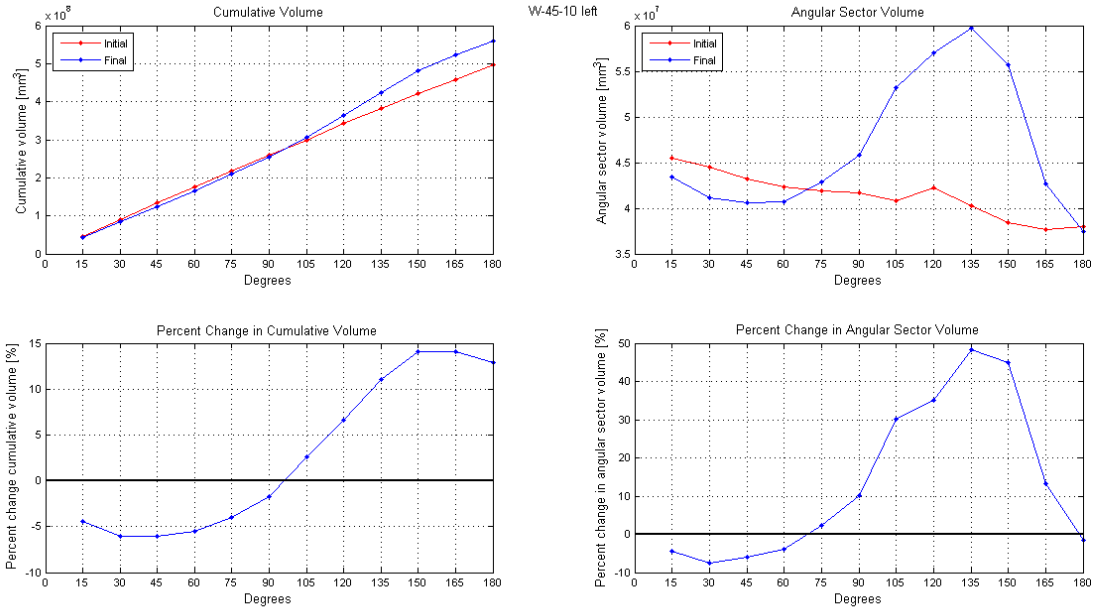

Figure 88 Complete results for W-45-10 Left angular sectioning

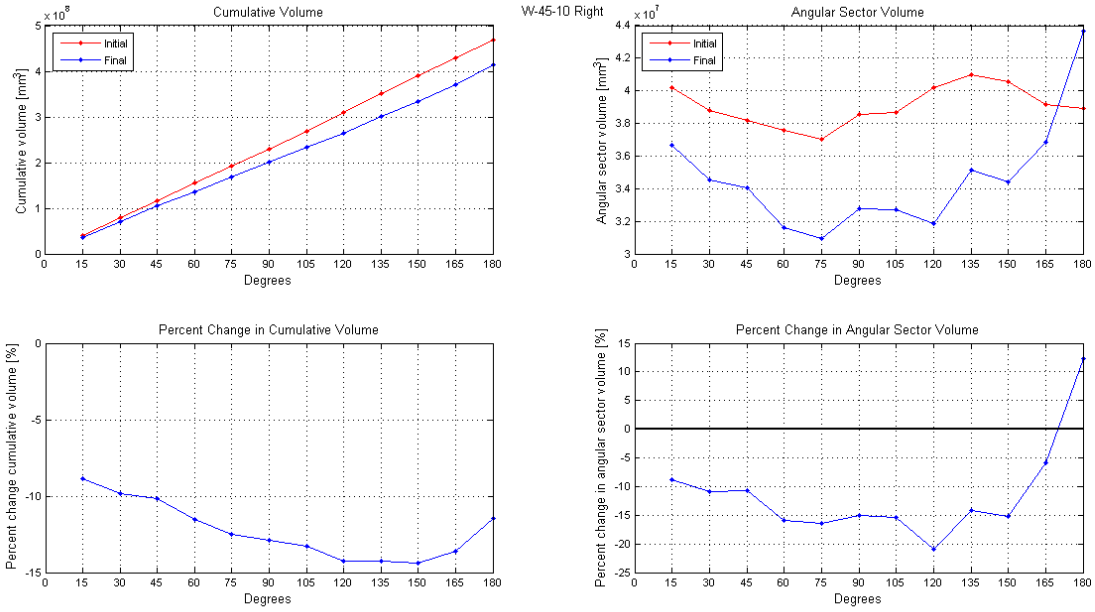

Figure 89 Complete results for W-45-10 Right angular sectioning

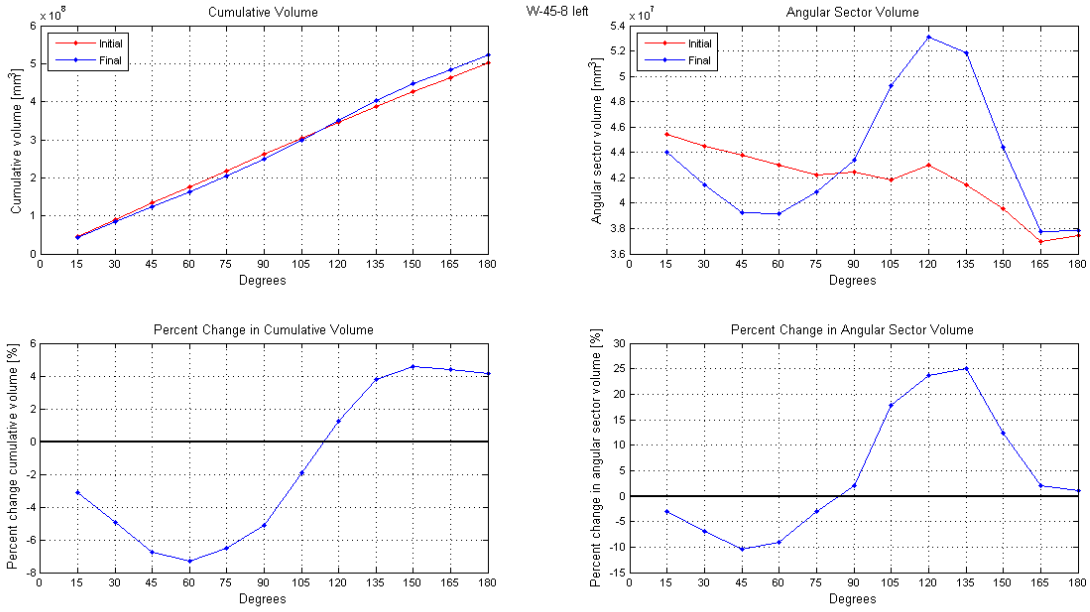

Figure 90 Complete results for W-45-8 Left angular sectioning

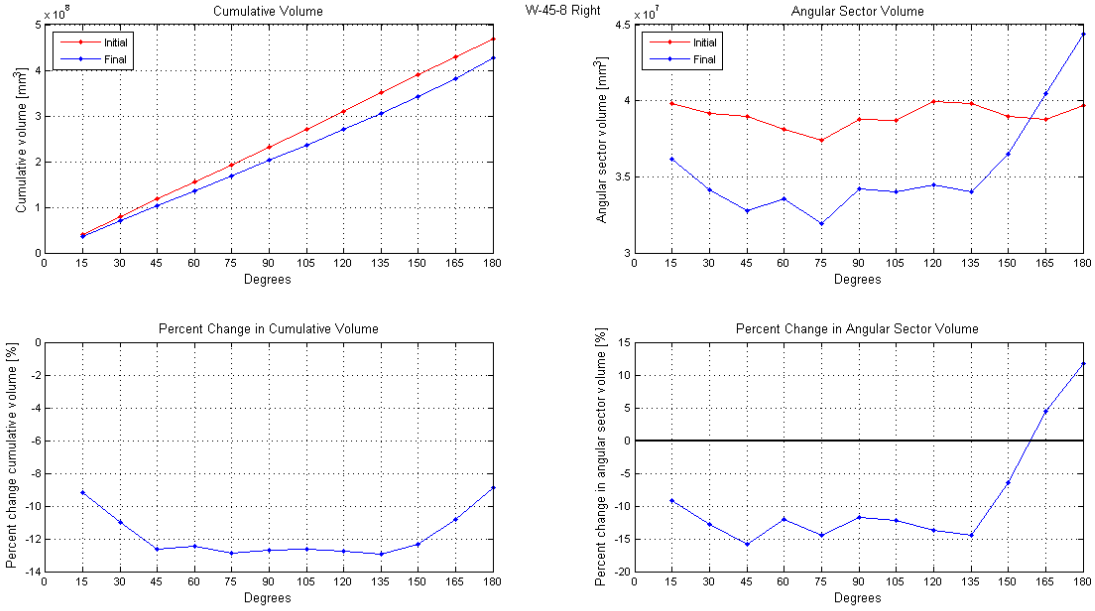

Figure 91 Complete results for W-45-8 Right angular sectioning

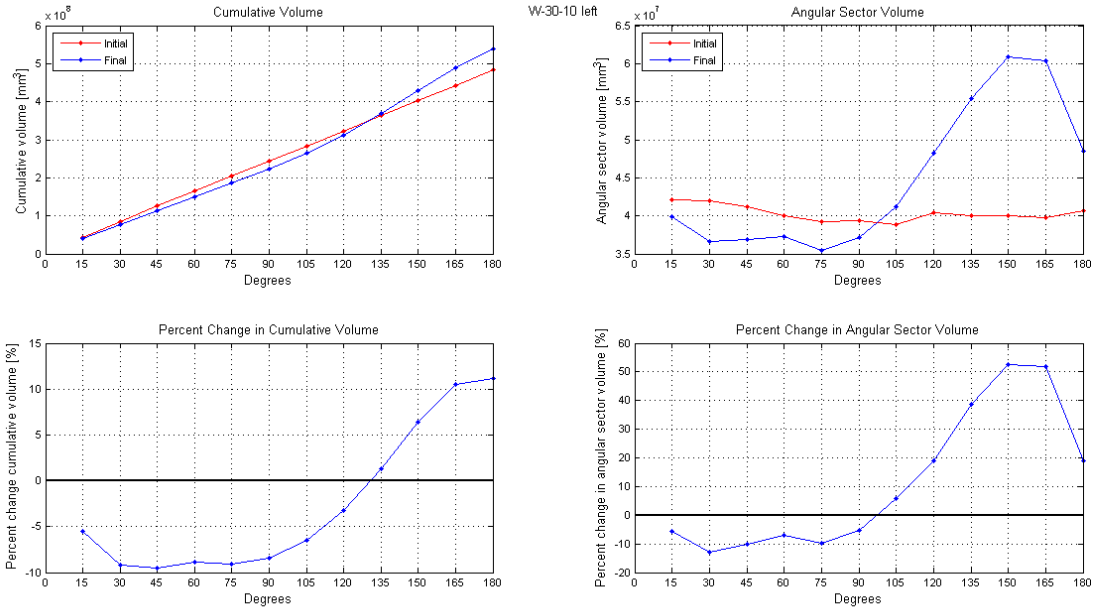

Figure 92 Complete results for W-30-10 Left angular sectioning

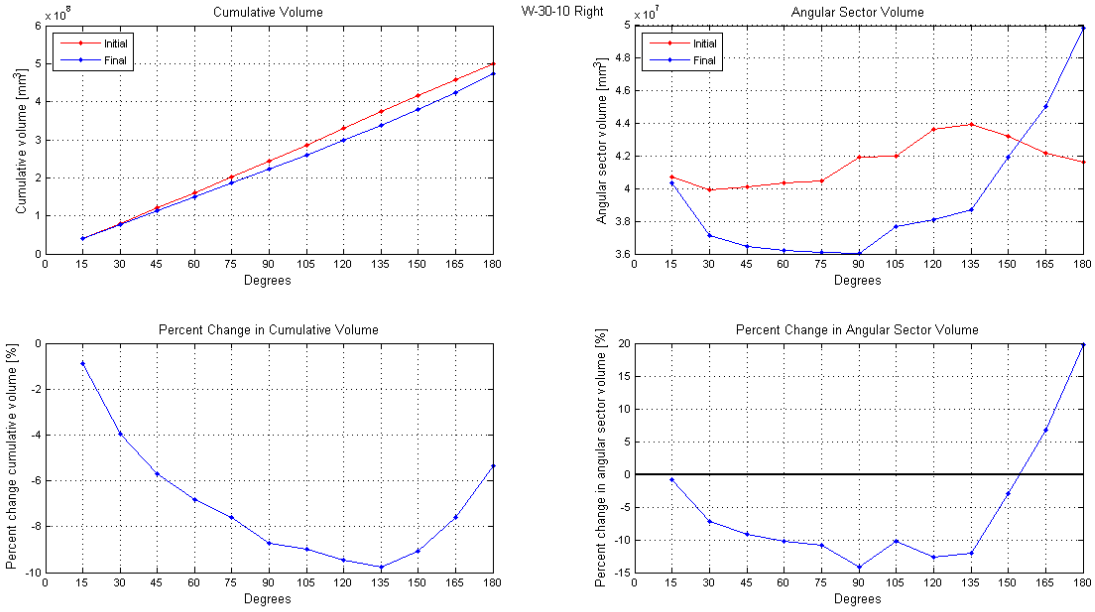

Figure 93 Complete results for W-30-10 Right angular sectioning

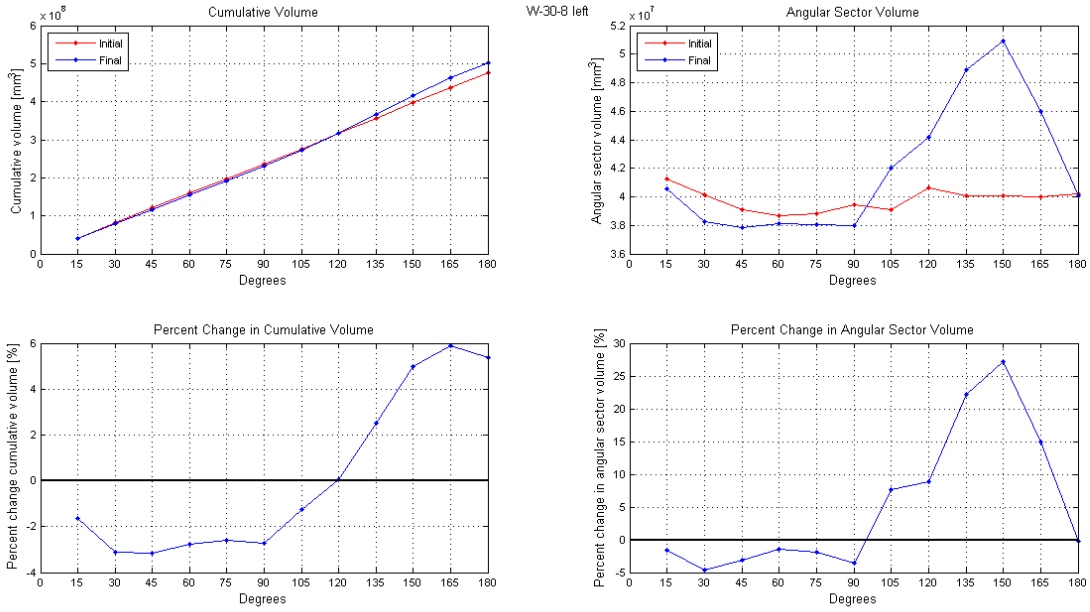

Figure 94 Complete results for W-30-8 Left angular sectioning

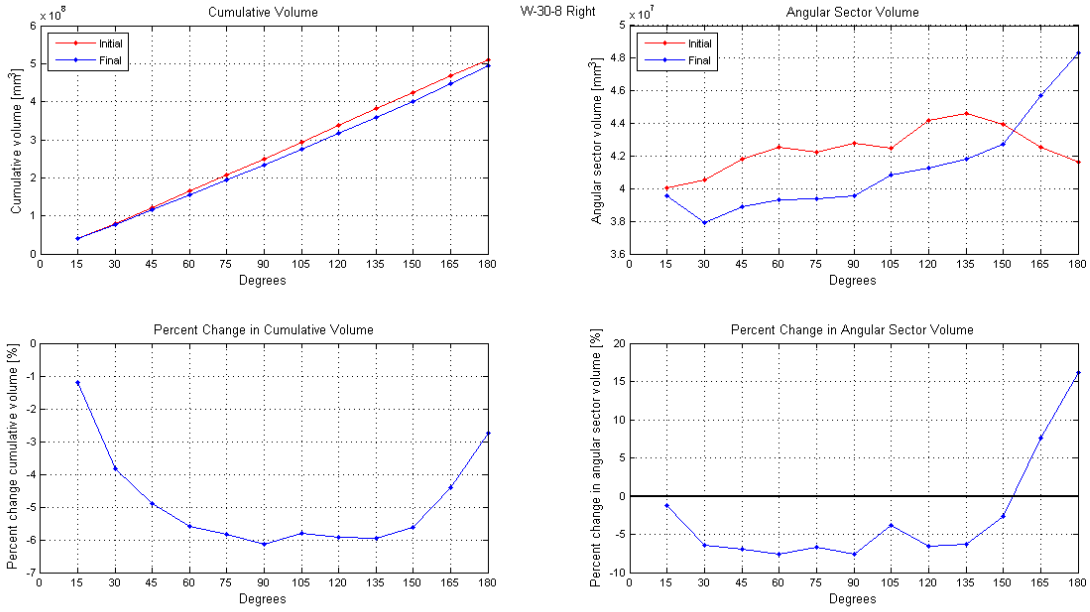

Figure 95 Complete results for W-30-8 Right angular sectioning

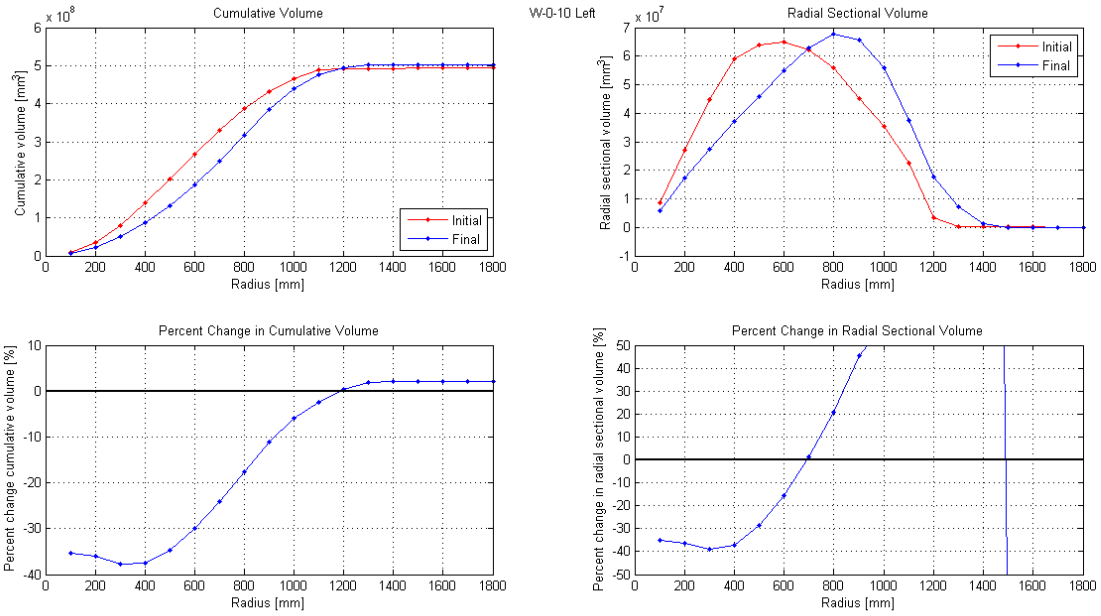

Figure 96 Complete results for W-0-10 Left angular sectioning

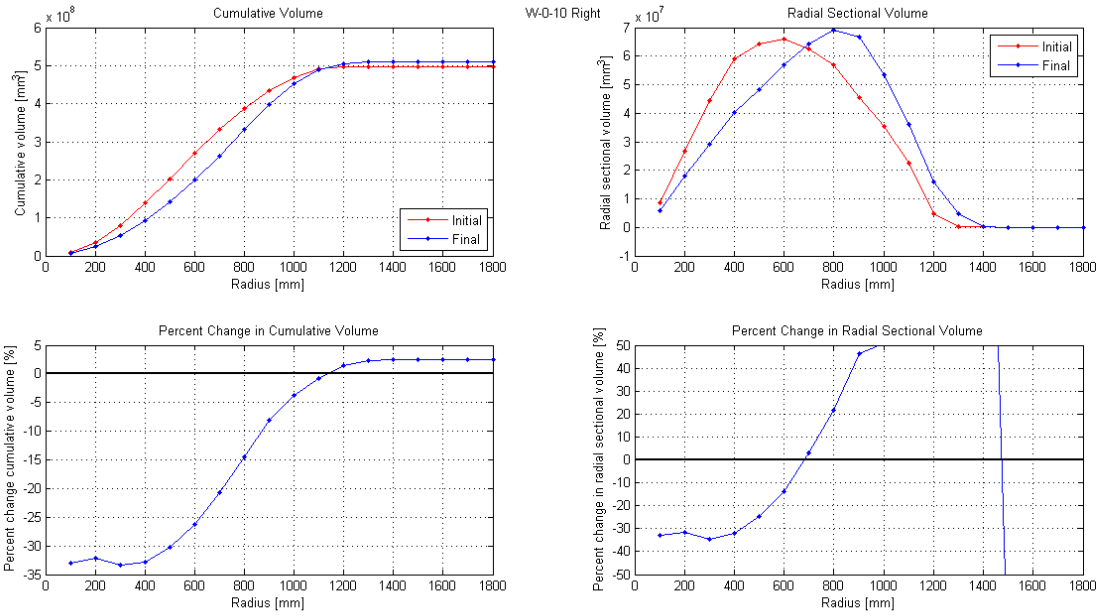

Figure 97 Complete results for W-0-10 Right angular sectioning

8 References

IRIA, CUR, & CETMEF. (2007). *The Rock Manual; The use of rock in hydraulic engineering (2nd edition).* London: C683, CIRIA.

Kennisbank Waterbouw. (2013). Retrieved from http://www.kennisbank-waterbouw.nl/

Maciñeira, E. and H.F. Burcharth. 2008. Spatial damage distribution over cube armoured roundheads, Proc. ICCE 2008, World Scientific, Vol.4. pp.3449-3460.

Matsumi, Y., A. Kimura and K. Ohno. 2000. Stability of armour units on breakwater heads under multidirectional waves, Proc. ICCE 2000, ASCE, Vol.3., pp.1946-1958.

Mulders, P. (2010). *Breakwaters under construction exposed to oblique waves.* Delft: Delft University of Technology, MSc Thesis.

Mulders, P., & Verhagen, J. (2012). Breakwaters under construction exposed to oblique waves. *Coastal Engineering Proceedings, 1(33), structures-15.*

Van der Meer, J. (1988). *Rock slopes and gravel beaches under wave attack.* Delft: Delft University of Technology, PhD Thesis.

Van Gent, M., & Van der Werf, I. (2011). Stability of Breawater Roundheds during Construction. *Coastal Engineering Proceedings, 1(32), structures-33.*

Van Hijum, E., & Pilarczyk, K. (1982). *Equilibrium profile and longshore transport of coarse material under regular and irregular wave attack.* Delft Hydraulics.

Verhagen, J. J., D'Angremond, K., & Van Roode, F. (2012). *Breakwaters and Closure Dams.* Delft: VSSD.

Verruijt, A. (2010). *Soil Mechanics.* Delft: VSSD.

Vidal. C, M.A. Losada and R. Medina. 1991. Stability of mound breakwater's head and trunk, J. of Waterway, Port, Coastal and Ocean Engrg, ASCE, Vol. 177, No.6 Nov/Dec, pp.570-587.